Shallow P-wave seismic reflection event for estimating the static time corrections: implications for 3D seismic structural interpretation, Ellis County, Kansas

by

Christian Tucci

B.S., University of Oklahoma, 2017

A THESIS

submitted in partial fulfillment of the requirements for the degree

MASTER OF SCIENCE

Department of Geology
College of Arts and Sciences

KANSAS STATE UNIVERSITY
Manhattan, Kansas

2020

Approved by:

Co-Major Professor
Dr. Matthew Totten

Approved by:
Co-Major Professor
Dr. Abdelmoneam Raef

Copyright

Abstract

In a processing flow of 2D or 3D seismic data, there are many steps that must be completed in seismic processing to produce a dataset in suitable for seismic interpretation. In case of land seismic data, it is very essential that the data-processing work flow create and utilize a static time correction to eradicate variations in arrival time associated with changes in the topography and low-velocity near surface geology (Krey 1954). This project utilizes velocity analysis, based on a near-surface reflection, to estimate near surface statics corrections to a datum at elevation of 1300 ft (Sheriff and Geldart 1995, Rogers 1981). Reviewing and Rectifying errors in geometrical aspects of the field seismic data is essential to the validity of velocity analysis and estimation. To this end, geometrical aspects of the data were validated based on spatial aspects of the survey acquisition design and acquired data attributes. The seismic workflow is a conglomeration of many steps, of which, none should be overlooked or given insufficient attention. The seismic processing workflow spans from loading the data into a processing software with the correct geometry to stacking and binning the traces for exportation to interpretation software as a seismic volume. Important steps within this workflow and ones that will be covered in this thesis include; the framework to reverse engineer a survey geometry, dynamic corrections, velocity analysis, and building of a static model to account for the near surface, or low velocity layer. This seismic processing workflow seeks to quality control most, if not all, seismic datasets in hopes to produce higher quality and more accurate three-dimensional seismic volumes for interpretation. The developed workflow represents cost-effective, rapid approach of improving the structural fidelity of land seismic data in areas with rugged topography and complex near-surface velocity variation (Selem 1955; Thralls and Mossman 1952).

Table of Contents

List of Figures

List of Tables

List of Equations

Acknowledgements

Foremost, I would like to express my sincere gratitude to my advisors, Dr. Matthew Totten and Dr. Abdelmoneam Raef for the continuous support of my Master's Thesis and research. Without their support and immense patience, this task could not have been completed. I would also like to than the Kansas State Geology Department for financial support and for the opportunity to use such advanced software supplied by Schlumberger and Halliburton. I would also like to thank Paul and Deana Strunk for their generous contributions to further my education, for without them, I could not have completed this thesis. Finally, I would like to thank God for granting my perseverance and commitment to bettering myself within the scientific community.

Chapter 1 - Introduction

Within the discipline of seismic processing and interpretation, there are many important, and sometimes underappreciated, steps that must be taken to create an accurate and usable product for oil and gas exploration. Within the processing workflow, or the early stages of the seismic data workflow, the fundamentals and groundwork is laid to create an accurate dataset. If proper attention is not paid, an inaccurate and unusable dataset may be the result. The fundamentals of the seismic processing workflow incorporate: correctly loading the data, assigning the correct geometry to the data (ground-truthing the data with the native data), editing the data with amplitude, bandpass filters, and deconvolution, then applying statics corrections, running a velocity analysis, stacking and finally post-stack analysis. Much care should be taken to make sure that these steps are completed with the most accuracy and precision so that the final product, one that will be interpreted to explore for hydrocarbons, will correctly reflect the subsurface.

Seismic surveys have greatly increased the chance for drilling success in hydrocarbon exploration. They have not, however, eliminated dry holes. There are abundant cases where "the seismic did not work" within the industry. The post-mortem typically centers on the interpretation of the seismic volume. Inaccurate processing of the data is also possible, but rarely investigated.

This project and associated research will illuminate that there is a need for further study into the seismic processing workflow, especially with regards to the quality control of the data and how to remedy data that lacks sufficient quality and that is not up to industry standard. Within the scope of the seismic data provided by an acquisition and processing company, it can be determined with preliminary quality control that the processed data provided lacks accuracy

in that the topography is directly paralleled in the subsurface, and while in some cases this situation might be true, with knowledge of the geology and subsurface of Ellis County, Kansas, one can say that there is inherent error in the interpretation (Figure 1 and Figure 2). Herein lies the substance of the project, to understand what the error in the data is, propose methods to remedy this error, and finally to communicate the results, comparing the original dataset to the remedied.

We have proposed hypotheses regarding the data and what might remedy the issues seen in the data. One hypothesis we will explored is the static corrections datum, as mentioned previously in the seismic processing workflow, as it is often seen that if the seismic data does is not accurately represented, there is often an issue with the static datum and associated near surface velocity (Cox 1999; Frei et al. 2015). We have also conjectured that there was an issue with the way that the seismic geometry was formulated, in that there seemed to be little no coherence among shot and receiver points within the dataset, and to remedy this we will reverse engineer a system to assign geometry from what was given as well as what is observed within the actual dataset.

Chapter 2 - Seismic Data

l Information

The 3D seismic data received from Stroke of Luck covers an area of 1.9 square miles (1.2 Acres) with inline and crossline spacing is equal to 82.5 feet (97 inlines and 133 crosslines). With seismic datum at 2100 feet and replacement velocity of 9000 feet/s used. The processing information lacked details on the quality of the statics solution applied as well as the adequacy of using 9000 ft/s replacement velocity. The spectral content of the data has a bandwidth of 10-80 Hz (Figure 3) with lower energy levels on the higher frequency part of the spectrum. The data

can be improved in terms of bandwidth with data enhancement techniques to boost the higher

frequency content and thus the resolution and potential reservoir signatures (Figure 4). The

structural fidelity of the data is likely to improve with better statics solution in order to account

for velocity and topography changes above the seismic data (Cox 1999). As can be seen in

Figure 1and Figure 2 the local high seen in the time structure map is directly correlated to the

topography seen at the surface when superimposed. The quality of the seismic data is therefore

hindered by the fact that structure observed here is inaccurate. Before moving further into the

bulk of the thesis, we must define some of the terms that will be used throughout. Definitions

adapted from Sclumberger Glossary as well as Yilmaz (2001).

Offset: In surface seismic acquisition, the horizontal distance from source to geophone. In a
vertical seismic profile, geophone offset is the horizontal distance between the source and
the wellhead or the surface projection of the geophone in the case of a deviated well. Offset
between seismic source and receiver creates a delay, or moveout, in the arrival time of
a reflection that can be corrected before stacking and can be used to determine velocity
(Schlumberger Glossary).

Source Line: A collection of source points within the seismic geometry, often in a
linear arrangement.

Receiver Line: Similar to a Source Line but with the geophones arranged in a linear fashion,
typically on the same line a source line as well as offset between two source lines.

Channel: a collection of traces, defined by acquisition parameters, that make up a source or
receiver line.

Trace: the actual recorded seismic impedance change data as a function of velocity and
density contrast.

First Arrival: The first response that a geophone (receiver) picks up as the reflection from
an impedance change.

RMS Velocity: Root Mean Squared Velocity calculated from the first arrival to the first
reflector, giving interval velocity for near surface.

Gather: a collection of seismic traces which share some common geometric attribute. There exist many different kinds that give different results for interpretation of attributes.
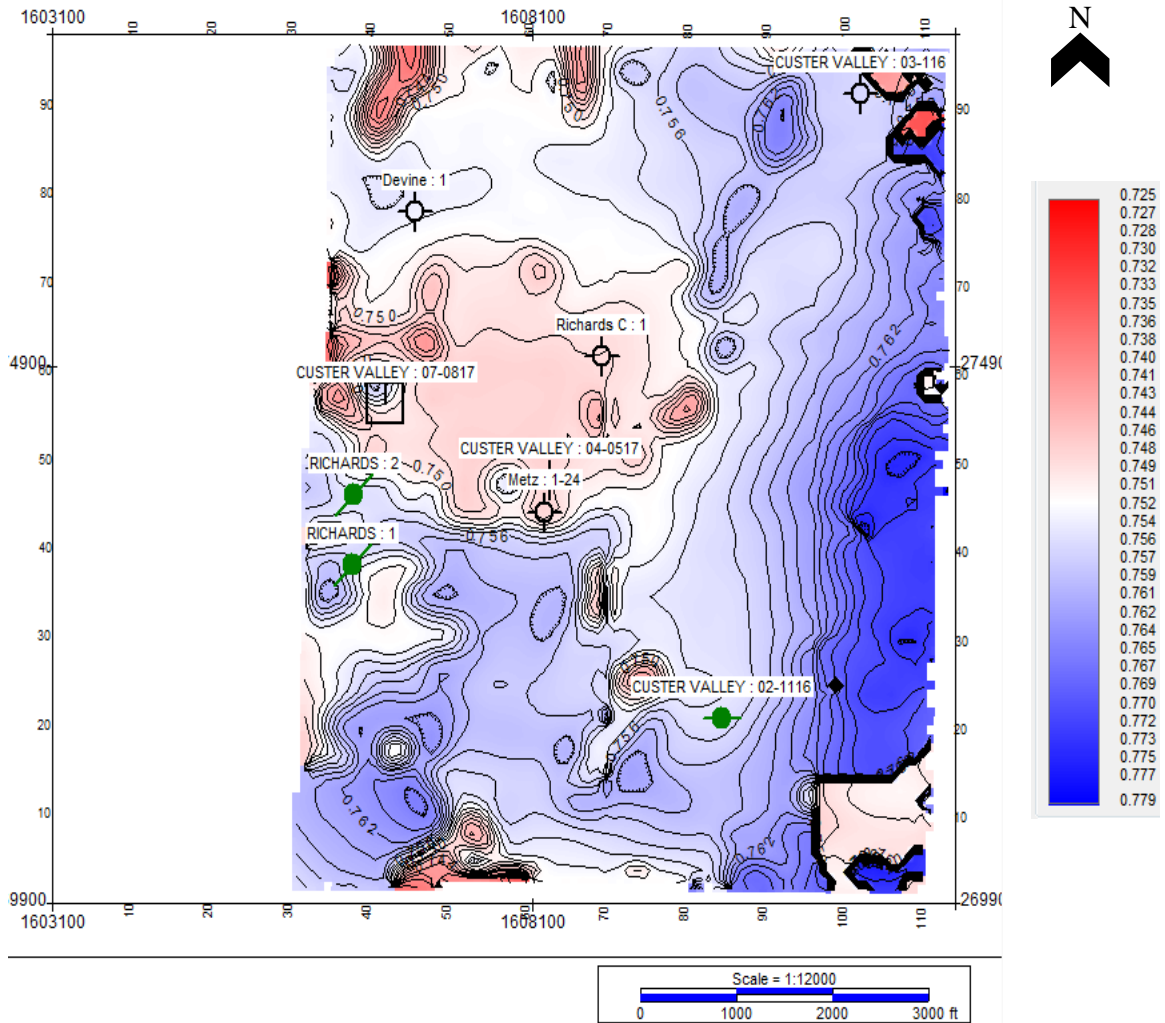
Figure 1 Amplitude attribute time slice as it pertains to structure in the subsurface. The red color correlates to the structural high seen in Figure 2. The structure mirrors the subsurface which is an indicator of poor static corrections.
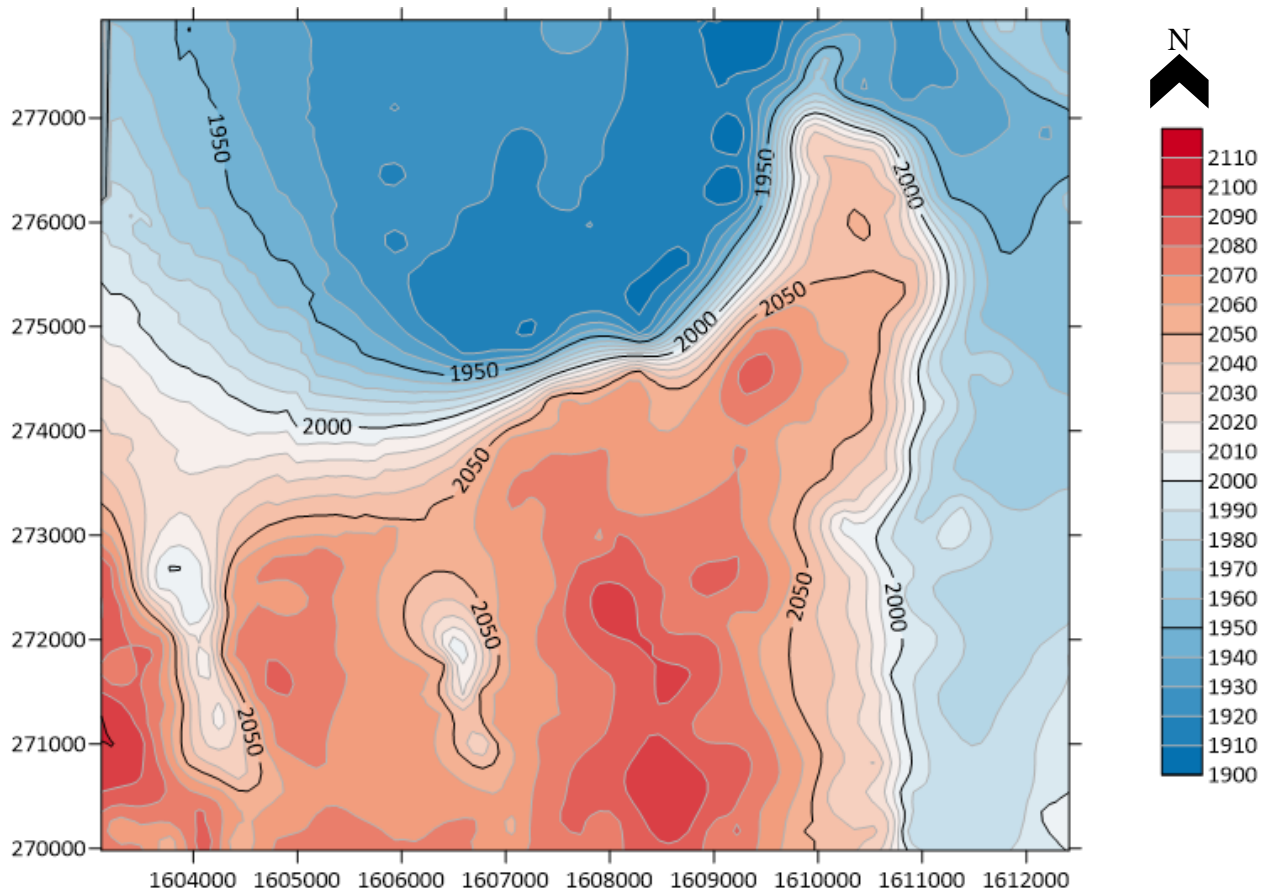
Figure 2 The study area in topography and it is important to note that overlain on top of Figure 1, the topography and subsurface structure are the same, this should not be the case. For this reason, further analysis of the seismic datum must take place.
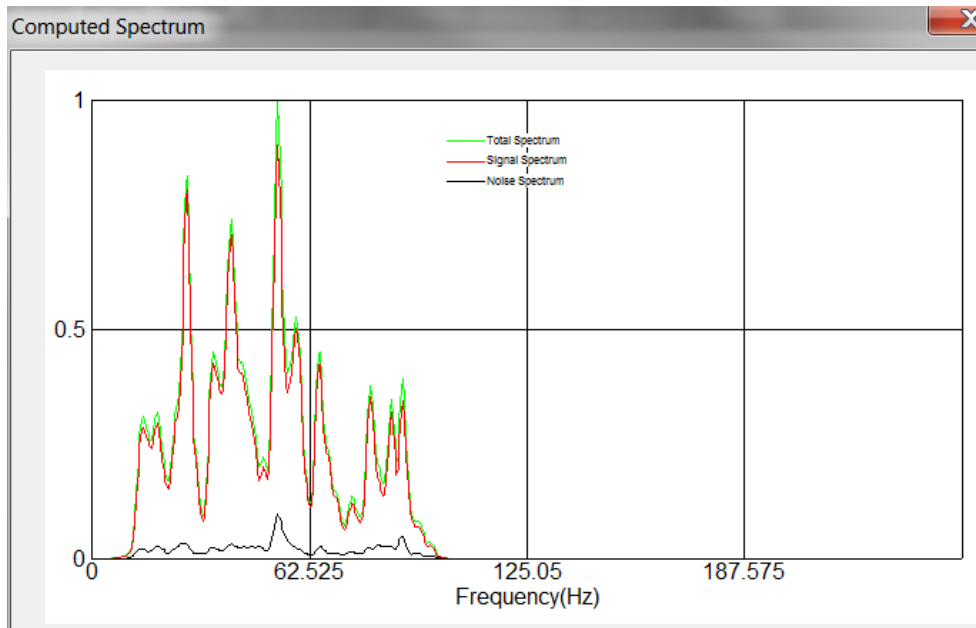
Figure 3 Usable frequency bandwidth from the previously shot seismic survey. Ranges from 10 to 80 Hz with missing frequency amplitude within the spectrum. This can be fixed with reprocessing and datum correction and is conceptualized in Figure 4.
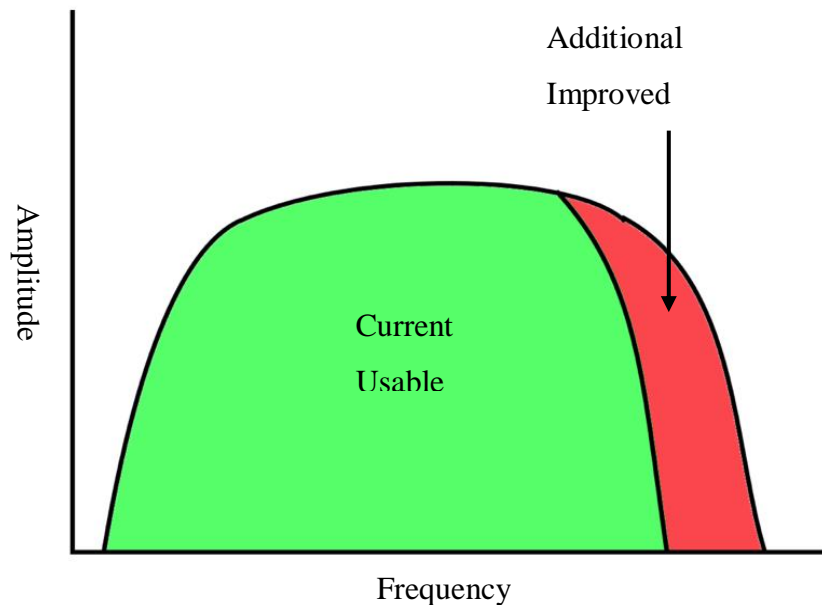
Figure 4 An idealized scenario of x where the higher frequencies are increased, and the amplitude or power is increased for higher signal to noise ratio. This concept is crucial to understanding the improvement of seismic data.

The seismic processing workflow is pertinent in the generation of a useable and accurate 3-Dimensional seismic volumes. For the purposes of this thesis project, data was provided in pre-stack and post-stack form, with the intention of reprocessing the pre-stack data using a different workflow to help elucidate better results. A sample seismic processing workflow has many steps and the ones used are listed as such: (1) Data Initialization, (2) Assigning Correct Geometry, (3) Amplitude Processing, (4) Noise Attenuation, (5) Deconvolution, (6) Multiple Attenuation, (7) Velocity Analysis and Normal Move Out (NMO), (8) Migration, and (9) Stacking. However, many problems can be encountered in any of the steps listed above, and for this dataset, as it was attained from the acquisition and processing companies, it was noticed that the data was incomplete in regard to the spatial geometric data as well as to the parameters and headers presented in the load sheet.

The seismic processing workflow proposed by many sources and processors around the industry agree that the workflow illustrated in Figure 5 is commonly used. However, this thesis finds that this workflow is lacking regarding accuracy and redundancy to validate that the data is correct in all its aspects. This thesis will discuss further the aspects of iterative quality control for major steps within the processing workflow. It will also discuss the problems that plague data processing and why iterative QC is vitally important ensure an accurate completed dataset.
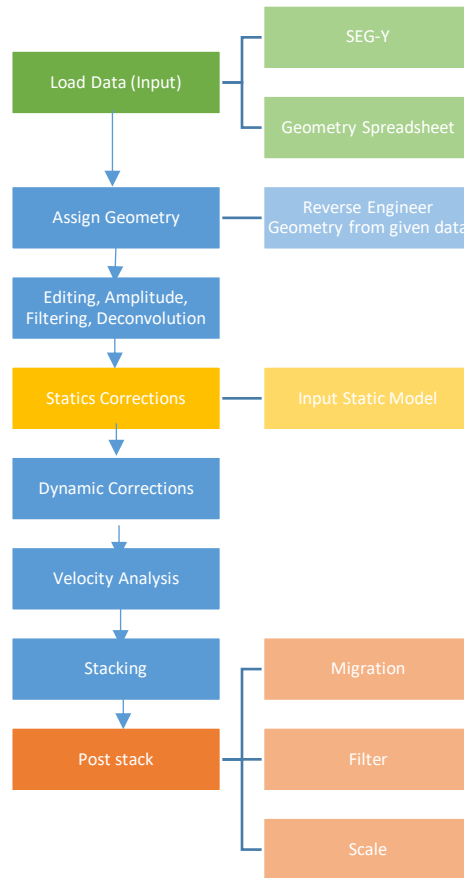
Figure 5 The general seismic workflow used on pre-stack data by most geophysicist and processors in order to generate accurate data. For the purpose of this thesis, many of the steps in this workflow will contain additional QC steps to validate processing iterations and interpretations.

Data Geometry

In seismic data processing, the multitude of traces are loosely organized based on the assigned headers that are written to each individual seismic trace during data acquisition, these can be anything from Individual Trace Number, Field File Identification Number, or Source Number. Native data is much more complicated than simply assigning a header, or "tag", to a dataset because when factoring in topographic variance, irregular source and receiver locations, and curving ray paths, the ideal model get somewhat convoluted based on these variables. These headers are important in assigning values to the geometry spreadsheet as they help correlate the latitude and longitude, or X and Y, as well as the elevation, Z, data. According to Yilmaz (2001),

the step in the seismic processing workflow that is most susceptible to error is the defining of the geometry for the survey and merging this geometry with the seismic data. This error, as Yilmaz explains, is human error which means that within all the pre-stack data as it is native, the largest source of inaccuracy will be geometry. The importance of recognizing this source of error lies in the fact that geometry is often the most overlooked step in seismic processing, as it is often assumed that the geometry is correct when it is supplied to the seismic processor. The result of improper assignment can be seen in Figure 6 where the traces are paced improperly within the geometry. In Figure 6c we can see that the velocity semblance spectrum has ambiguous peaks that cause failure in the normal-moveout correction to flatten the primary reflection events in the data (Thomas 1963). These errors are due to improper geometry placement and the examples listed below are the varying effects of improper geometry and how severe these may be. An ideal scenario would have the data appear as the first example (a) wherein the discrepancy between approximation and moveout it minimum.
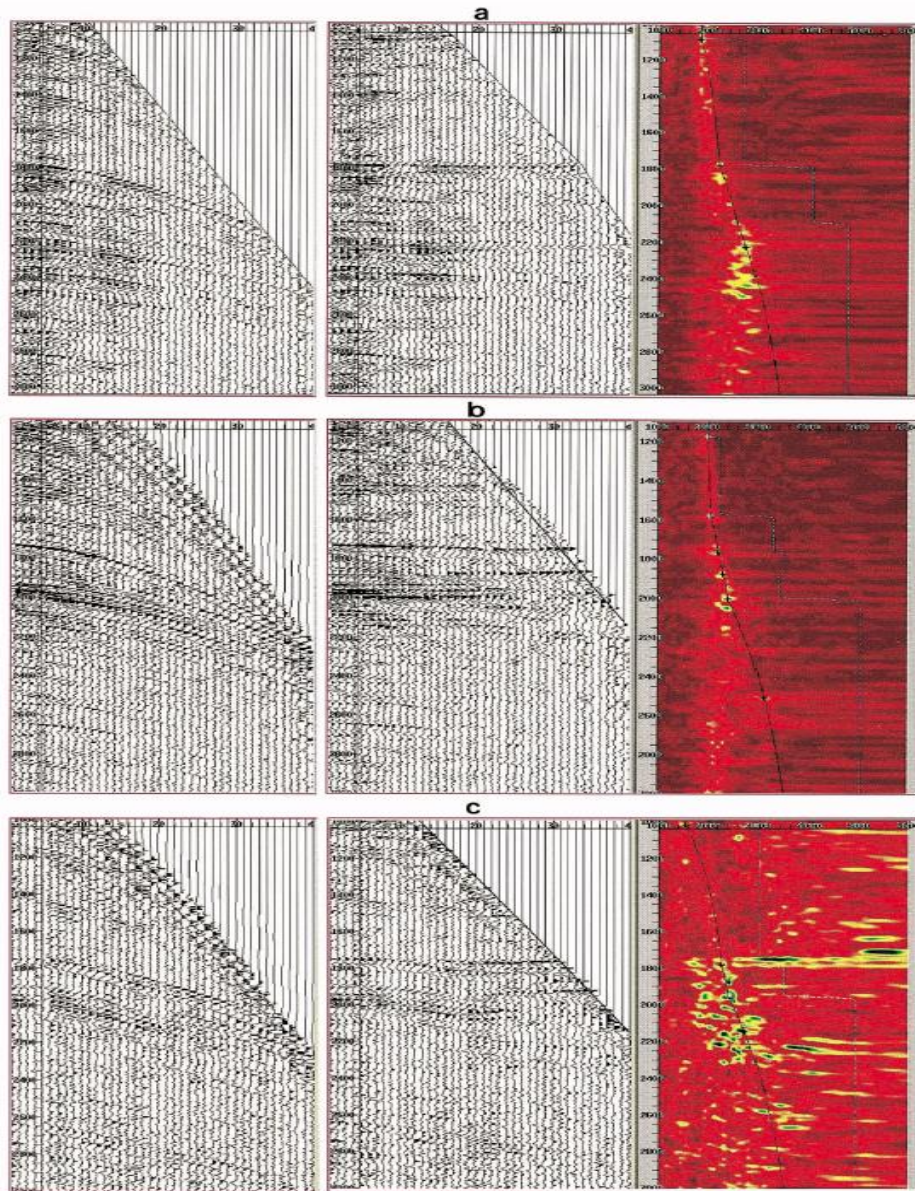
Figure 6 This figure, borrowed from Yilmaz (2001) illustrates the effect of improper geometry assignment within seismic data in 3 different locations along a seismic traverse. In Figure (a) there appears to be no abnormal moveout correction or velocity function trend. Figure (b) illustrates some minor moveout abnormality with offset, with no noticeable aberrant velocity function. Figure (c) illustrates the most parabolic moveout disparity as well as almost a chaotic velocity spectra and velocity function. (Yilmaz 2001).

Seismic data geometry is often set up in terms of source and receiver lines, and for the purpose of this thesis and the program used to process the seismic data, they may be referred to as S_LINE and R_LINE respectively. The importance of understanding the source and receiver

lines is dictated in the number of channels, or traces, within each. There exists a hierarchical scheme to geometry as sources are situated into source lines and receiver lines respectively. Within the data geometry, the FFID's that corresponded to each source, or source number, had a certain number of active receiver lines for any given source. Within these source lines, or cables, there are a certain number of channels. The hierarchical representation of how the data is arranged is seen in the graphic below (Figure 7). For the superset of the geometry to be correct and accurate, there must exist a coherent pattern where all the sources in numerical order must have the correct number of source lines active and the correct number of active channels within each source line. For example, within each source line if there are 40 channels active within the native data, there must be 40 channels active within the associated geometry spreadsheet so that there is no discrepancy. If there is a discrepancy between the number of channels active within the native data and the geometry spreadsheet, then this will cause errors in the way that the X and Y data is assigned to each individual channel. If there is a source line, or unique cable that is active with 56 channels within the spreadsheet but the native data shows that there are only 40 channels for that unique cable, then the extra 16 channels associated with the cable will be taken from the next numerical cable and associated in X and Y space with the first cable and not the second. It can be seen through previous explanation that the native data and the geometry spreadsheet rely heavily on hierarchical patterning and if any of the associated headers, or sorting keys, are awry then the data itself will exhibit flaws regarding the actual spatial positioning of wiggle traces, or channels.
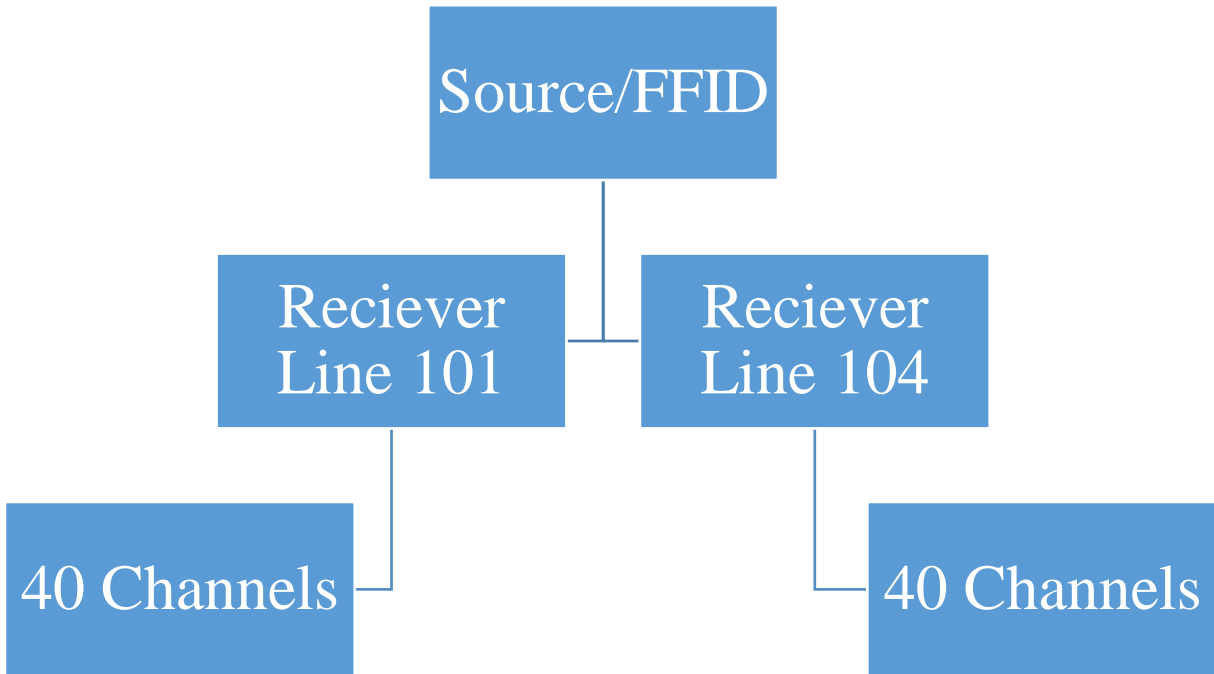
Figure 7 This illustrates the hierarchy of sources, receivers, and channels within the seismic data geometry wherein reverse engineering of the poorly organized data must take place to create a proper acquisition geometry for reprocessing and seismic datum creation.

For the geometry to be placed properly in 3 Dimensional space, there needs to be at least two headers assigned to the data during acquisition that match the data in the geometry load-sheet, otherwise there will be problems correctly spacing the traces, sources, and receivers in 3-Dimensional space, seen in Table 1. This process can be seen as an analogous to triangulating a point in GPS wherein the location can be derived on three radii intersecting at a point, and in the case of the seismic data headers, there needs to be at least two matching header fields within the geometry spreadsheet, seen in Table 1, for the wiggle traces and shot-receiver points to be correctly located in three dimensional space.

TRACENO	SOURCE	RECNO	CHAN	FFID	S_LINE	SOU_X	SOU_Y	R_LINE	REC_Y	REC_ELEV	OFFSET	CDP_X
1	343	1001	1	1	122	1607265.70000	273474.50000	101	269955.10000	2074.39990	5378.12451	1605232.35000
2	343	1002	2	1	122	1607265.70000	273474.50000	101	269954.60000	2067.39990	5254.13525	1605315.30000
3	343	1003	3	1	122	1607265.70000	273474.50000	101	269949.10000	2072.39990	5139.29053	1605395.95000
4	343	1004	4	1	122	1607265.70000	273474.50000	101	269951.80000	2047.69995	5018.46924	1605478.55000
5	343	1005	5	1	122	1607265.70000	273474.50000	101	269951.80000	2066.19995	4899.81689	1605562.85000
6	343	1006	6	1	122	1607265.70000	273474.50000	101	269948.90000	2089.80005	4790.56348	1605644.00000
7	343	1007	7	1	122	1607265.70000	273474.50000	101	269947.50000	2070.00000	4680.69336	1605727.10000
8	343	1008	8	1	122	1607265.70000	273474.50000	101	269947.40000	2052.39990	4575.51367	1605808.40000
9	343	1009	9	1	122	1607265.70000	273474.50000	101	269945.90000	2060.39990	4470.45264	1605893.30000
10	343	1010	10	1	122	1607265.70000	273474.50000	101	269943.60000	2071.80005	4374.12256	1605974.80000
11	343	1011	11	1	122	1607265.70000	273474.50000	101	270065.10000	2070.50000	4180.43701	1606056.15000
12	343	1012	12	1	122	1607265.70000	273474.50000	101	270089.00000	2064.80005	4060.50806	1606144.75000
13	343	1013	13	1	122	1607265.70000	273474.50000	101	270107.20000	2072.80005	3962.39087	1606221.45000
14	343	1014	14	1	122	1607265.70000	273474.50000	101	270122.40000	2075.19995	3865.41455	1606303.30000
15	343	1015	15	1	122	1607265.70000	273474.50000	101	270141.70000	2073.00000	3768.73926	1606385.95000
16	343	1016	16	1	122	1607265.70000	273474.50000	101	270223.70000	2070.00000	3619.82324	1606469.55000
17	343	1017	17	1	122	1607265.70000	273474.50000	101	270224.30000	2074.69995	3549.14355	1606552.85000
18	343	1018	18	1	122	1607265.70000	273474.50000	101	270240.90000	2068.69995	3470.84912	1606635.10000
19	343	1019	19	1	122	1607265.70000	273474.50000	101	270237.40000	2063.19995	3418.21606	1606716.75000

Table 1 Values directly from the geometry spreadsheet as they appear in the seismic dataset. The headers are in the top row, shaded in grey. Some of these headers were assigned when the data was recorded, such as trace number (TRACENO), and source line (S_LINE). However other headers had to be generated by the author to create matching fields such as source number (SOURCE) and Channel (CHAN) in order to create accurate geometry.

Without knowing the proper Common Depth Point, or CDP, as well as the Source Line enumeration, there will be no way to place shots and gathers correctly in space. If the data is not correctly spatially located, the traces will not sequence correctly and when trying to stack the data because as the software reads the traces and combines them into cables and enumerates them as source and receiver lines, traces for other shots and receivers will be incorrectly placed within gathers they do not belong to. This misplacement provides side-effects seen in the data such as aberrant offset which will interfere with gathering and binning of the data further into processing. The processing workflow, aside from loading the initial SEG-y data is dependent on a corrected geometry model, without a corrected geometry, performing complex analysis of amplitude or velocity, the generated model will not be true to the subsurface conditions and render the data useless.

Seismic data within a 2D frame, wiggle traces or the seismic amplitude and frequency content of a line, are placed sequentially on an increasing axis of known distance and time

(Figure 8). When the geometry is incorrect and traces are misplaced, then the amplitude and frequency of the data will be incorrect and the subsequent seismic processing steps in the workflow will be affected substantially. A comparison of the same dataset at different geometric representations can be analyzed to properly grasp the importance of proper trace representation and how geometry affects properties such as offset, this can be seen in Figure 8 and Figure 9.

Figure 8 Within this example, as Source Number and Channel increase from left to right, it can be seen that however there is some consistency to the placement of the wiggle traces in the geometry, when checking quality control of the Offset, we can see that it does not reflect the semi-parabolic shape that is desired for correct offset geometry, as seen below, in 14.
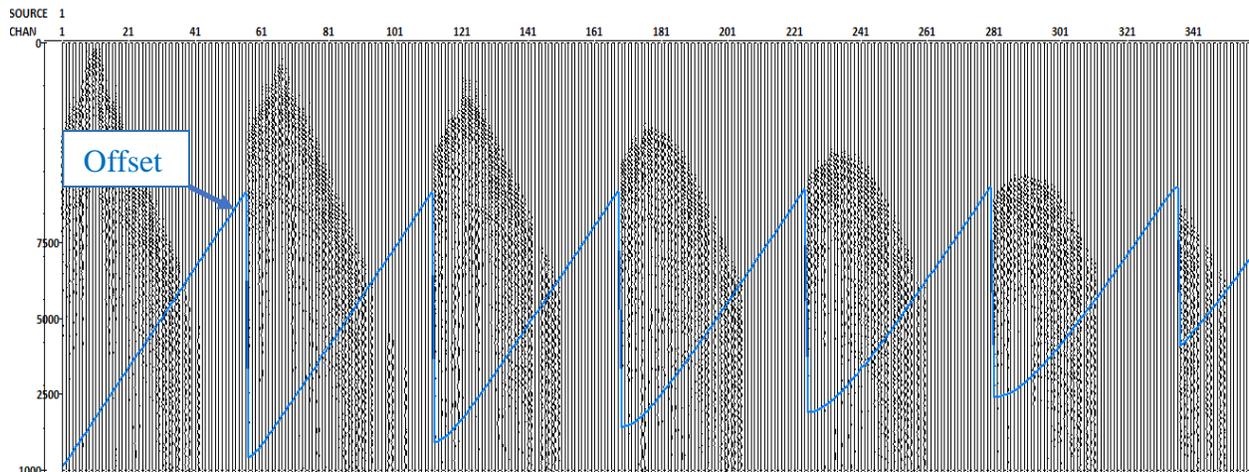
Figure 9 As Source Number and Channel increase with left to right within the survey, the correct wiggle traces are placed within the geometry, allowing for the correct amplitude and frequency data to be presented. This can be quality controlled by analyzing the absolute offset within the windowed data. The offset calculated from the geometry, shown in blue, is representative of corrected data.

Corrections

Within the realm of seismic processing, after an accurate seismic geometry has been formulated and quality controlled for accuracy, statics corrections are then applied to ensure that the spatial relation of the reflectors is accurate within the seismic section. Statics corrections are corrections that are applied to seismic data to compensate for the effects of petrophysics in the near surface that may interfere with the accuracy of reflection placement (Frei et al. 2015). These effects include variations in elevation (the more relief, the more severe the effect), the near-surface low-velocity layer (LVL) and its thickness, and the reference to the selected seismic datum. The key objective for this step is to adjust the seismic data so that it appears as if all reflection arrival times were observed on a flat plane with no low-velocity layer present (Rogers 1981). The figures below indicate the seismic survey experiment as well as what data appears as before statics corrections and after. The figure illustrates the seismic experiment as a common midpoint gather, CMP gather, where the sources are denoted S_1, S_2, S_3, with increasing offset

16

away from the midpoint. R_1, R_3, R_5 are the receiver as they increase in offset away from the

midpoint with their associated height h as a function of thickness of the topography to the

seismic datum. In panels (b) and (c) of this figure the reflectors are positioned as they would be

if no correction were applied and with one applied, respectively. It is important to note the time

shift of the reflections from (b) to (c) as they are correctly placed within the time domain (Opara

and Ebeniro 2018).
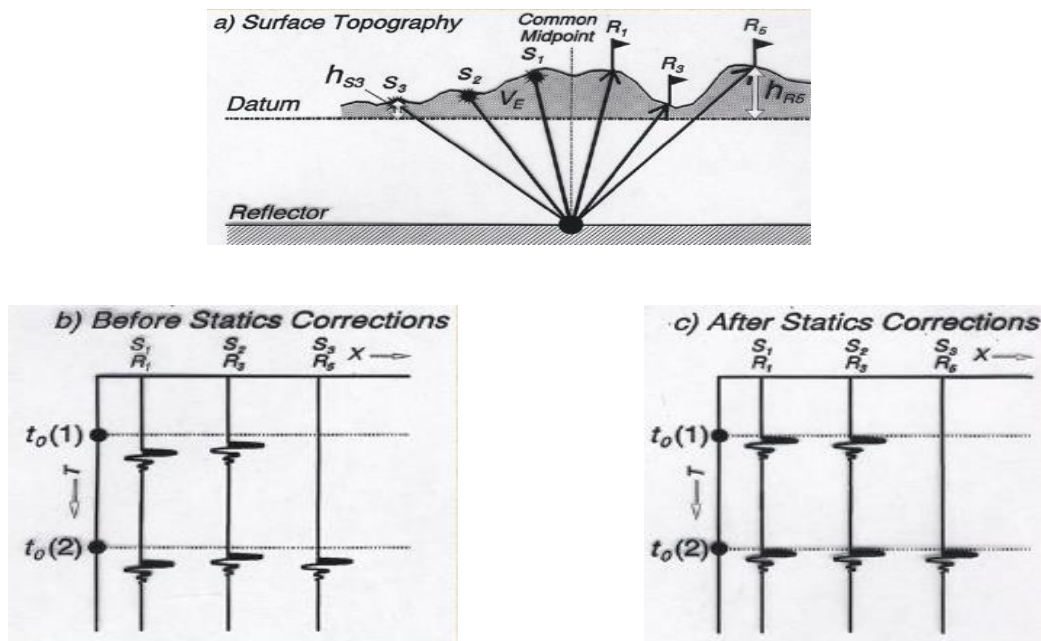
Figure 10 (a) illustrates the surface topography of the seismic survey using a CMP gather where the datum is defined below the near surface (b) illustrates the reflections before and (c) after statics corrections, where the seismic traces are flatter and do not have imprint of the surface topography (Adapted from Dr. Ali Osman Öncel, Professor of Geophysics (2009).

The near surface generally coincides with the area of substratum that is filled with air

rather than water, the reason for this is that as a seismic wavefront propagates through this

medium, the air within the pore space attenuates the waveform far more than a liquid. For this

reason, as well as many others that will be covered, the area known as the low-velocity layer, or

LVL, must be thoroughly understood before dynamic corrections can be made. It is important to

understand the change in velocity between the base of the weathered layer and the first reflector because, as Snell's law indicates, there is a subsequent refracted ray path angle. To mitigate this affect, the statics correction experiment implies in a shot and gather, there is an identical shot and receiver point in the subsurface vertically beneath the original shot and receiver points. This suggests that the datum below the base of the weathering layer, which is established by the seismic processor, would then be the established top of the seismic data where all subsequent reflectors would be positioned thereafter. This simple approach works well in most areas, however as is the case with most of processing, certain steps must be taken to minimize errors introduced as a result of this simplified approach (Cox 1999). The key features that are analyzed when computing a static correction are: surface elevation, the base of the weathered layer, and the velocities below the weathered layer (Cox 1999). This approach may seem oversimplified but within each of these characteristics are many subcategories and variables that must be considered to properly grasp the scope of the experiment. For example, in many areas in Ellis County, the topography and profile of the near surface changes rapidly in the lateral direction and based on the given parameters for calculating the static corrections for seismic data, this poses a problem. To understand the profile of the near surface in seismic terms, some of the seismic properties must be analyzed; namely velocity. Goupillaud (1961) stressed the idea that near velocities must be understood to properly grasp the lower velocities in a statement:

> *We conclude by stressing again the importance of near-surface velocity information,*
> *so rarely available with our present techniques, hoping that, when this information*
> *is properly used, the efficiency of the seismic method will be increased sufficiently to*
> *make it applicable to a new range of exploration problems.*

It is the writer's opinion that this excerpt summarized the importance of the near surface and associated velocities quite concisely, while this was stated in 1961 when the seismic method was

somewhat in its infancy, the sentiment is applicable today, when certainty in the quality and validity of seismic data must be high.

Analysis

It can then be stated that the velocity of the near surface may have one of the principal impacts on the static correction, and therefore the velocities that can be derived from any data about that area will be of import. This chapter will explore the velocity analysis gained from the native data as it will give sufficient data for calculating the character of the near surface and LVL (Sheriff and Geldart 1995). More specifically, this seismic workflow will look to elucidate this data from the first arrivals associated with the native data. The purpose of looking to the native data for the information about the near surface velocity lies in that it simply comes as a part of the data already collected. It may be more effective for the static model to resample the survey area with the specific purpose of collecting the first arrivals and refracted waves previously discussed, however within the realm of the oil and gas industry, this method may not be the most cost and time efficient (Opara and Ebeniro 2018). Therefore, it is the author's impression that looking to the original seismic data and deriving the first arrivals from that data set prove to be the most effective way of establishing the seismic static model.

First arrivals are characterized as the earliest arrival of energy propagated from the energy source at the surface to the geophone as the first indication of seismic energy on a seismic trace. On land, the first break is commonly associated with the base of the weathering and is used for establishing static corrections, defined by Schlumberger. In ideal cases, the data that would generally be used to calculate the velocity profile of the near surface would be check shots along the well bore, as they are more accurate in the depth domain, however this method is limited to

19

the wireline operator and is not done in most cases, especially in older wells and those with limited budget. Refraction data is often looked at as a supplementary method to improve the accuracy of the check shot velocities but as previously stated, it is often more time and cost effective if the seismic gather is already completed and there is no supplementary data present. For the purposes of this study and given what data is available, the refraction method will be used. Therefore, the data that will be analyzed is: reflection data, refraction data, and numerical interpolation. Another data input can be considered in this case, geological data, if it is available from a suite of well logs, which is unavailable for this thesis. However, refraction data will be the primary data input that will be analyzed and interpolated because of the redundancy of refraction data within the dataset. This data will provide information about the subsurface ranging from the topographic surface layer down to the refracting surface and give a velocity profile therein. However, a seismic refraction survey is often limited to the number of refractors that can be imaged because each refractor requires, for optimum definition, the recording of data from a range of different offsets (Cox 1999). This leads to another issue associated with this type of static model build, even though there are discrete locations associated with each trace, there exists a duality of quality; the choice between a smooth near-surface velocity profile and an irregular depth profile, or a smooth depth profile and an irregular depth profile.

The velocity data for the static corrections and the normal moveout is gathered from the hyperbolic approximation of the first and second reflector and then associated with the interactive velocity analysis semblance spectrum to guide the picking (Li et al. 2011). To assemble the velocities for picking, the data must be super gathered from the original data file so that they are in common depth point gather, or CDP gather. After the seismic data has been assigned its proper geometry and everything has been QC'd for accuracy, as was done in the

20

previous steps, the next step is to assign a binning geometry based on parameters that were

assigned to the geometry in headers and calculate what is known as common depth point, or

CDP, in the x and y direction. This process is done as a fucntion of the headers that were

assigned. To achieve this, the offset of the points must be taken into account. For the offset

calculation the fucntion must be used:

$$OFFSET = sqrt(sqr([SOU\_X] - [REC\_X]) + sqr([SOU\_Y] - [REC\_Y]))$$

Equation 1 The offset equation takes into account the source x and source y as well as the receiver x and receiver y, squares the difference of the x and y in both headers, sums that value and takes the square root of that sum.

Thereafter, another set of equations must be used to calculate the common depth point of

the x and y coordinates of te source and reciever in the equations:

$$CDP\_Y = ([SOU\_Y] + [REC\_Y])/2$$

$$CDP\_X = ([SOU\_X] + [REC\_X])/2$$

$$CDP = trunc([CDP\_X]/100.0)$$

Equation 2 This series of equations are used to calculate the common depth point, CDP, of the points taken from the geometry headers, for it is necessary to know the CDP_X and CDP_Y and truncated CDP in order to establish accurate binning geometry, as this is the primary filter.

For binning the geometry, the maximum distribution of common depth points is

desired within each bin while keeping the amount of redundantly used CDP's per bin to a

minimum. It is often typical for a processor to use the cell dimensions as half of the receiver

group spacing in the inline direction, in the case of this geometry the distance is approximately

100 feet. When the CMP's are placed into bins, what results is called a common cell gather,

where the number of gathers within a bin dictate the amount of fold in the geometry. It is

important to note that maximum fold allows for the highest consistency within the binned data as

the signal that is compounded and averaged often filters out aberrant traces within itself.

However, while trying to maximize the fold of the bin, there may arise irregularities in the gridding geometry. In real world application there is often irregularity in the way that seismic is shot because of local topographic constraints, and therefore there is often a nonhomogeneous distribution of the CDP gathers. Therefore, it is often important to QC the data and assign individual bins within the grid different values. This can be done by shifting or translating the geometry grid in different ways. This process is known as flexible binning, as it seeks to optimize the CDP distribution in order to maximize the fold within the data. The optimal distribution for this data was calculated using the distance between the receiver points at approximately 165 feet on average. This gives a value of 82 feet as the bin length and width, or 82'x82'. However, after applying a correctly sized grid, a rotation and translation must be applied to the binning geometry to avoid what is called acquisition footprint. Acquisition footprint comes from inadequate sampling geometry and irregular azimuth distribution, which can be mitigated by the rotation and translation.

Attributes and Interpretation

Seismic interpretation is the actual evaluation of a post-stack 3-dimensional cube viewed in voxel format. This is often the final product that is achieved by all of the aforementioned seismic processing steps and is considered the final product given to exploration geologists and geophysicists. Seismic interpretation can only take place when both static and dynamic corrections have taken place and the dataset has gone through the seismic processing workflow with proper iterative quality control analysis. Many consider the seismic interpretation the most important step in the life of seismic data, however the finished product cannot be attained without proper construction by the seismic processor. The basic petrophysical properties seen in

the 3D seismic cube are directly derived from the pre-stack data and its inherent accuracy. For instance, many of the seismic attributes that are used by interpretation software is directly dependent on the accuracy of frequency, velocity and amplitude data in the seismic cube. As this thesis does not directly pertain to the interpretation of seismic data, the nuances of interpretation with be limited in definition for the sake of brevity. However, this thesis will include a sample of attributes that a seismic data interpreter might find useful for analyzing structure, stratigraphy and petrophysical properties, and ones that were used on the final product of the dataset pertaining to this thesis, for comparing the results gleaned from the seismic processing workflow. Some seismic attributes that allow for an increased chance of finding oil are as follows; Amplitude, Minimum and Maximum Curvature, Spectral Decomposition, and Coherence.

<u>Amplitude:</u> considered one of the more basic but important of the seismic attributes used for analysis, amplitude is the expression of seismic impedance and velocity as a wavelet passes through a given media. Seismic amplitude is often the format in which 3D data is expressed naturally in data, either as wiggle traces or as dual gradational color scheme as to help elucidate polarity of the expressed seismic impedance, positive (+) or negative (-). As a wavelet travels through the earth and encounters media of different density, the wavelet velocity is directly impacted and thus the signature of the wavelet is recorded as a change. This allows interpretive geologists to discern things such as change in lithology and structure (Brown 2011).

<u>Curvature:</u> a derivative of dip and azimuth and therefore a second derivative of structure, it is evident that this seismic attribute will allow for structural interpretation. Curvature helps identify flexures in structure (Brown 2011).

Spectral Decomposition: a seismic attribute that decomposes a section of seismic data with normal frequency bandwidth into a set of equivalent sections each with a very narrow bandwidth. The basic concept behind this attribute is that a reflection from a thin bed has a characteristic expression in the frequency domain that is indicative of bed thickness. It is useful for bed thickness below tuning thickness, and in the case of Kansas geology, this may be very common (Brown 2011).

Coherence: a time derived attribute that aims to convert a volume of continuity into a volume of discontinuity (the faults and other boundaries). This attribute operates in the time domain and uses a variety of mathematical approaches. The importance of this attribute is that it is derived directly from the processed data and is free of interpretive bias in contrast to horizon attributes such as Curvature. This attribute is especially useful when interpreting faults (Brown 2011).

Within this chapter, many of the results will be presented as formation top maps within seismic two-way-time (TWT). The purpose of this is to compare the effects of the seismic workflow developed for pre-stack data in comparison to the data and maps there supplied by the original processing and interpretation companies. As previously mentioned, the 3D interpretation of seismic data is closely related to the final product in terms of prospection or hydrocarbons, and as such the similarities and differences seen between the two datasets will allow one to see the overall effect of this workflow on what an exploration and production company would realistically base drilling on.

The Stone Corral is the formation on which the interpretation and comparison will be made. We will compare the previous interpretation supplied by the last interpreter to the interpretation made by the author based on the seismic workflow proposed. The interpretation will be made in two-way time (TWT) as well as the depth domain as the depth domain can be

tied to well reports and reflects the accuracy of normal moveout and statics corrections. It can be seen in Figure 53and Figure 54 that the maps are TWT and depth domain and the Stone Corral lies at around 305 milliseconds and 1147 ft depth. In the pre-stack data interpreted by the author, the Stone Corral existed at an average depth of around 400 milliseconds in TWT depending on the local variation. Also, the Stone Corral is picked at 1147 feet in depth, but it is known from drilling reports in the area that the Stone Corral sits at around 1410-1420 feet in the subsurface. Even before looking at a reinterpreted section of the Stone Corral, based on the evidence provided by well control, the previously interpreted section is indeed incorrect. Whether or not this is due to misinterpretation of the actual Stone Corral reflector or the incorrect application of velocity and static modeling will be explained in the hitherto section.

Chapter 3 - Field Location and History

ocation

The field location sits within Ellis County (Figure 11) wich is relatively flat but feeder channels cutting across stratigrpahy as well as quaternary alluvium have created a topogrpahy that is unlike the rest of the area (Figure 12). There is importaqnce in this, that the seimic datum in this area used a model assuming the topogrpahy was flat, where that is not the case and there were not adequate statics corrections. The lcoation of the field allows us to focus on the importance of qulaity statics corretions.
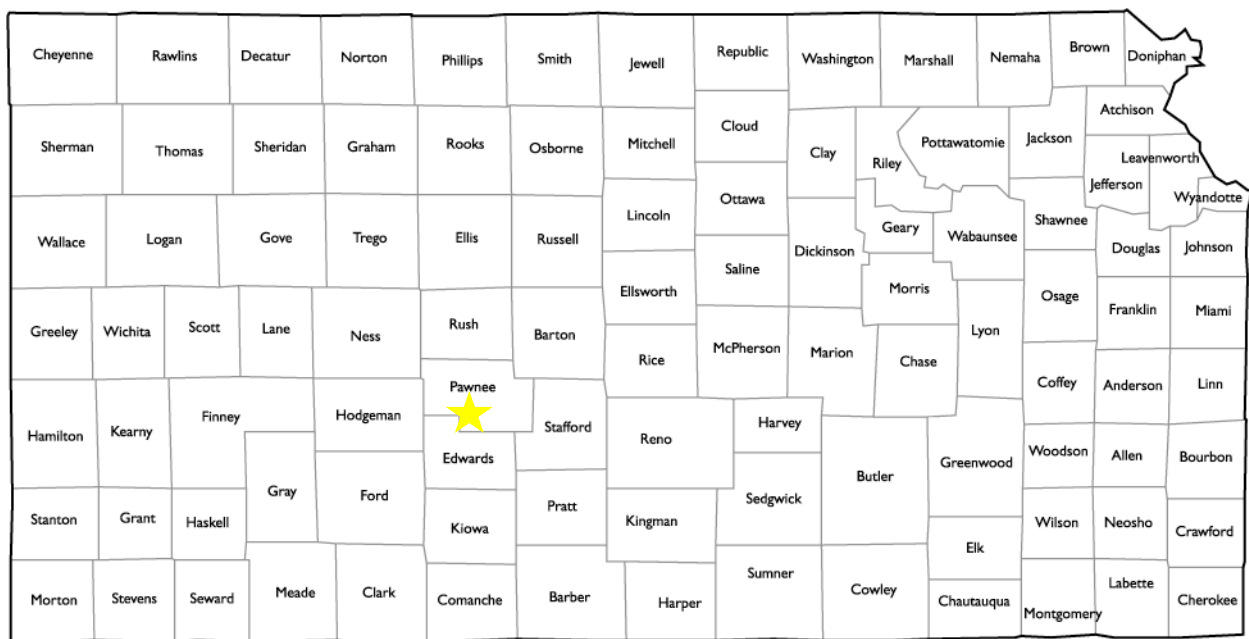
Figure 11 Location of Ellis County within Kansas as well as the field of study within Ellis County, denoted by red box and yellow star, respectively. (Map provided by Kansas Historical Society).
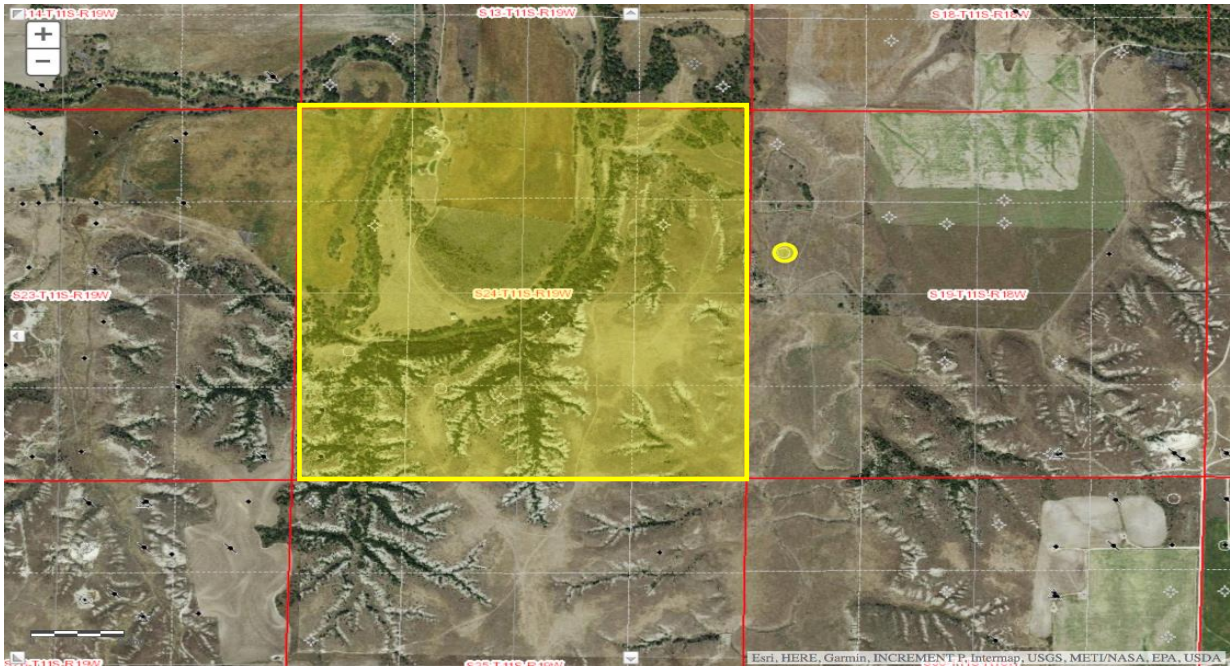
Figure 12 Topography of the field location in Ellis County. Important to note the topographic highs in the North West corner (map provided by Kansas Geologic Survey).

The proposed field is an offset wildcat location located between two proven fields, the Riverview and the Solomon to the East and West, respectively. The target formation proposed by the Intent to Drill report is the Arbuckle formation. Therefore, there is no production data from this new field, however there were a set of wells drilled in the area that had a suite of well logs run for them. With regards to the production in the area, some wells have cumulatively produced into the hundreds of thousands of barrels individually and in some areas, bringing the total of the field into the millions of barrels (Kansas Geologic Society). This would suggest that the wildcat field between the Riverview and Solomon fields has potential to yield productive wells. However, as previously mentioned, the wells that were drilled either missed productive zones or had such insignificant shows that they were plugged and abandoned due to financial infeasibility.

27

The area in which this new field sits shows signs of potential, and given the proper attention in seismic detail, this field shows signs of potential production.

aphy and Stratigraphy

Situated upon the Central Kansas Uplift, which separates the Hugoton Embayment of the Anadarko Basin on the West from the Salina and Sedgewick Basins on the east, the geology of the area is denoted with complex folding and faulting within the subsurface. The relation of Ellis County and its oil fields to the Central Kansas Uplift make it so that the target formations will be shallower in the subsurface to its correlative formations further west in the Hugoton Embayment. However, this does not detract from the availability of hydrocarbon accumulation within the area, specifically the accumulation of crude oil, as a trend of fields is seen across the majority of the Central Kansas Uplift, almost in its entirety (Figure 13).
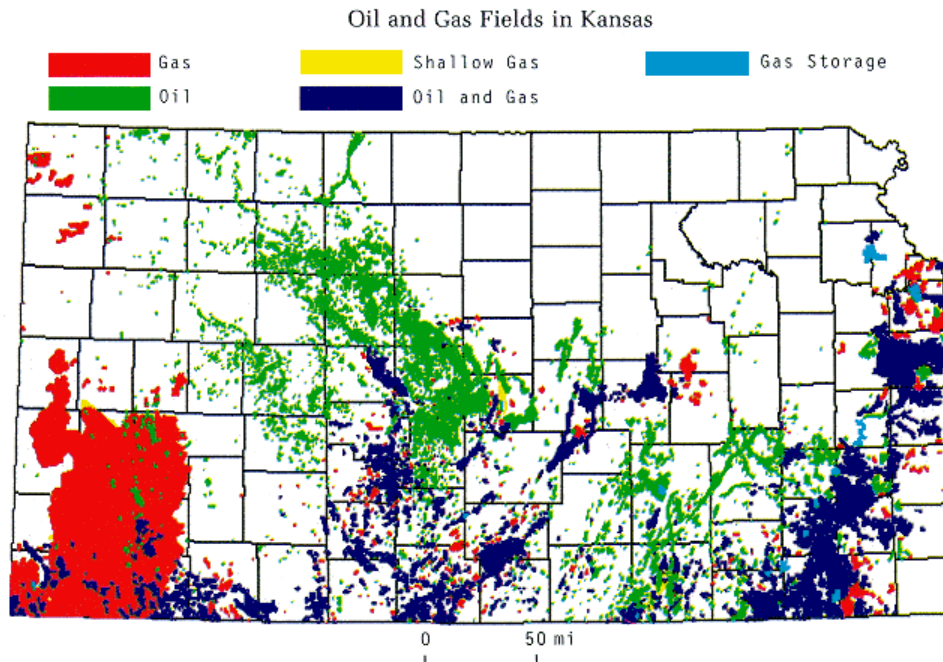
Figure 13 In the figure above, the respective hydrocarbon accumulations across Kansas, it can be seen that the majority of the strictly oil fields within east-central Kansas are located along the Central Kanas Uplift, with a high density of these fields situated within Ellis county and the surrounding area (map from United States Oil and Gas Historical Society).

28

The stratigraphy as well as the topography of the Ellis County region are integral in understanding the application of general 3D seismic data as well as shallow reflection seismic data (Zhang et al. 2016). The immediate topography of Ellis County is relatively flat and consists of upland benches that are deeply incised by drainage channels. The broad benches and their channels are controlled by the harder rocks that crop out to the surface, which include the Ogallala formation, the Fort Hays Limestone member of the Niobrara formation, and the Greenhorn limestone. These benches decrease in elevation from the Ogallala to Greenhorn respectively. All of these units are derived from the Mesozoic Era, specifically the Cretaceous System and are the primary weathered units in the area and cause the most distortion in the 3D seismic if they are not properly accounted for using shallow reflection to establish a seismic datum. The surficial units found in the area are primarily carbonaceous and weather accordingly. In most petroleum geology related studies, the focus is on the subsurface, specifically the target production zones, however to fully grasp the scope of the problems facing the seismic processing workflow, the near surface must be taken into account because the static correction survey is based almost explicitly in this area. This near surface area has experienced the least amount of compaction, is the most readily water saturated, and experiences the most weathering, all these factors contribute to the variability in petrophysical properties, which seismic data acquisition is invariably tied to.

Deeper below the shallow subsurface and subaerial rock, lithology known as the Absaroka Sequence, the Pennsylvanian through the Triassic contains many of the producing formations that are drilled in the Ellis County area. Most notably in this sequence is the Pennsylvanian aged Lansing-Kansas City groups, which account for a large portion of oil and gas production within all of Kansas, not limited to Ellis County. Upper Pennsylvanian lies directly atop the

Precambrian surface in local areas on the Central Kansas Uplift, after this deposition occurred, the entire region began subsiding, where the basins were falling at a much faster rate than the faulted uplifts, allowing for more accommodation space for the Absaroka Sequence in the flanks of the Central Kansas Uplift and into the basin areas. In conjunction with this subsidence came movement among the structures in the uplift causing variations in depositional patterns as well as complex structures that is reflected in the topography as well as subsurface imaging. This period of structural disorder, a product of collision between two continental plates, was complicated by cycles of sea level change due to glaciation pattern. These patterns caused sea levels to rise and fall repeatedly, where the shoreline would migrate several hundred miles transgressive and regressively with the accompanying depositional facies. These sedimentary units can be traced for thousands of square miles throughout the United States, however the import of the conjunction of this shoreline wandering with the complex folding and faulting of the Central Kansas Uplift has led to myriad structural and stratigraphic traps, at one time being one of the most densely drilled targets in North America. Where most of these drilling targets are looking for production in the Lansing-Kansas City (Baars et al 2001).

Ogallala Formation

The deposits in the Ogallala Formation accumulated as an apron of clastic sediments that were shed eastward by the Rocky Mountain Uplift and erosion. However due to the feeder conduits from the Rocky Mountains, little lateral north-south certainty exists in the homogeneity and similarity of the Ogallala formation as it trends north-south. Due to this uncertainty, it is proposed that each of the feeder channels has a unique erosional and depositional history (Chapin 2008). Each of the feeder channels has a specific lithofacies description warranting the names; Valentine, Ash Hollow, and Kimball Members all in ascending order.

Fort Hays Limestone

The Fort Hays Limestone is a massively bedded cream-colored chalk or chalky-limestone and is a member of the Niobrara formation, derived again from the Rocky Mountain uplift and erosion. The Fort Hays Limestone is permeated by bedding structures that range anywhere from 6 inches to 6 feet and average about 2.5 to 3 feet. These beds are separated by beds, 1 to 4 inches thick, of light gray to dark gray chalky gray shale. The bedding gets progressively thinner towards the top and weather to almost a pure white. The Fort Hays Limestone contains rounded, coarsely ribbed pelecypod shell fragments which are more prevalent in the harder bedded regions (Kansas Geologic Survey).

Greenhorn Formation

The Greenhorn Formation's four members are prevalent in Ellis County and amass to a thickness of approximately 100 feet. However, it does not account for much of the surficial exposure in Ellis County, primarily due to the steepness of its slopes. However, it is extensively exposed in the southern and southeastern portion of the county. In basal, the Lincoln Member is characterized by an abundance of skeletal grainstone and bentonite seams. Overlying that is the Hartland Member with little skeletal grainstone but contains 3 widely traceable, time-parallel, beds of burrow-mottled chalky limestone (Hattin 1975). The Hartland Member is overlain in central Kansas by the Jetmore Member which is characterized by 13 ledge-forming beds of chalky limestone that can be traced with confidence for hundreds of miles. Comprising the upper portion of the Greenhorn Formation is the Pfeifer Member which is best characterized by its content of concretionary beds of chalky limestone. Greenhorn carbonates are predominantly of

pelagic origin and were deposited on the broad, flat eastern region of the Western Interior region. The formation was deposited near the peak of and eastwardly directed marine transgression (Hattin 1975).

Lansing-Kansas City

The Lansing-Kansas City Groups are part of the Missourian Stage of the Upper Pennsylvanian and are composed of interbedded carbonates and shales with minor coals and sandstones. These are referred to as cyclothems. The carbonate units display a variety of depositional environments ranging from phylloid algae-bearing, lime mud banks to oolite shoals (Heckel, 1975; Mossler, 1973). The Lansing-Kansas City Limestones are described as thickening, merging, and becoming more massive from north to south toward the Anadarko Basin. However, the thickness is not as large as the soon to be mentioned Arbuckle Group and is seen to be under approximately 50 feet thickness in well log and core data. The Lansing-Kansas City is a known producing formation in the Ellis County area but due to its relatively small thickness, it is hard to see in seismic resolution.

Arbuckle Group

The Arbuckle is present in most of Kansas and is absent only in the areas of northeastern and northwestern Kansas, and over ancient uplifts buried Precambrian highs (Walters, 1946). The Arbuckle is also locally absent along the Nemaha Uplift, Cambridge Arch, and the Central Kansas Uplift due to pre-Pennsylvanian uplift. The Arbuckle rocks occur at depths of ranging from 500 feet to 7,000 feet from southeastern to southwestern Kansas respectively. The Arbuckle group is part of the craton-wide Sauk Sequence, which is bounded at its base and top by irregular unconformities seen in Figure 14 (Sloss, 1963). These irregular unconformities represent major regressions of the sea and erosion and subaerial exposure of vast area of the craton. The

Arbuckle Strata thickens from north to south as seen in Figure 15 (Franseen et al. 2003). The basal contact of the Arbuckle Group in Kansas is an unconformity on Precambrian rocks or Cambrian strata. The upper bound of the Arbuckle group is an unconformity as well and lies stratigraphically under the Simpson Formation, however in this field area the Lansing Group overlies the Arbuckle Group. The Arbuckle formation includes 4 formations listed as; the Cotter Dolomite, Jefferson City Dolomite, Roubioux Formation, Gasconade Formation, and the Eminence Dolomite (Franseen et al. 2003).
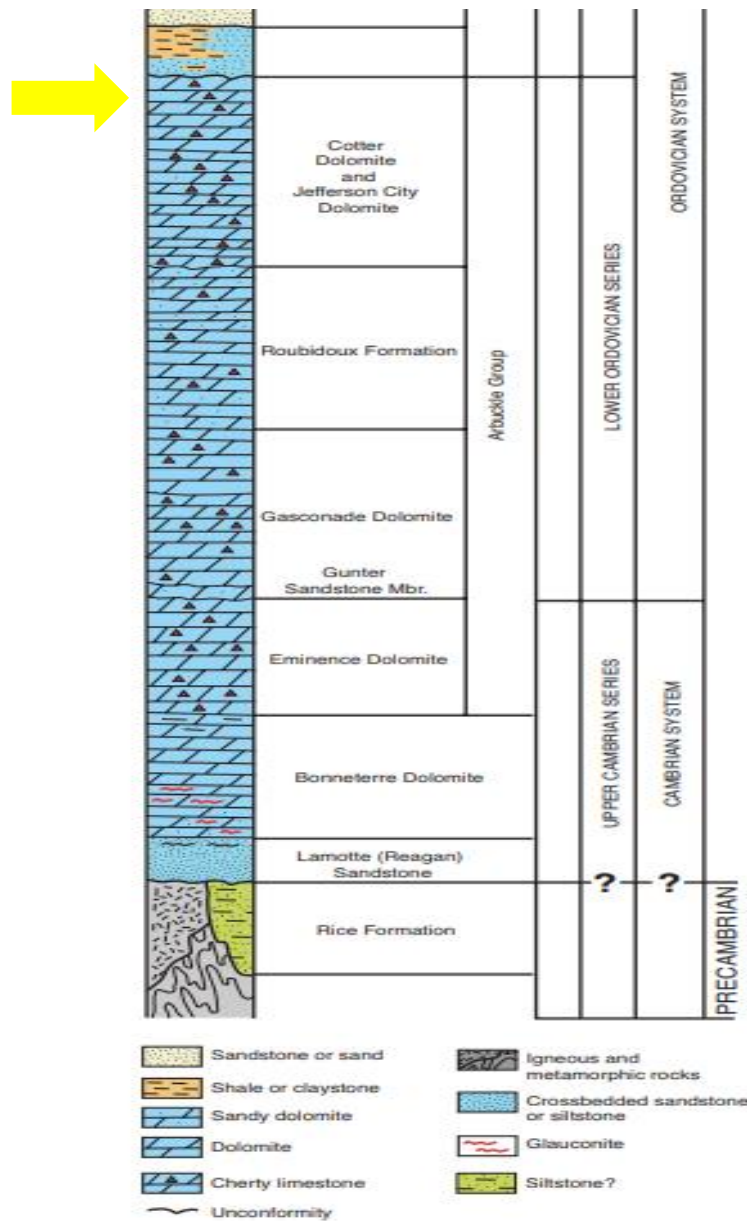
Figure 14 Stratigraphic column of the Arbuckle Group with lithology and relative ages. The Arbuckle Group represents one of the largest producers in Kansas and sits atop an aquifer. Most of the previous drilling and production were in the upper 25 feet, labeled with the yellow arrow. Borrowed from Franseen et al. 2003.
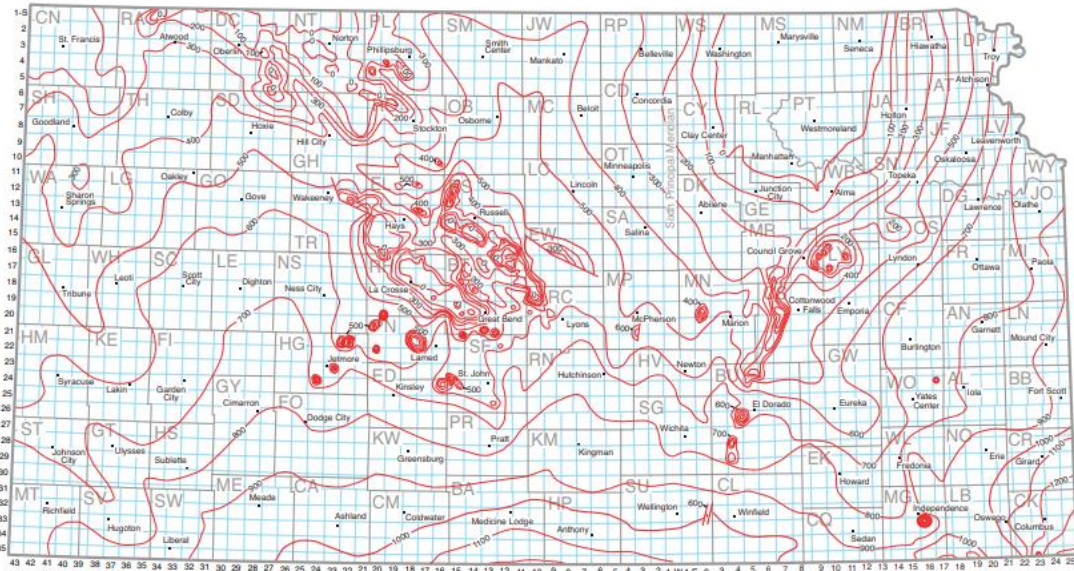
Figure 15 Isopach map of the Arbuckle Group Strata from well data up to 1965. This map illustrates the notion that there is significant variability within the subsurface if Ellis county and if analyzed in conjunction with the topographic map, can be seen that there will be significant effect on seismic datum interpretation. Contour interval 100 ft. From Cole (1975).

Chapter 4 - Seismic Data Geometry

of the Data Provided

Seismic data geometry is often set up in terms of source and receiver lines, and for the purpose of this thesis and the program used to process the seismic data, they may be referred to as S_LINE and R_LINE respectively. The importance of understanding the source and receiver lines is dictated in the number of channels, or traces, within each. There exists a hierarchical scheme to geometry as sources are situated into source lines and receiver lines respectively. Within the data geometry, the FFID's that corresponded to each source, or source number, had a certain number of active receiver lines for any given source. Within these source lines, or cables, there are a certain number of channels. The hierarchical representation of how the data is arranged is seen in the graphic below (Figure 7). For the superset of the geometry to be correct and accurate, there must exist a coherent pattern where all the sources in numerical order must

have the correct number of source lines active and the correct number of active channels within each source line. For example, within each source line if there are 40 channels active within the native data, there must be 40 channels active within the associated geometry spreadsheet so that there is no discrepancy. If there is a discrepancy between the number of channels active within the native data and the geometry spreadsheet, then this will cause errors in the way that the X and Y data is assigned to each individual channel. For instance if there is a source line, or unique cable that is active with 56 channels within the spreadsheet but the native data shows that there are only 40 channels for that unique cable, then the extra 16 channels associated with the cable will be taken from the next numerical cable and associated in X and Y space with the first cable and not the second. It can be seen through previous explanation that the native data and the geometry spreadsheet rely heavily on hierarchical patterning and if any of the associated headers, or sorting keys, are awry then the data itself will exhibit flaws regarding the actual spatial positioning of wiggle traces, or channels.
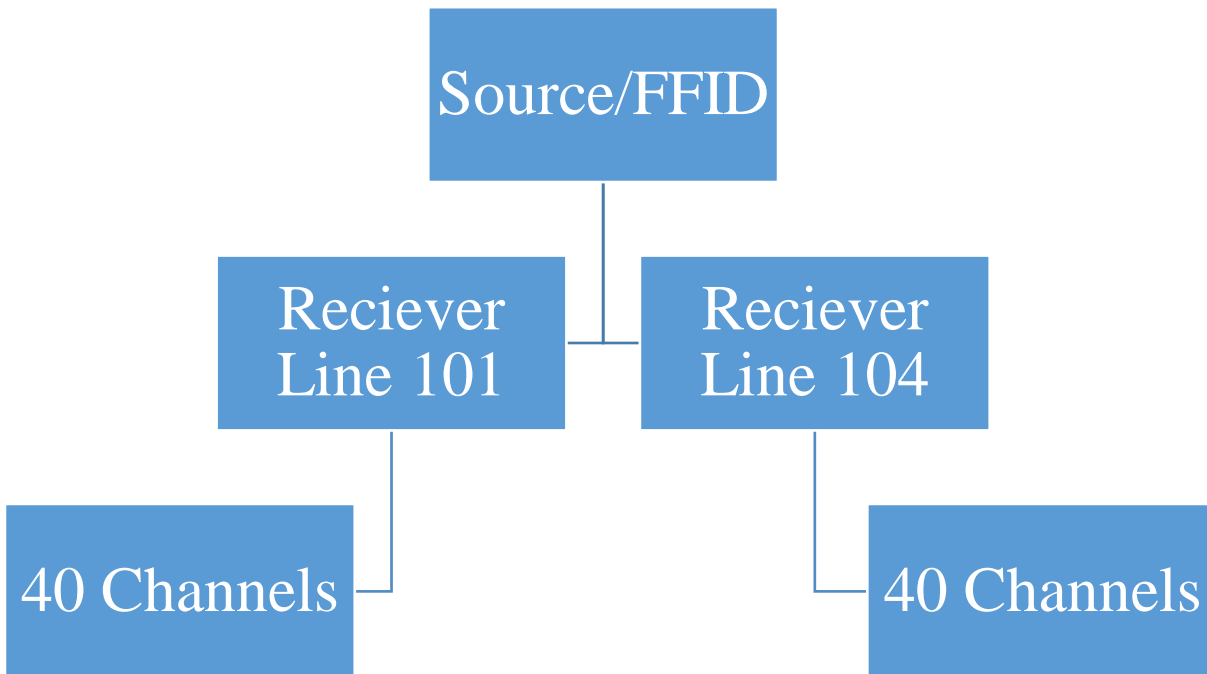
Figure 16 This illustrates the hierarchy of sources, receivers, and channels within the seismic data geometry. If any aspect of the seismic acquisition geometry is flawed, any subsequent reprocessing or seismic datum placement will therefore be incorrect.

For the geometry to be placed properly in 3 Dimensional space, there needs to be at least two headers assigned to the data during acquisition that match the data in the geometry load-sheet, otherwise there will be problems correctly spacing the traces, sources, and receivers in 3-Dimensional space, seen in Table 1. This process can be seen as an analogous to triangulating a point in GPS wherein the location can be derived on three radii intersecting at a point, and in the case of the seismic data headers, there needs to be at least two matching header fields within the geometry spreadsheet, seen in Table 1, for the wiggle traces and shot-receiver points to be correctly located in three dimensional space.

TRACENO	SOURCE	RECNO	CHAN	FFID	S_LINE	SOU_X	SOU_Y	R_LINE	REC_Y	REC_ELEV	OFFSET	CDP_X
1	343	1001	1	1	122	1607265.70000	273474.50000	101	269955.10000	2074.39990	5378.12451	1605232.35000
2	343	1002	2	1	122	1607265.70000	273474.50000	101	269954.60000	2067.39990	5254.13525	1605315.30000
3	343	1003	3	1	122	1607265.70000	273474.50000	101	269949.10000	2072.39990	5139.29053	1605395.95000
4	343	1004	4	1	122	1607265.70000	273474.50000	101	269951.80000	2047.69995	5018.46924	1605478.55000
5	343	1005	5	1	122	1607265.70000	273474.50000	101	269951.80000	2066.19995	4899.81689	1605562.85000
6	343	1006	6	1	122	1607265.70000	273474.50000	101	269948.90000	2089.80005	4790.56348	1605644.00000
7	343	1007	7	1	122	1607265.70000	273474.50000	101	269947.50000	2070.00000	4680.69336	1605727.10000
8	343	1008	8	1	122	1607265.70000	273474.50000	101	269947.40000	2052.39990	4575.51367	1605808.40000
9	343	1009	9	1	122	1607265.70000	273474.50000	101	269945.90000	2060.39990	4470.45264	1605893.30000
10	343	1010	10	1	122	1607265.70000	273474.50000	101	269943.60000	2071.80005	4374.12256	1605974.80000
11	343	1011	11	1	122	1607265.70000	273474.50000	101	270065.10000	2070.50000	4180.43701	1606056.15000
12	343	1012	12	1	122	1607265.70000	273474.50000	101	270089.00000	2064.80005	4060.50806	1606144.75000
13	343	1013	13	1	122	1607265.70000	273474.50000	101	270107.20000	2072.80005	3962.39087	1606221.45000
14	343	1014	14	1	122	1607265.70000	273474.50000	101	270122.40000	2075.19995	3865.41455	1606303.30000
15	343	1015	15	1	122	1607265.70000	273474.50000	101	270141.70000	2073.00000	3768.73926	1606385.95000
16	343	1016	16	1	122	1607265.70000	273474.50000	101	270223.70000	2070.00000	3619.82324	1606469.55000
17	343	1017	17	1	122	1607265.70000	273474.50000	101	270224.30000	2074.69995	3549.14355	1606552.85000
18	343	1018	18	1	122	1607265.70000	273474.50000	101	270240.90000	2068.69995	3470.84912	1606635.10000
19	343	1019	19	1	122	1607265.70000	273474.50000	101	270237.40000	2063.19995	3418.21606	1606716.75000

Table 2 Values directly from the geometry spreadsheet as they appear in the seismic dataset. The headers are in the top row, shaded in grey. Some of these headers were assigned when the data was recorded, such as trace number (TRACENO), and source line (S_LINE). However other headers had to be generated by the processor to create matching fields such as, source number (SOURCE) and Channel (CHAN).

Without knowing the proper Common Depth Point, or CDP, as well as the Source Line enumeration, there will be no way to place shots and gathers correctly in space. If the data is not correctly spatially located, the traces will not sequence correctly and when trying to stack the data because as the software reads the traces, combines them into cables and enumerates them as source and receiver lines, traces for other shots and receivers will be incorrectly placed within gathers they do not belong to. This misplacement provides side-effects seen in the data such as aberrant offset which will interfere with gathering and binning of the data further into processing. The processing workflow, aside from loading the initial SEG-y data is dependent on a corrected geometry model, without a corrected geometry, performing complex analysis of amplitude or velocity, the generated model will not be true to the subsurface conditions and render the data useless.

Seismic data within a 2D frame, wiggle traces or the seismic amplitude and frequency content of a line, are placed sequentially on an increasing axis of known distance and time

(Figure 8). When the geometry is incorrect and traces are misplaced, then the amplitude and frequency of the data will be incorrect and the subsequent seismic processing steps in the workflow will be affected substantially. A comparison of the same dataset at different geometric representations can be analyzed to properly grasp the importance of proper trace representation and how geometry affects properties such as offset, this can be seen in Figure 8 and Figure 9.

Figure 17 Within this example, as Source Number and Channel increase from left to right, it can be seen that however there is some consistency to the Offset (blue) of the wiggle traces in the geometry, when checking quality of the Offset, we can see that it does not reflect the acquisition geometry as manifested by the semi-parabolic shape; the example in Fig. 18 shows the correct offset geometry in match with moveout of the data.
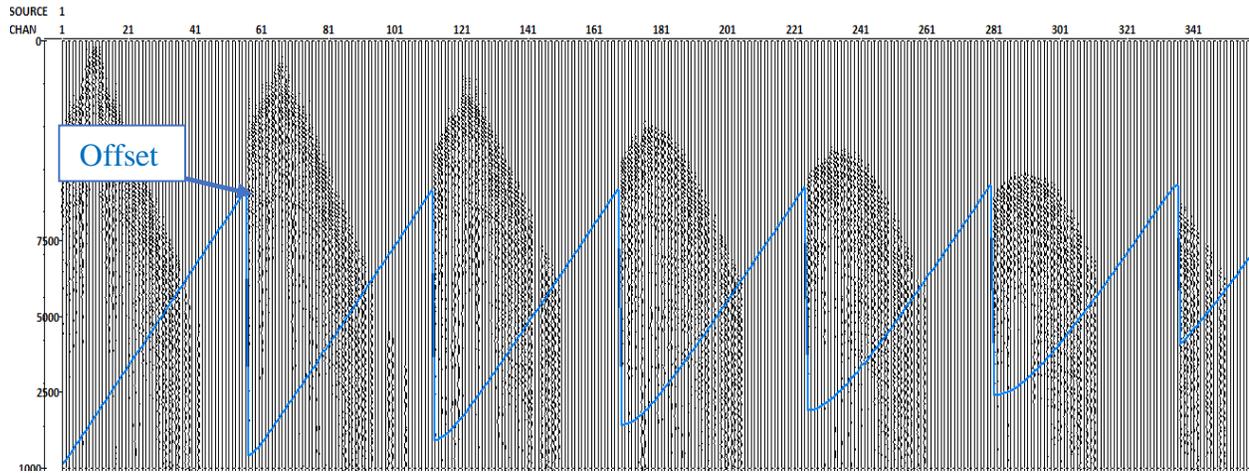
Figure 18 As Source Number and Channel increase with left to right within the survey, the wiggle traces are placed within the geometry; the Offset pattern is matched to the moveout of the data, indicating a correct representation of acquisition geometry.

The way that the data was supplied in its native form as well as the supplemental load sheet illustrated a basic lack of uniqueness to spatial properties. There was insufficient numbering to the traces and the unique receivers to be able to properly assign correct geometry. Facing this problem was strenuous and took considerable creativity and perception to overcome, giving rise to a robust seismic processing workflow for quality control. Upon investigating the data, it was found that the data was acquired in a linear fashion, from west to east in row and resetting going from south to north. This fact was made apparent by studying the pre-stack seismic data noting how the offset and moveout changed moving from west to east instead of the reverse, east to west. With the distance increasing from the nearest traces to the farthest, moveout increases, allowing interpretation of distance from origin of source and receiver line as well as local positioning of source and receiver location, correlating to individual channels of traces. It was also found that the common depth point (CDPX) assigned to each Reciever within a specific reciever line increased from west to east. This trend can be seen in Table 3, as with increasing X values, the CDPX also increases, allowing inference that this apparent pattern will give some basis to a correct geometry.

Receiver_	CDPX	x	y	elevation	R_Line	Chan
101	485	1603199	269955.1	2074.4	101	1
101	486	1603365	269954.6	2067.4	101	2
101	487	1603526	269949.1	2072.4	101	3
101	488	1603691	269951.8	2047.7	101	4
101	489	1603860	269951.8	2066.2	101	5
101	490	1604022	269948.9	2089.8	101	6
101	491	1604189	269947.5	2070	101	7
101	492	1604351	269947.4	2052.4	101	8
101	493	1604521	269945.9	2060.4	101	9

Table 3 This table gives an excerpt of the values given by the acquisition and processing companies. By evaluating the assigned numbers to each receiver line, R_Line, as well as CDPX, a pattern was seen and the basis for an enumeration scheme was formed.

The geometry is shown in Figure 19 where the Receivers are denoted with blue triangles and the Sources are denoted by red circles. In terms of X and Y, data increases linearly across X in what is known as Source and Receiver lines and these lines increase in value going north or increasing Y value. By assigning each of these sources a unique number to each of these source locations, which are now labeled in groups based on the source line, the geometry can be properly arranged in a grid format that will allow for the interpolation of zero valued location data. Assigning individual values to the sources within the source lines creates a header within the geometry which generates a matching series within the seismic data and the load-sheet. This represents the first matching header used for correlation. By assigning each source its own individual and unique number, each trace can then have its own individual and unique number within this, as a subgroup, and each shot point location number can be given an individual and unique FFID, of Field File Identification Number. Within the survey, there exists over 556,000 individual data points, or channels, that correlate to individual source and receiver pairs. By

analyzing the geometry spreadsheet produced by the processing software, we can assign each

group of traces that correspond to a source point activation a unique value. This is done by using

the trace number associated with the source, which resets numerically each time a new source

point is displayed in data. Grouping each trace batch together under a common source number

allows for proper geometric representation. This process divides each numerically grouped

source line number into separate source locations within the line, each of which have their own

group of traces. By assigning numerical values in this manner, the CDP-X values given by the

load-sheet are rendered obsolete but still account for the way that they correlate with the data as

headers. This process of creating numerical values and reassigning values allows for a more

accurate way of pairing headers while remaining consistent with given data. This hierarchy of

numbering creates a recognizable pattern within the data that again allows for consistency as

well as uniqueness, both of which are pertinent for properly assigning seismic geometry.
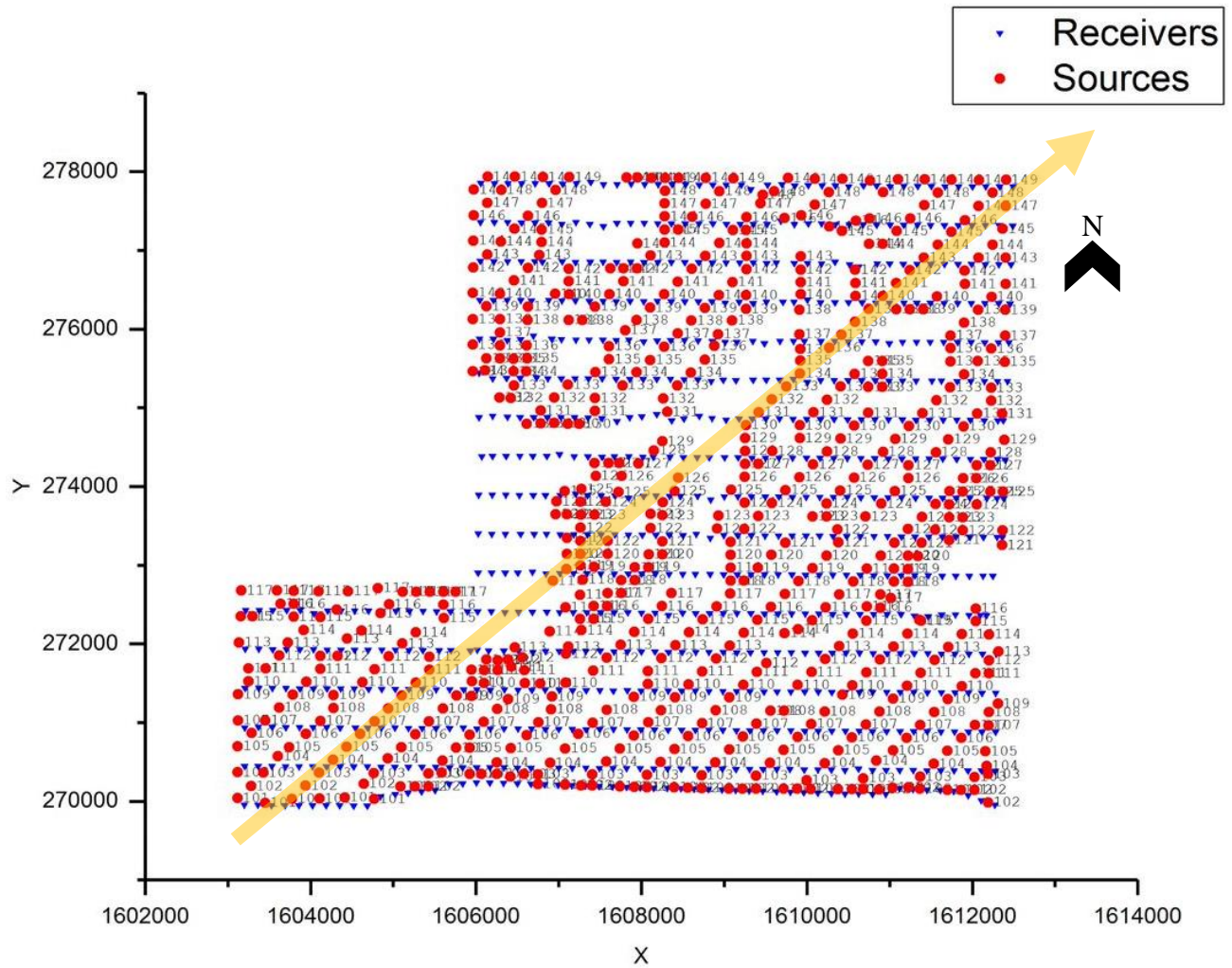
Figure 19 The figure shown indicated the numeration of source and receiver points as they increase in value in X and Y, as the trend is denoted with the semi-transparent line. This geometry was created using ArcMap software, loading the supplied X and Y data.

This zero-value location lacks X and Y values in the geometry load-sheet but exists as a spatial point within the data. In order to account for this, we again turn to interpolation between known values from the load-sheet that we have correctly assigned values to matching the data. This is important to take care of so that no impactful data is cut or filtered from the processing flow, because for a thorough and complete survey, the more data that is used in creating the

model, the more reliable the model is, and the less uncertainty is present within the process. In terms of seismic data, the more data points that are available, or more traces that are able to be used in the interpretation, the more valid a model will be when it comes to stacking and velocity analysis. The more points that can be stacked and the more traces whose velocity can be analyzed, the more accurate the associated static model will be. By assigning X and Y spatial data to these data, it can be used in the interpretation of the subsurface and influence the 3-D modeling.

ance of Matching Headers on Seismic Data Geometry

By Creating headers within the data from the separate parts of the data, we were able to create a way to assign geometry of the shot points, receiver points and a hierarchical way to incorporate source lines, receiver lines, and their respective cables and channels. The significance of doing this lies in that the system had to be reverse engineered from the data that was represented in the SEG-Y files and read by the program, essentially the data that could not be affected by any human input, as well as with the sparse amount of data that was given by the acquisition and processing companies. In most standard seismic data processing workflows, as well as with most datasets, the companies that acquire the initial data and do the initial processing, assign a geometry to the data that is coherent and allows for input of the data into the processing software and the assignment of geometry to take minimal time and effort. It is in the experience of the writer that this has been the case for all datasets previously worked on, some semblance of coherency accompanied the data in the form of headers or within the geometry load sheet itself. When confronted with the problems that came with this dataset, it appeared that this may be more than a singular case and many other datasets may exhibit this problem more inconspicuously.

If this is the case, developing a way to quickly and efficiently assign geometry headers and to quality control the output became a priority so that it may be translated to other datasets that may exhibit some of the same symptoms. By successfully engineering a data geometry from what was supplied, the workflow has proven to be adequate in establishing the source lines and receiver lines in correct geometric space. The importance of the headers was found to be crucial in designing the geometry, because as previously stated, these headers are what give specific groups of traces, channels and cables a unique identity. The geometry that was created adhered to the native data as well as to the hierarchy of the data within the geometry spreadsheet and the load sheet.

Source Line and Receiver Line Enumeration

After the headers for the sources, FFID, and Channel (CHAN) were created and assigned, another problem arose within the data. This problem stemmed from the cable and channel configuration present within the geometry and how it was inconsistent with the native data. As data was filtered through and displayed by the primary key Receiver Line, secondary key FFID, and tertiary key, Channel, it was seen that there was a discrepancy between the actual length of the cable in the native data and what was proposed by the acquisition and processing companies in the geometry load sheet. In the geometry load sheet that was acquired, as previously mentioned, had problems regarding headers for matching the geometry to the native data, however this file came with other issues in that the file assumed that each cable in the receiver line was 56 channels long. When the data was loaded into the program based on this premise, offset issues were observed. As seen in the figure below, the green line indicated a stepping of receiver line, R_LINE, location as it corresponds to the number of channels within each receiver line, as previously discussed. The stepping of the receiver lines indicates that it is increasing

numerically within the hierarchy of the FFID or source, and these reset with a new FFID, done in a chronological order. What is important to note, as well, is that there is an apparent incorrect enumeration of the channels within the cables, or receiver lines that will give an incorrect location representation of each trace in three-dimensional space. This can be seen by the red lines indicating the actual length of the cables, or collection of channels, within the source. The discrepancy is seen in the difference in distance of the red and green line transition, noted as a yellow bracket (Figure 20). The significance of these extra channels is that they are subtracted from the subsequent receiver line and this results in an overall shift in the cable structure within the FFID. However, this cable shift is reset at the end of the source and is not carried over to the subsequent source. This pattern shows that instead of the cables consisting of 56 channels, they instead consisted of 40 channels. This left an excess of 16 channels per cable that was then shifted to the beginning of the cable that was seen in the native data. Each cable therefore had 40 traces until the source line expired, with some cables having less due to the amount of offset and moveout from the source point leaving no recorded channels at that length, i.e. a dead trace. With this solution formulated, correcting the channel length within the geometry spreadsheet was a matter of numbering the channels within a cable manually. The number of cables per source was variable but a pattern predominated. This pattern was seen in sources that had a total length of 774 channels in total length. Once these cables were corrected for the total length of the source, copying the pattern and applying it to the rest of the data was all that was required to fix the rest of the geometry spreadsheet. Each source thereafter had cables with a predominant range of 40 channels, seen in Figure 21, which further allowed for the correct placement of channels and traces within 3-dimensional space. The resulting geometry was corrected for general offset issues and the total channel count and trend per source exhibited a pattern that is coherent with general

offset and moveout away from a source point seen in Figure 22. The overall premise of this step within the quality control workflow is to recognize that pre-stack seismic data does not always come as completely reliable and coherent data. If a seismic processor was to assume that the receiver lines were correct in this case, the channel numbering would be incorrect, and source and receiver line coordination would result in incorrect spatial placement. Within the seismic processing workflow and hierarchy, the length of the cables comes as a finer resolution aspect of the data. The overall objective of this workflow is to allow for the organization of a seismic geometry given relatively little to rely upon other than the native pre-stack data. This step is to ensure the correct placement of channels while the previous steps were to ensure the correct assignment of sources and receivers, as shown in the hierarchical figure shown below (Figure 23).
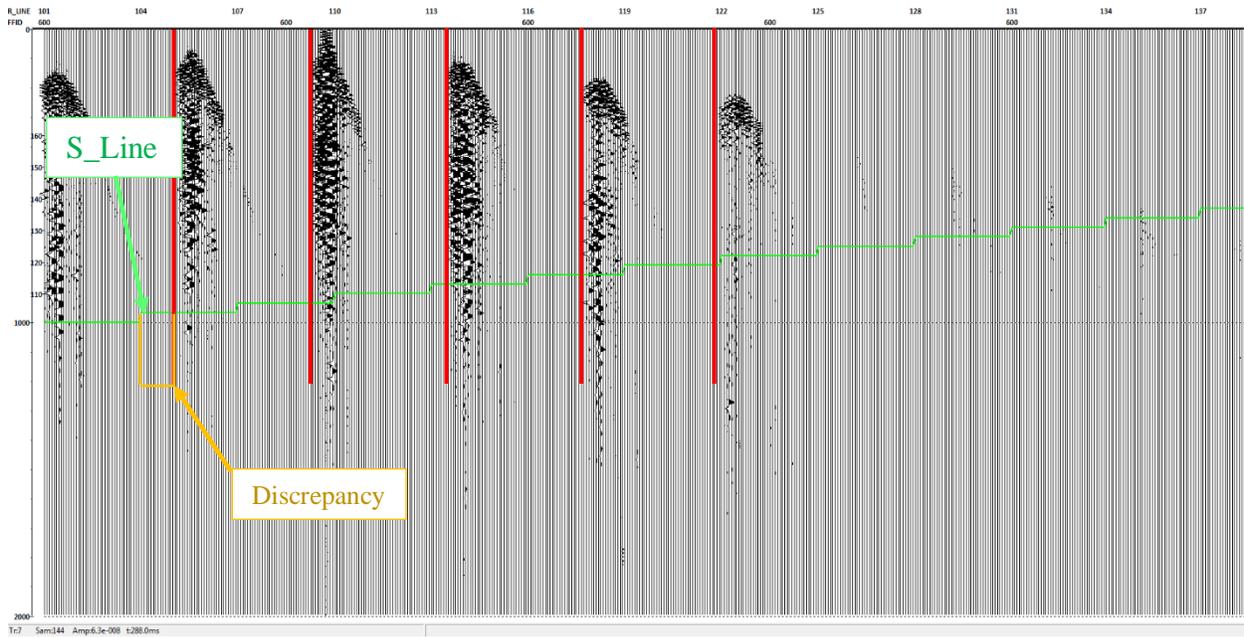
Figure 20 This figure illustrates the starting and ending points of each cable and their associated channels as well as the discrepancy between the starting and ending points. The red lines indicate the starting and ending points of the cables in the native data while the green S_Line header plotted indicates the cable length derived from the geometry spreadsheet. The yellow bracket indicates the amount of total discrepancy seen between the native data and the geometry spreadsheet.
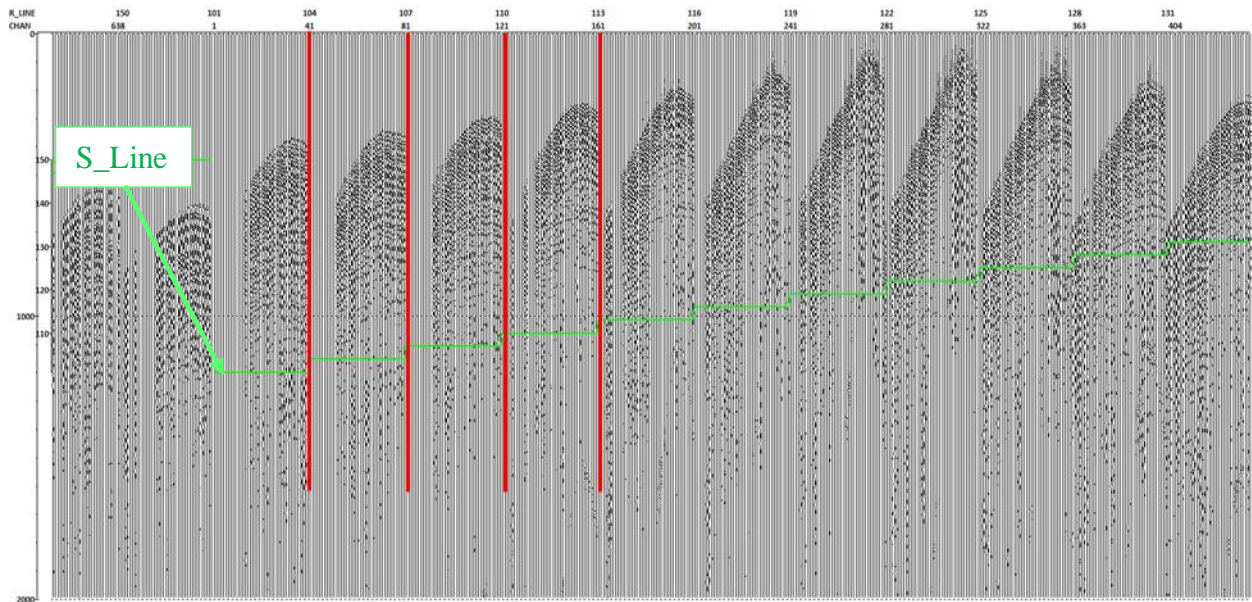
Figure 21 This figure illustrates the corrected S_Line geometry from both the native data as well as the geometry spreadsheet, as with the previous figure, the red and green lines indicate that start and ending of cables from the native data and spreadsheet respectively. However, since this data is corrected, there is no observed discrepancy and the source lines coincide at the same points.
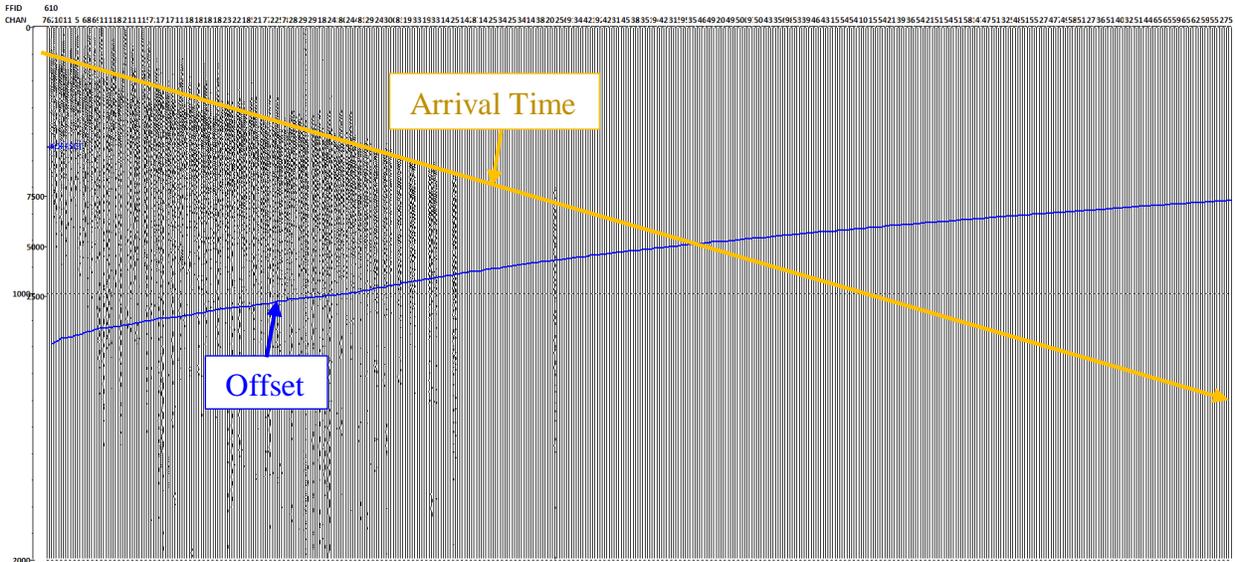
Figure 22 **The figure above illustrates the QC of the data after the receiver lines were fixed. From left to right the offset and moveout of the source increases, which is the blue line, absolute offset, increases in an approximately linear trend as the traces increase in distance away from the source point. As offset is defined, with increasing moveout, the offset should increase. This principle is what gives the inverse function of arrival time in yellow versus the offset in blue.**
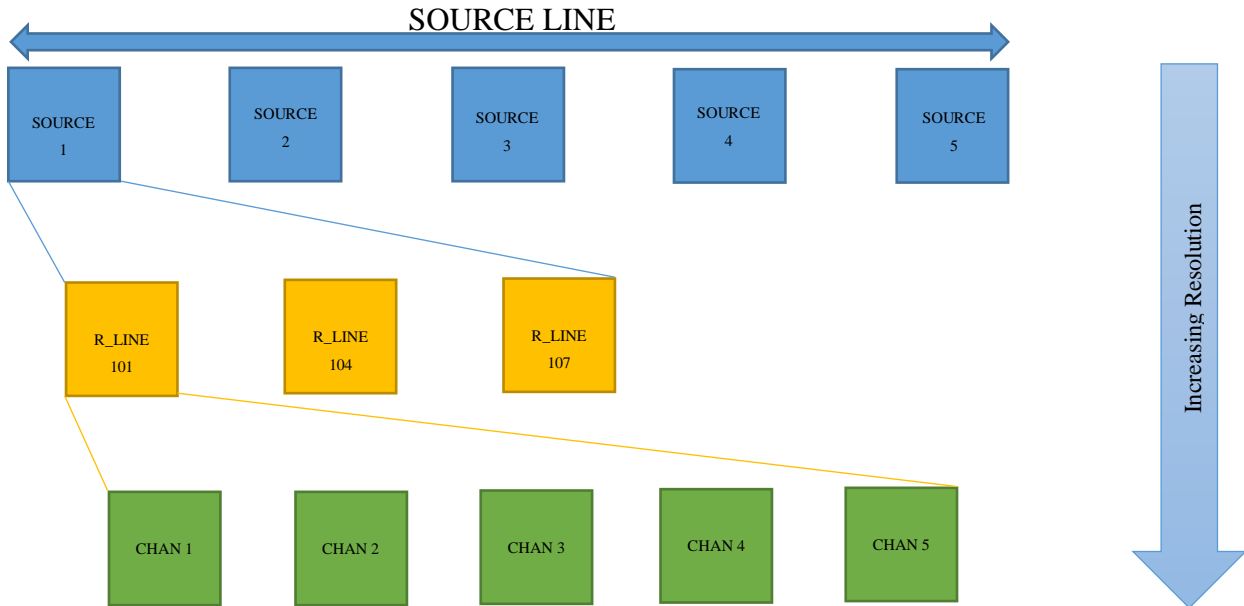
Figure 23 **The figure above illustrates the resolution of the processing workflow with the correct placement of the source lines and receiver lines at the beginning. Then work is done to establish the correct placement of individual sources and receivers (cables) within their respective lines. With finer resolution comes the correct numbering and placement of channels as they correspond to these sources and receivers.**

After the solution for the channel count within the cable was applied and that aspect of

the geometry rectified, another aspect of the geometry presented issues. These issues came in the

presentation of channels within the cable being reversed in numeration, seen in Figure 25. These

channels were inversed in their X and Y coordinates and resulted in parabolic seismic reflections

with offset coinciding with moveout. Realistically, as previously discussed, the offset of the

cable should vary directly with moveout, so that as moveout increases the offset should increase

as well (Figure 24). By sorting the geometry spreadsheet and the native data by the primary key

source and the secondary key as channel, the data was sorted so that each unique cable

associated with a source could be seen. The general trend of each cable within a certain source

was then analyzed, looking specifically for the trend of the offset within each cable. If the cable

was reversed, it was then noted, and if all the cables within a source were reversed, that too was

noted. These notations presented themselves as a pattern within the data, seeing most of the

source anomalies needing to be flipped in their entirety. There existed other patterns within the

data, suggesting that within some sources there were individual cables that needed to be flipped

or only one half of the cables within a source were reversed. Four categories were then created,

and all sources filed into one of these four categories. These include: (a) coherently numbered

channels, (b) reverse numbered channels, (c) sources with channels exhibiting patterns, and (d)

aberrant channel and offset correlation. These patterns can be seen in the figures listed below

with normal offset data as Figure 24, inverse offset as Figure 25, two types of patterned data as

Figure 26 and Figure 27, and finally aberrant offset as Figure 28. The predominant pattern that

permeated the data was one in which the first two receiver lines, or cables were aberrant and

needed to be cut from the source line so that the rest of the cables within the line could be

reversed, giving coherence to the offset and moveout pattern within the geometry. This patterned

fix, however, was not applicable to all the sources that exhibited a pattern. The sources that exhibited a pattern other than this were considered nonessential to the dataset and were removed. This solution may give rise to subtle problems but the redundancy of shots within the survey takes care of the excised sources with fold.

The only solution to this problem appeared to be categorizing each individual source based on the type of transformation that appeared to be needed, based on the native data. This meant that the dataset would then need to be broken up and partitioned based on the type of pattern each source. For instance, if all channels and all cables within a source exhibited the correct offset pattern with moveout it could be left within the original native dataset file. If a source exhibited the trait that all the channels within all the cables needed to be flipped then it would be excised and put into its own dataset where a bulk transformation could be applied easily. After these sources were individually shifted, each of the datasets were then stitched back together with the previous geometry steps applied. This generated a geometry spreadsheet that mirrored the native data coherently. This was the final step of processing and correcting the geometry data before further processing the data with regards to frequency, amplitude and velocity.
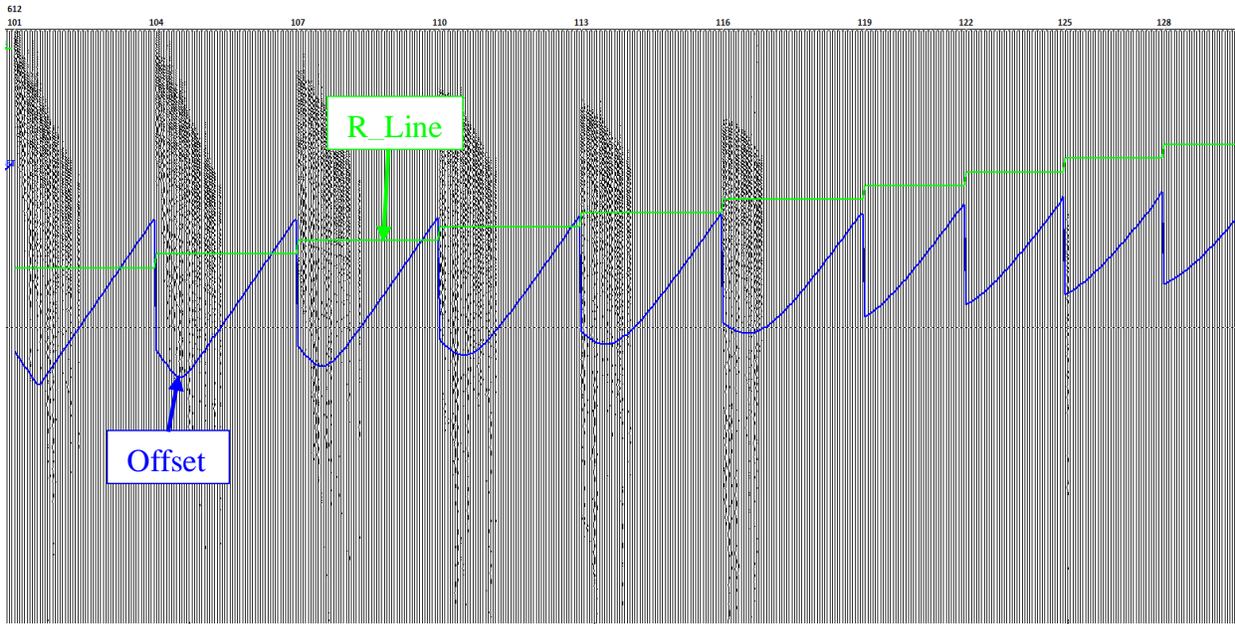
Figure 24

In this figure, the offset of the channels matches the moveout between the cables as the receiver lines increase in offset. The offset of the channel is indicated with the blue line while the step of the receiver line is indicated with the green line.
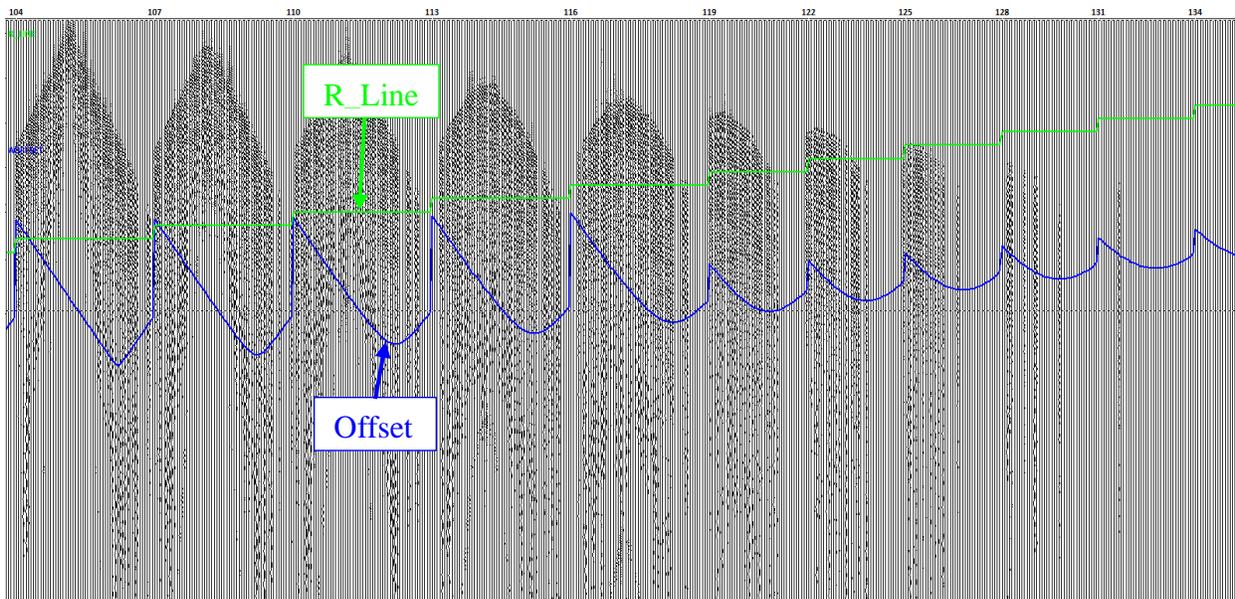
Figure 25 In the figure above, the channel moveout and offset are inverse, denoting that the channel number of each receiver line cable need to be inversed so that the offset and moveout are corresponding.
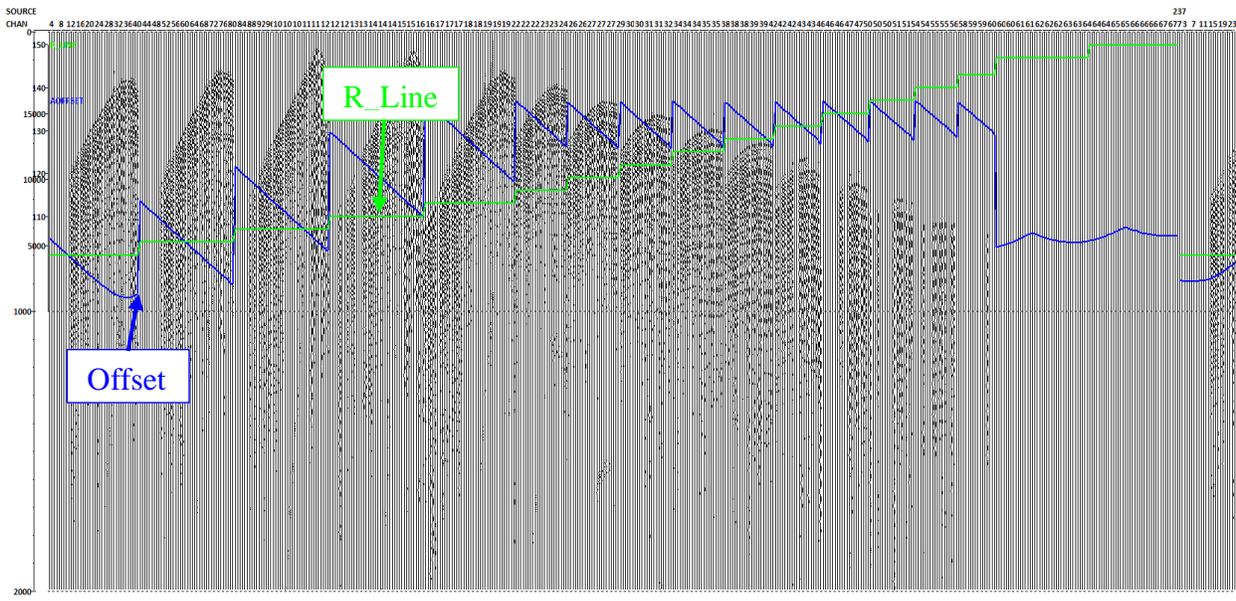
Figure 26 The figure above illustrates another pattern seen within the data. The sources exhibiting this pattern had receiver lines at the end of the gather that had dead traces, filtered out based on aberrant offset values. When these receiver lines were excluded, the sources produced useable seismic data.
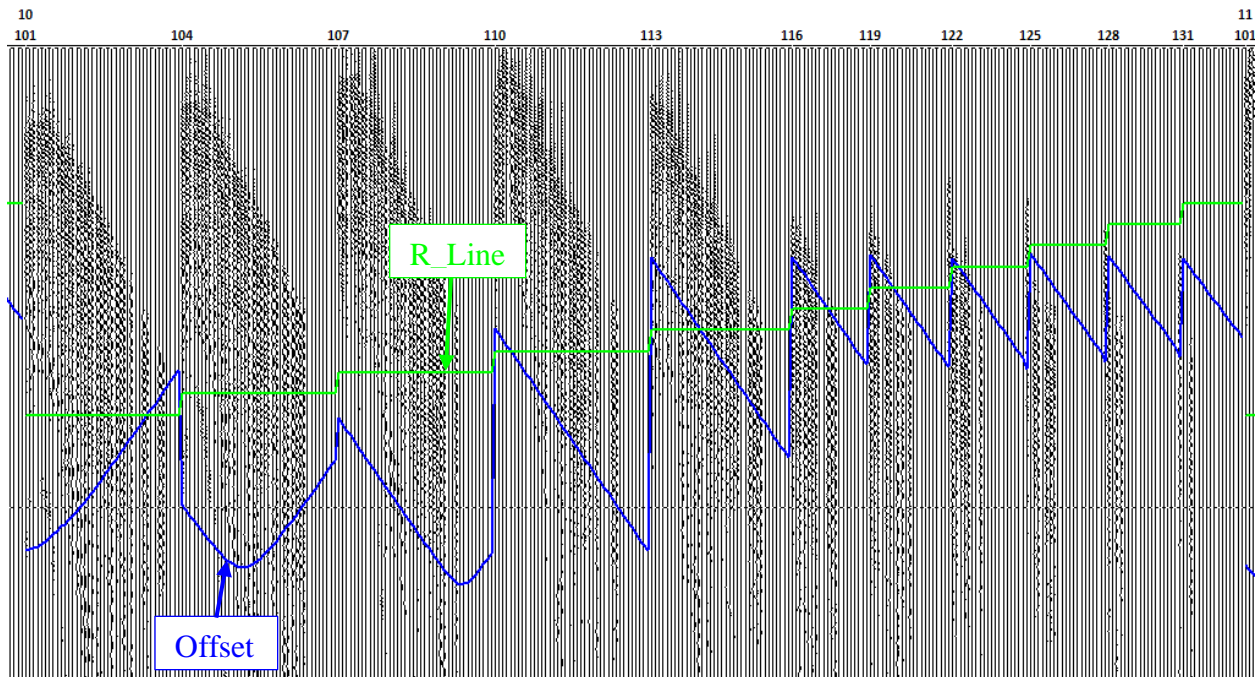
Figure 27 The channels and cables pictured above illustrate semblance of a pattern that had to be cut out. Receiver lines 101 and 104 exhibit offset and moveout trends that are anomalous but thereafter the cables exhibit a trend that needs a simple reversal of the channel number.
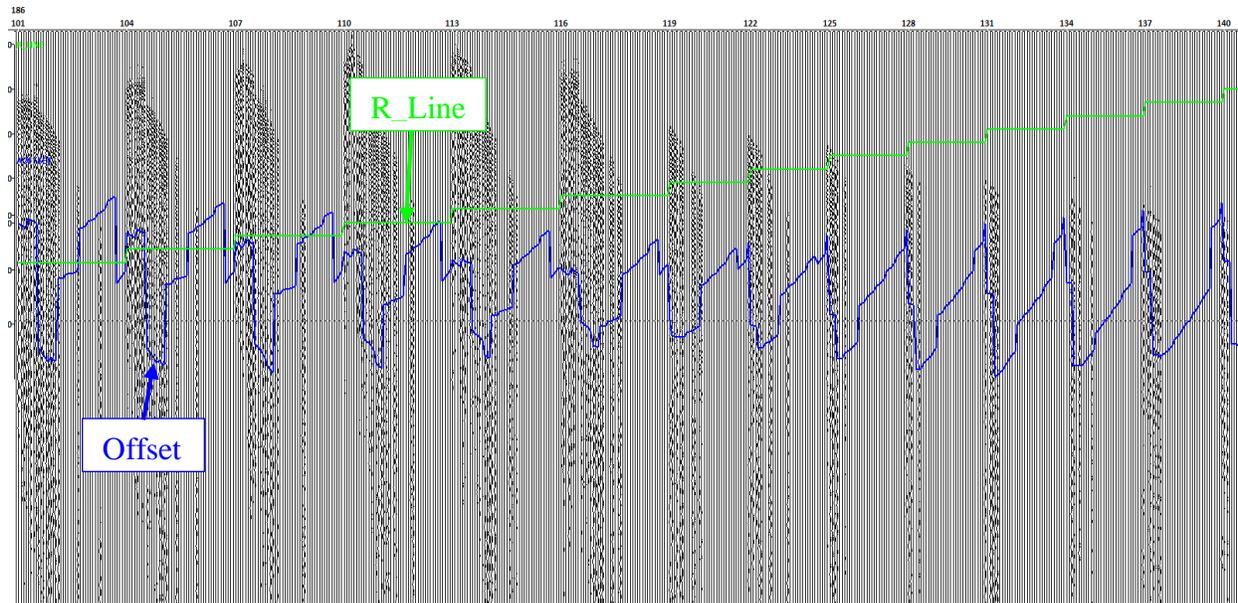
Figure 28 The source line pictured above illustrates a completely aberrant behavior and there seems to be no coherent pattern concerning offset and moveout of the channels within the cable. Therefore, in this case, this source must be excised from the data completely and cannot be put back in without causing harm to overall data quality.

n Depth Point Binning

As previously mention in the definition of velocity picking, the maximum fold of the data is desirable for binning and stacking and the maximum distribution of common depth points is desirable as well. To reiterate, the typical processing workflow uses cell dimensions half the receiver group spacing in the inline and crossline direction; 100 feet. With the maximum distribution calculated between receiver points at 165 feet the bin length and width is 82 feet by 82 feet. For this dataset, the rotation was of 25 degrees and translated to an origin point of (1602518.76, 270199.94) in NAD27 Kansas Northern. This step is pertinent to the geometry binning because it mitigates irregularity within the CDP fold. For the size of the survey and the bin size, the resulting inline and crossline count are 109 and 136 respectively. These values will be reflected in the seismic cube.
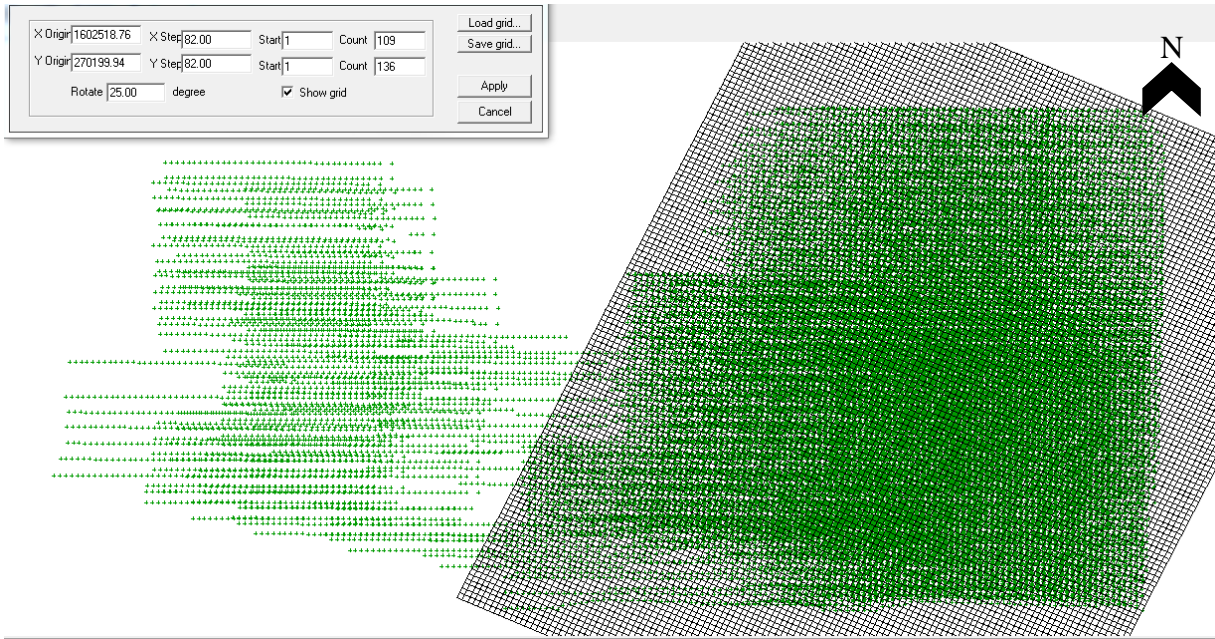
Figure 29 The 3D binning geometry above shows the translated and rotated from linear rectangular field. This allows for maximum CDP distribution as well as mitigating acquisition footprint. In the top left corner, the grid parameters are shown.
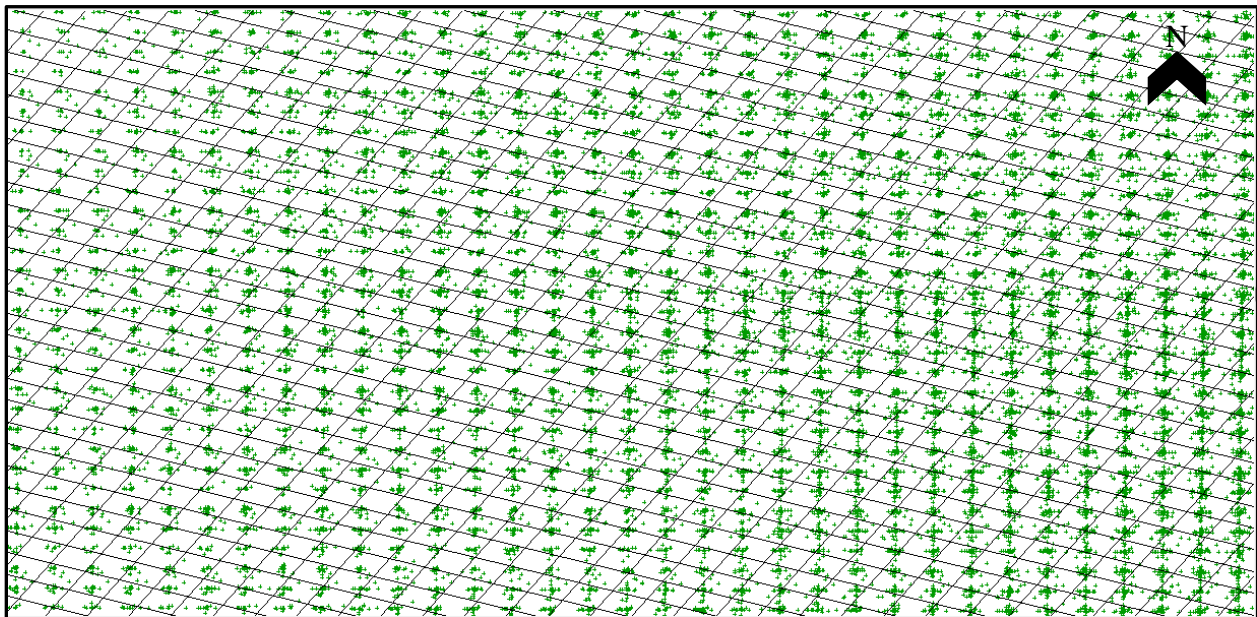
Figure 30 The Figure above is a more detailed view of Figure 29, showing the fold dispersion within the binning parameters, translated and rotated.
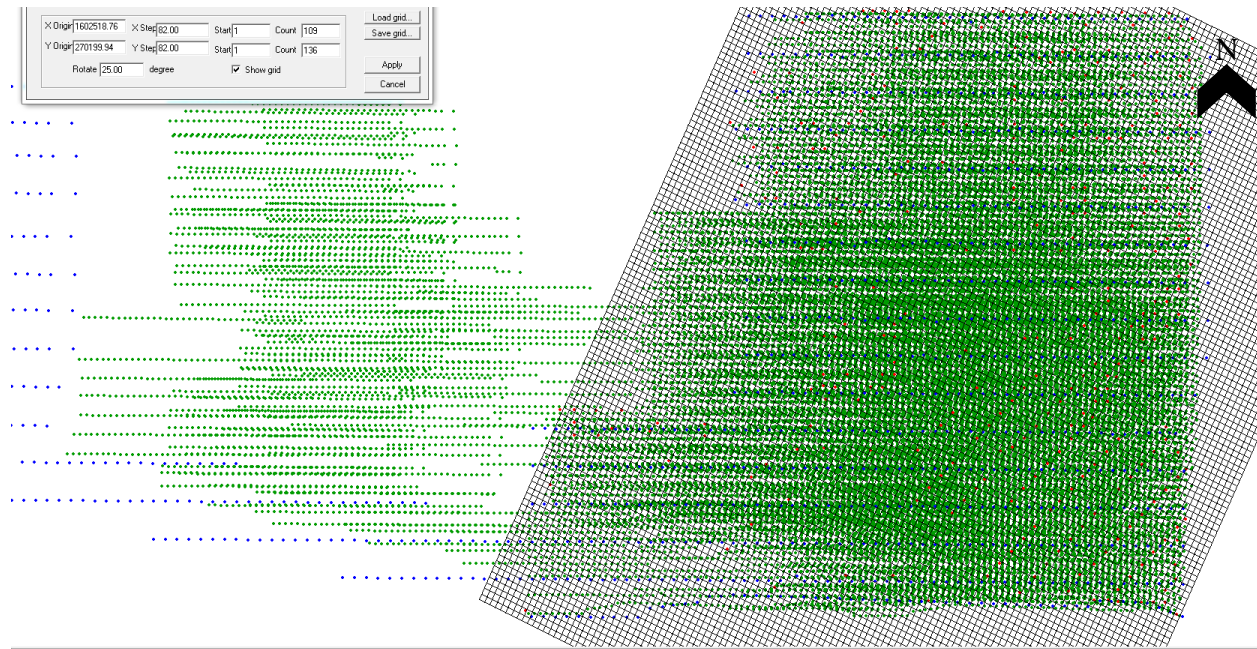
Figure 31 Plotted over the binning grid are the source and receiver points, blue and red respectively. This allows for quality control of the gridding geometry, making certain maximum fold is achieved.

It is important however to take note of the non-gridded lines to the left (east) of the main gridding geometry, this data exhibits source lines that were of incorrect spatial positioning, which can be seen by the sources in blue plotted out to the side of the geometry. This phenomenon gives rise to inaccurate CDP positioning that are not truly in the survey area. While this may seem to be a problem, given the high density and distribution of the correct CDP values within the binning grid, the incorrect ones can be excluded from the rest of the processing workflow with minimal impact to data quality.

Chapter 5 - Statics Corrections

Analysis

       Most of the accuracy in the static correction model is based on the velocities gathered from the data through interpretive velocity picking. After the data has been binned in super-gathers, experimental stacking (Sheriff and Geldart 199) enables interpretive velocity analysis to be accomplished. Through this process, the velocity picks are made on the semblance of the velocity data. The semblance analysis is done by developing a velocity spectrum of the data to determine the velocity through different layers at depth (Yilmaz 2001). This velocity and semblance spectrum represent a measure of signal coherency and semblance along the hyperbolic trajectories by velocity, offset, and travel time. While normally velocity data will be displayed in the semblance model previously mentioned, the interactive velocity module cannot be run on this dataset for a few reasons, namely that there is insufficient data at the lower depths to properly sample the full velocity field. Therefore, the semblance spectrum will not yield proper velocity picks to generate an accurate velocity function as seen in Figure 32. To then generate a proper velocity function for the dataset, manual velocity sampling must be done within the native data to generate the velocity function. Within the RadEx Pro software, there is a tool to approximate the hyperbola associated with individual reflectors and this hyperbola can give the velocity function with sufficient accuracy to apply normal moveout (NMO).
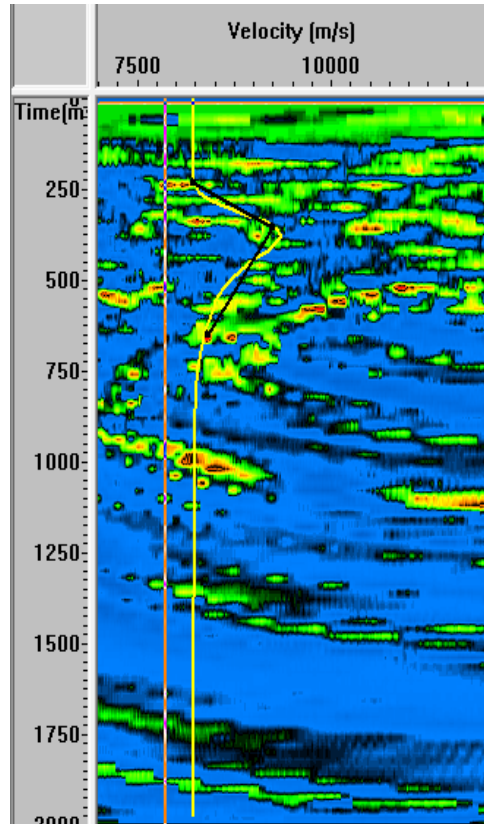
Figure 32 This figure shows the velocity semblance spectrum without a precompute, it shows the densest semblance in the warmer colors (red). This figure also shows the average velocity function for the dataset shown with the yellow line.

Sufficient sampling throughout the dataset must be done in order to gather enough

velocity information to generate a reliable velocity function, within the native dataset, 20 unique

points sampling the first unique reflector will suffice. This reflector, as seen in the data is

speculated to be the Stone Corral formation, a very distinct anhydrite layer that shows high

impedance on seismic section. By analyzing the RMS velocity hyperbola approximation, the

average velocity of the Stone Corral formation ranges from 9,100 ft/s to 9,300 ft/s. However, this

velocity range changes depending on the area of the seismic survey. For instance, there are some

areas in this survey which the stone corral has velocities lower than 9,000 ft/s and closer to 7,900

through 8,200 with variable dip within the area. This gives rise to a certain amount of

discrepancy within the dataset and proves that the assumption of a blanket velocity for the static

corrections, as previously done with this dataset, is insufficient. However, the average velocity of 9,000 ft/s for the stone corral is sufficient in its redundancy across the survey to be acceptable as a layer velocity for the calculated velocity function for this first reflector but not the static datum. This velocity range is in accordance with what was given to this thesis as the replacement velocity for the near surface datum which leads the author to believe that the LVL velocity was calculated based on the Stone Corral for the seismic datum. In conjunction with the misplaced spatial geometry within the survey, this assumption of the Stone Corral being the seismic datum will provide inaccuracy to the data in that it does not properly account for the variation in lithology and compaction above the anhydrite (Sheriff and Geldart 1995). The process of picking velocities based on the hyperbolic approximation works well for calculating approximate velocity values for lower layers as well to help build a robust velocity function. With the combination of what is known about the layer velocity that was gathered from the hyperbolic approximation, the interactive velocity analysis will be used, yielding varying degrees of success. To do this, knowing the depth of the reflector in two-way-time as well as the approximate velocity value will allow for guided picks on the semblance spectrum that will yield NMO corrections that make the seismic dataset more coherent. With the amount of and quality of the data given for this project, this is the best process for establishing a robust velocity function for normal moveout. While this process is not typical for most datasets, it will suffice in bringing correct moveout to the data.

A way to test the picks on the semblance spectrum is to see how they respond in the stack as well as the constant velocity stack (CSV) seen in Figure 33 and Figure 34. This allows for any changes seen in the semblance picking to display as a stack response on stacked velocities as well as the response to individual velocity spectrum within the stack. This process acts as a sort

of quality control when the semblance spectrum does not give helpful data as well as when it does. The stack response gives an immediate response to where the wiggle traces are located in TWT. For instance, if a velocity pick is made on the semblance spectrum where there is confidence in a reflector location, based on time-depth and velocity, the stack response will give more coherence to the wiggle traces at that time-depth. This is where the hyperbolic approximation step becomes more important in building a more robust model for NMO, as it allows for knowing where the primary reflectors sit and at what average velocity they have.
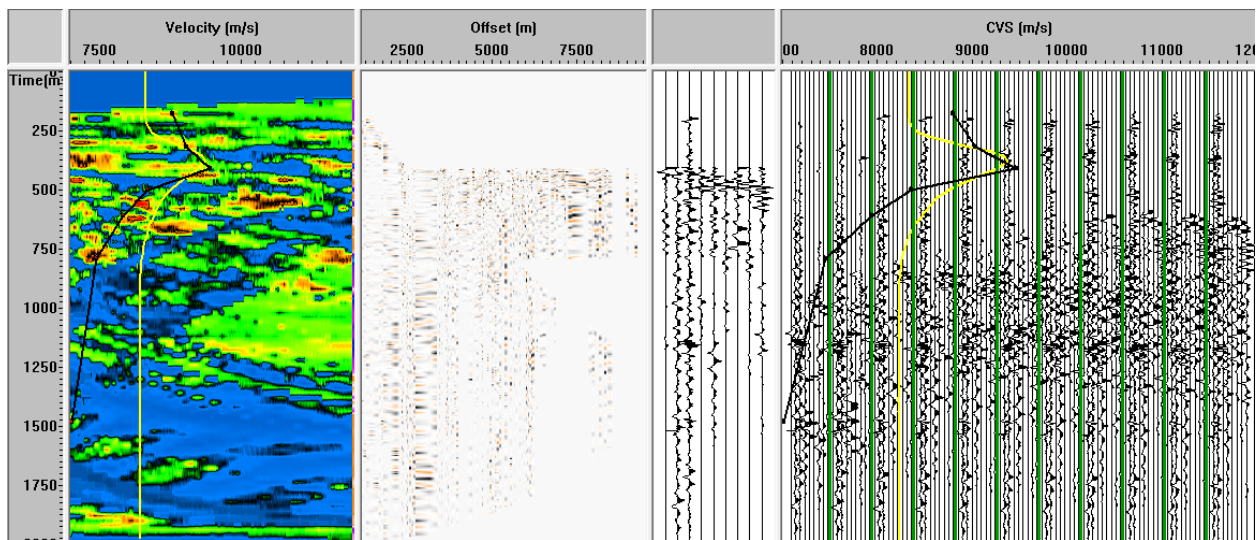
Figure 33 The semblance spectrum in the far-right pane gives relatively coherent data for picking velocities, however the reliance on parabolic approximation and stack response allows for a meaningful velocity analysis.
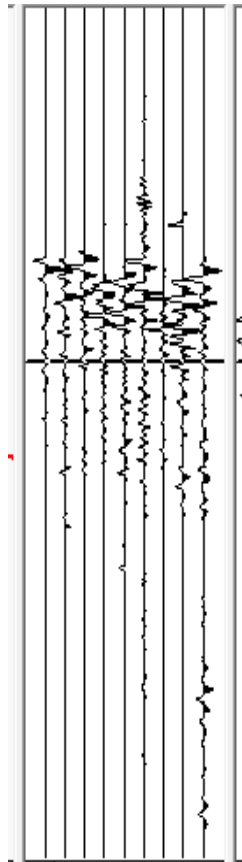
Figure 34 This is a stack response to picking velocity on the semblance spectrum as well as coordinating with the parabolic approximation of the target reflectors seen in the native data.

After picking a sufficient number of inline and crossline velocity spectra seen in Figure 35 , noting how it impacts the stack response and CVS response, a velocity function will be averaged for the data, which will then be used for normal moveout corrections as well as stacking. For the shallow reflectors which are approximated to be the Stone Corral reflector and others, this data will be sufficient for the subsequent steps of seismic processing, as seen in Figure 36. It can also be seen in this figure that the overall average velocity function denoted by the yellow line and the actual pic for velocity at this inline and crossline are differing in location on the semblance spectrum. This is since even though the approximate value of 9,000 ft/s as a velocity for the Stone Corral is a safe assumption over the whole survey, the actual velocity varies based on location due to many lithological influences such as compaction, dip, topography

and characteristic of the LVL (Sheriff and Geldart 1995). It can also be seen in Figure 37 through Figure 39 that the velocity function as a line changes from crossline to crossline even along the same inline. This further backs the idea that even though the average of 9,000 ft/s as a velocity for the Stone Corral is useable across the survey, line by line the velocity varies. This should be considered by the processor when looking at a dataset so that in the event of aberrant velocities somewhere in the survey area, a blanket assumption is not used and hinders the data in any way. As this process plays into static modeling, the local variability of velocity within a survey impacts the location of reflectors and refractors alike, moving both in normal moveout to correct or incorrect locations, therefore an iterative approach must be taken to properly understand the velocity profile of the subsurface throughout the entirety of the survey (Miller and Xia 1998). As discussed previously, these assumptions are quality controlled by the stack response of the data when velocity is picked, therefore giving a degree of certainty to the picked velocities.
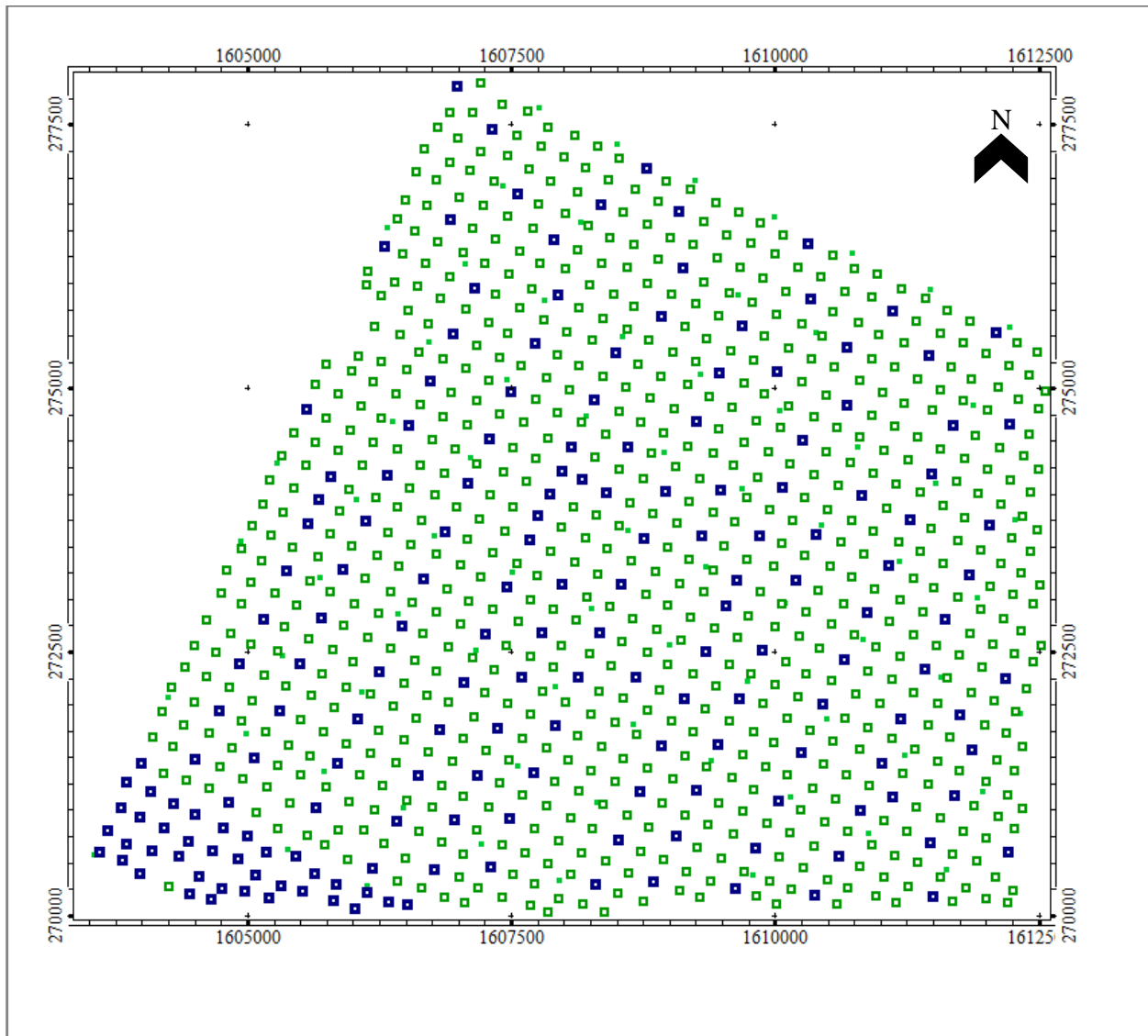
Figure 35 Shown above is the super gathered common depth points. The blue nodes are the super gathers with that have velocities picked within. The green nodes show the super gathers without picked velocities. The spatial extent of the picking is to give maximum spread to the velocity function, making it more robust.
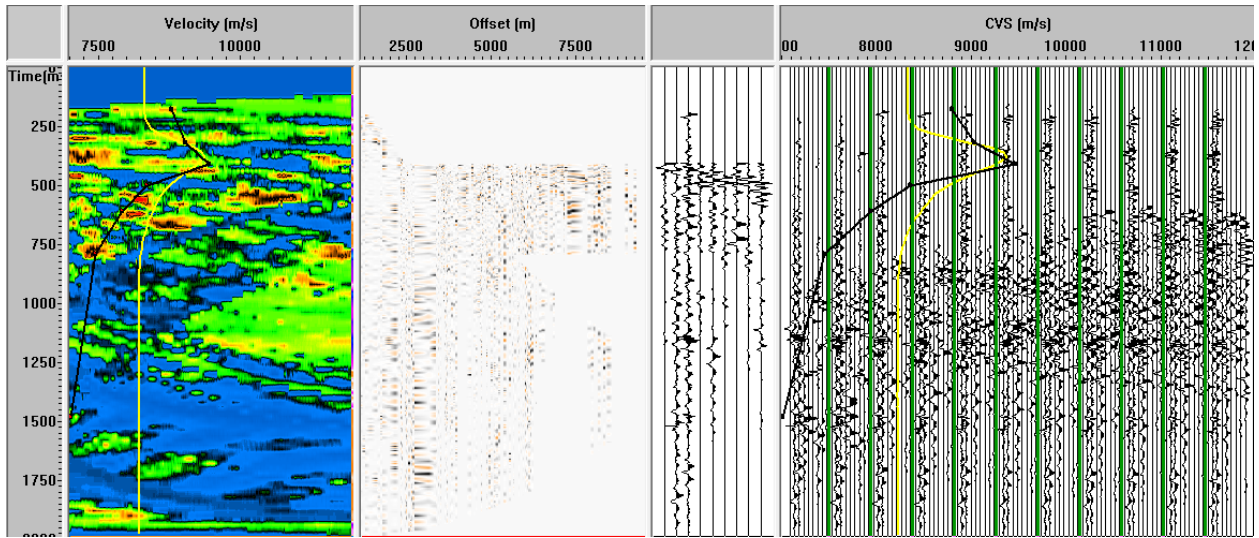
Figure 36 The figure above illustrates, from left to right, the semblance spectrum, the NMO correction, and the stack response based on the picked velocities. In the semblance pane, the yellow line indicates the overall average velocity function picked with the black line and points as the velocity picked at this inline and crossline.
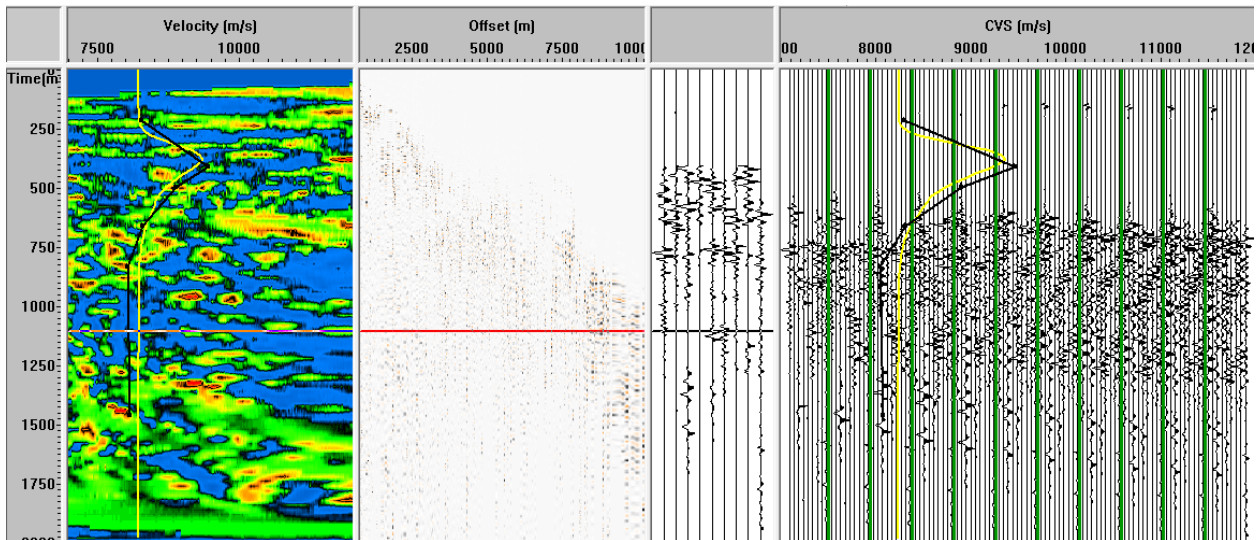
Figure 37 Velocity profile at inline 52 and crossline 70.

65
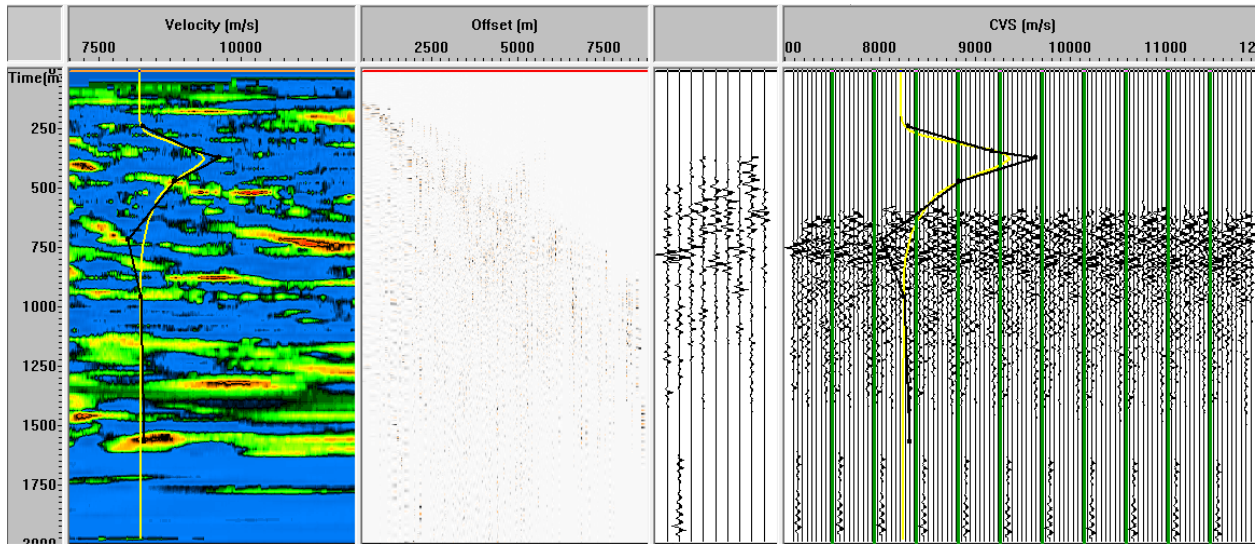
Figure 38 Velocity profile at inline 64 and crossline 76.
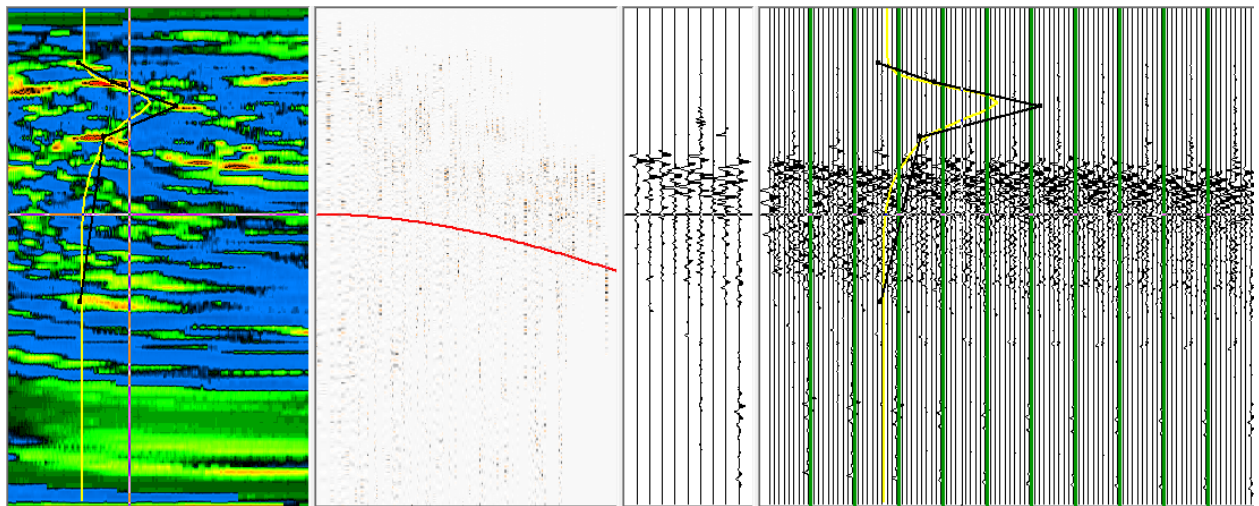
Figure 39 Velocity profile at inline 79 and crossline 67.

After the velocity picking is done, the next step in the seismic process is to stack the data in an ensemble as well as applying normal moveout (NMO). To do this, a dataset with CDP gathered geometry must be loaded into the workflow so that the proceeding modules will be able to apply the steps according to the proper headers. After the input traces are loaded, the normal moveout will be applied based on the velocity function given to the program from the previous interactive velocity analysis. As previously mentioned, the quality control of the velocity function is of the utmost importance because this function dictates the moveout of the data and

the correction that is applied to the offset to get data on the proper plane and of correct coherence. In the NMO module the mute percent is 60 percent so that the amount of NMO stretching effect is minimized while still preserving the overall effect of normal moveout bringing the reflectors into coherent linearity. After the NMO process is finished the next module is the Ensemble Stacking which will improve the overall data quality by reducing the noise and boosting the signal. Essentially this process adds the reflections from NMO and sums the trace to increase resolution. However, there are operating parameters to the stacking module, these being trace correction or trimming. In the case of this dataset, an alpha-trimming filter was used to decrease the amount of aberrant traces collected within the stack, further improving the quality of the ensemble stack. Alpha trimming organizes traces by common parameter, such as amplitude or corrected moveout and the ones that are the outliers, or in this case the 30 percent outliers on the high and low end are then filtered out to give the data more coherence.

reak and First Arrival

To properly account for the near surface, the first break in each cable in the seismic section must be analyzed and tracked. The refracted energy associated with the base of the weathering layer is closely associated with the first arrival on the shot gather. These occur in varying degrees of quality depending on the source type and the near-surface conditions (Yilmaz 2001). The shape of the refractor on the native seismic data can be influenced by the topography of the region as well as the character and shape of the weathered layer (Lawson 1989). Wherever there is a point in the refraction data where the shape and slope changes, this is called a crossover where the change of velocity or profile of the low velocity layer changes. There exist multiple causes for changes in the refraction character including compaction differences as well as shape of the low velocity layer in conjunction with the topographic profile, or a combination of the

two. Knowing the behavior and character of the refractor, the first break can be computed interpretively or by numerical methods, or both. This allows for an accurate representation of the first break as it corresponds to the LVL. Within the processing software RadEx Pro, there is a module to automatically track the first breaks as they appear in seismic section which is a methodology proposes by Hatherly (1982). The first break as it appears in seismic section coincides with the refraction data that will be used to calculate the static correction model Figure 40. The module that allows for this operates on specific sampling parameters within defined by the seismic processor, the most important parameter is to define the first break by the sign convention of the seismic impulse, and operating within American Standard polarity, which coincides with a positive reflection. Therefore, allowing for the sample size of the first break within amplitude bounds defined by the user, the first break can be tracked as the first positive reflection seen in the trace (Steeples et al. 1998). Using this first break pick, the seismic data will have an established datum to which the static correction can be assigned, which can then be imported into another module that references this pick and established the static correction. It can also be seen in Figure 40 that there is a differing character of refractor as previously defined within this chapter. The slope of the refractor changes from one cable to the next and this leads the interpreter to believe that there is indeed topographic and shape variation of the LVL. This fact supports the need for an iterative and robust analysis of the near surface and first break picks so that the subsequent reflectors and their velocities and share are preserved and mapped correctly within three-dimensional space.
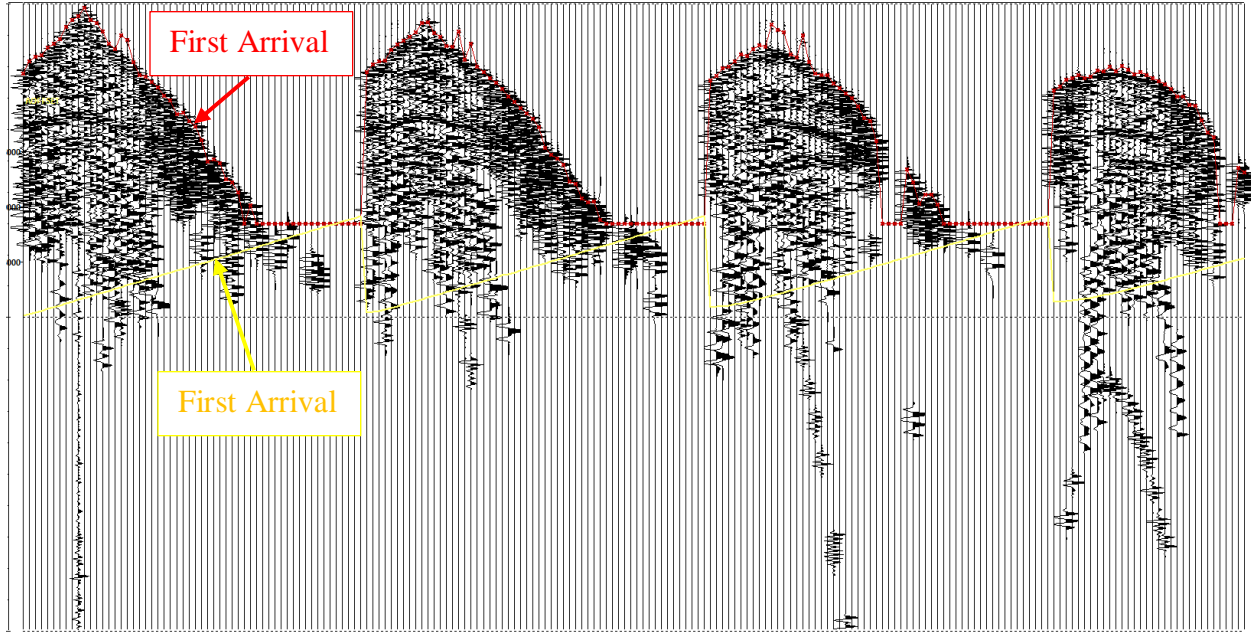
Figure 40 This figure illustrates the module of first break picking, which will be used in establishing the static model. The first break is denoted in the red color with offset in yellow. This method helps approximate the interval velocity of the LVL which is then used in defining the limits of velocity for the interactive velocity analysis.

n-based Statics Analysis

Another approach to statics and velocity corrections is what is known as Horizon Static

Modeling or Horizon Velocity Analysis (Yilmaz 2001) wherein the picked velocities for a

certain known horizon are then applied. There exist a couple ways to execute this process; a

more simplified one being that the velocity field for a given horizon over the entirety of the

survey will be calculated and applied to a previously interpreted horizon in three dimensions. By

calculating the velocity field for the horizon based on the newer interpretation, the difference in

layer velocity for the horizon can be calculated, effectively providing a velocity shift that will

place the horizon correctly in space. The initially interpreted horizon will be deconvolved with

its time depth in order to produce its velocity function as a surface within the survey. This will

then be subtracted from the new velocity surface to produce the corrected difference in velocity

which will then be reapplied to the surface to shift it into correct position based on the parameters defined by the new seismic workflow. This process is applied to the Stone Corral as it was picked based on the previously established workflow, not the current workflow that the author has defined in this thesis. This interpretation can then be further validated by stacking the new data and reinterpreting the Stone Corral based on the picked velocities from the IVA in order to provide a robust quality control of the data. Figure 52 below depicts the Stone Corral picked based on the data that was previously interpreted, not the corrected version. Using the software package, Surfer, to map the velocity, time and 3-domensional points of the data (Figure 41), the difference in time, or Δt, correction for the data can be applied graphically. The equation for this correction is:

$$\Delta t = \frac{h}{v}$$

Equation 3 This equation for the time correction, Δt, is calculated using *h* as the depth to the seismic datum and *v* as the interpreted replacement velocity down to the datum.

By using this equation, the difference in the time from calculated from the replacement velocities will allow for numerical mapping of the velocity field, allowing for a correction in time to be applied to the surface. The surfaces seen in the figures below depict the surfaces that were calculated using the equation above and how they were used to create the static time shift that can be applied to any surface within the seismic volume. The surfaces that were created to help achieve this outcome correlate to the time depth of the Stone Corral formation as previously picked in the seismic volume, the subsea depth of the Stone Corral as picked in the volume, the velocity map of the Stone Corral as it was picked in the author's workflow, as well as a map of the topography in the survey area. These maps and surfaces are pertinent in establishing the quality control of the velocity picks as well as the statics correction that was calculated (Beck and Steinberg 1986). As previously mentioned, the statics correction that was applied to the

Stone Corral can be applied to any surface in the seismic volume if it has been picked with accuracy. This calculation is a summation of the velocity work previously completed. The Stone Corral correction iterations are completed and listed below. Each iteration was completed to find the most effective way to compensate for the effects of the imprinting of the topography upon the subsurface. As previously mentioned, this effect is due to the variable velocity of the near surface and inaccurate placement of the seismic datum in the subsurface. By calculating a velocity field corresponding to the near surface, above the stone corral and below the topography, as well as establishing a datum by trial and error, the maximum correction could be found to mitigate the effects of the topographic imprint. Using this workflow of incorporating the velocity field and seismic datum, the optimal seismic datum is placed at 1300 feet above sea level, which created a corrected Stone Corral time-structure map that flattened the subsurface as much as possible without overcorrection. The spectrum of datum locations ranged from 1100 feet above sea level to 2000 feet giving a robust analysis of the effect of different datums on the seismic data. This is the final step in the proposed workflow wherein the initially incorrect horizon in two-way-time is now corrected for an accurate representation of the subsurface.
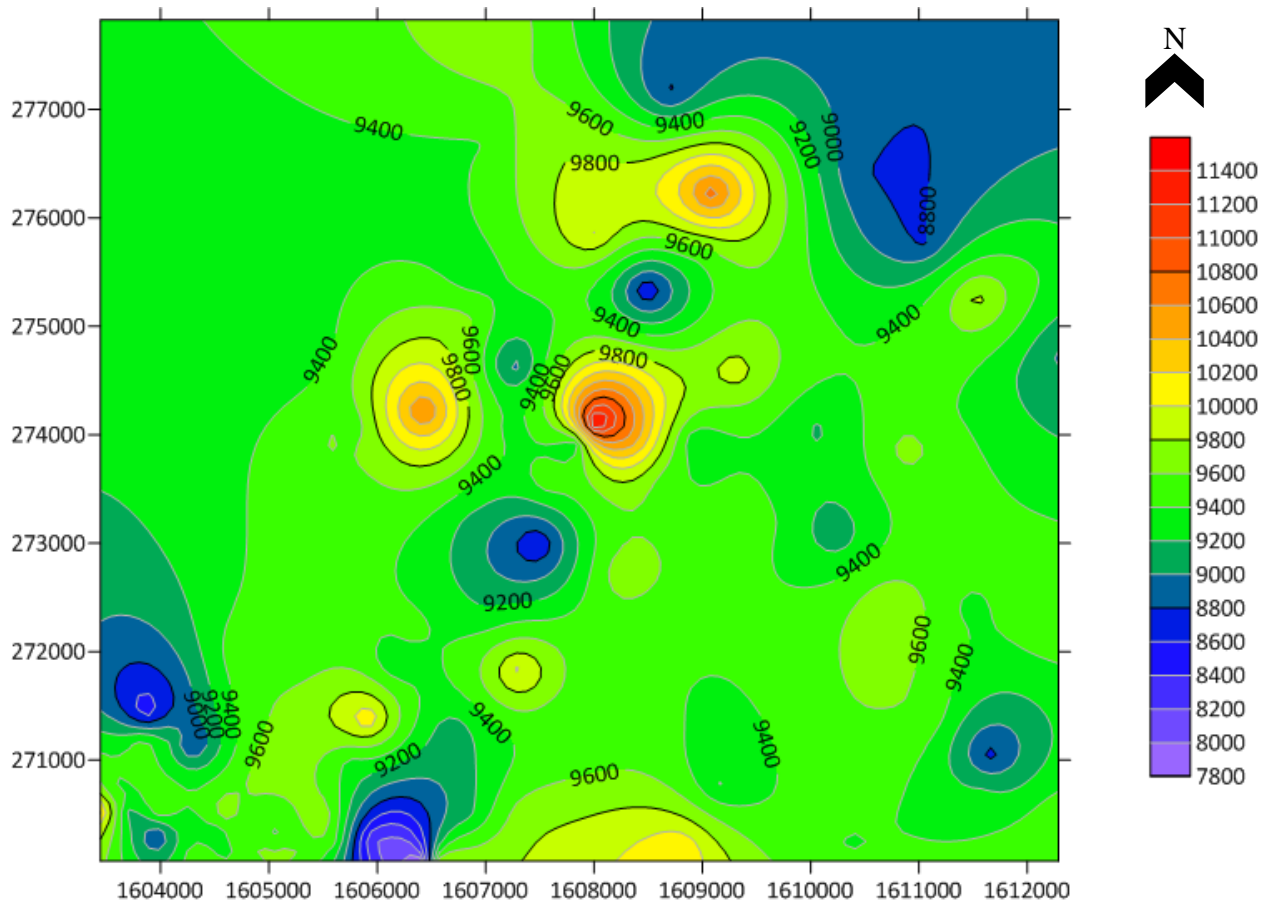
Figure 41 The figure above illustrates the velocity field picked across the survey area with the warmest colors being the highest velocities and the cooler colors being the slowest velocities. This map shows that there is variable velocity values and therefore a constant velocity analysis would be improper in creating a seismic datum.
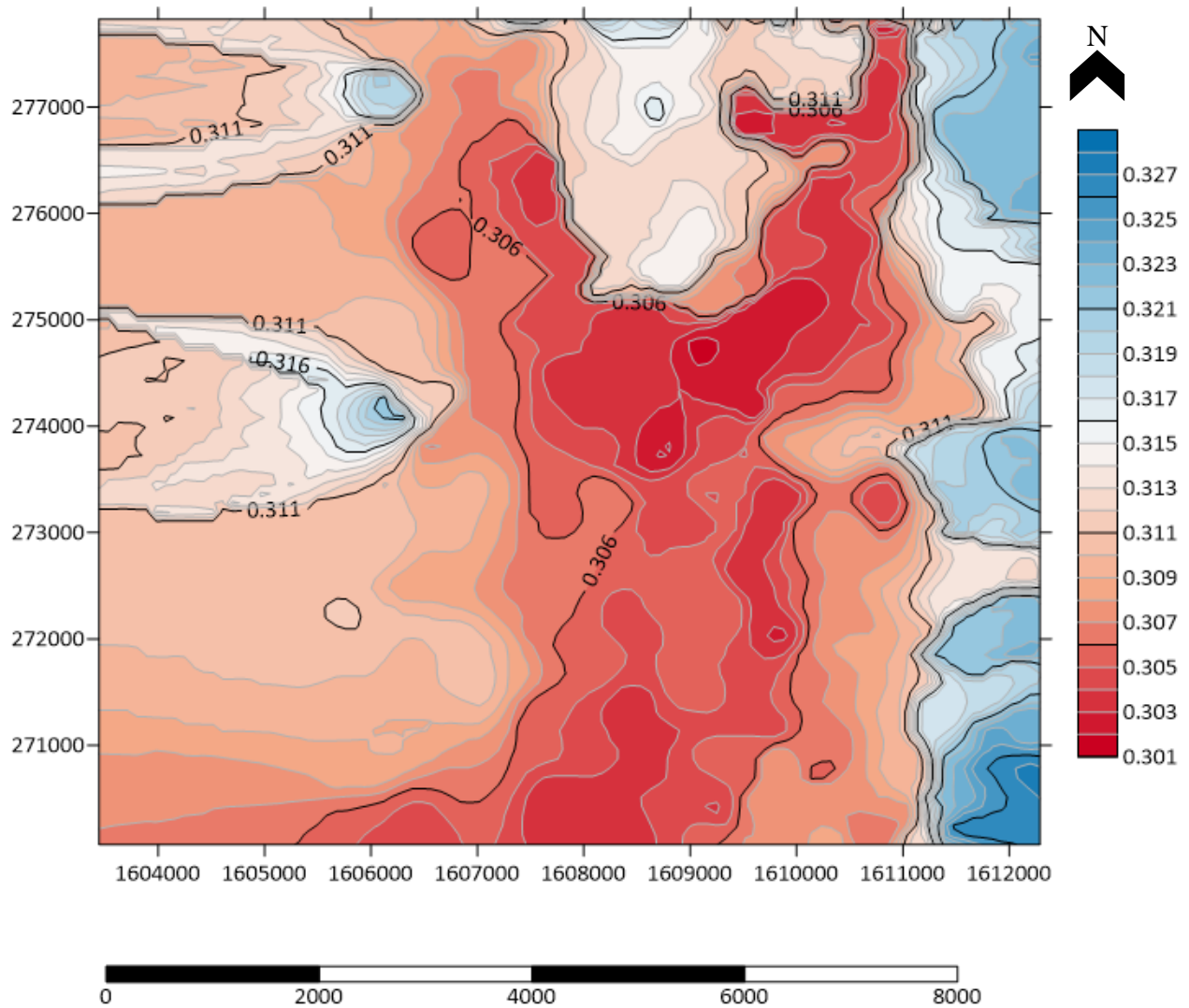
Figure 42 **The figure above illustrates the time structure map of the Stone Corral, and when referencing the topographic map of the area, they mirror one another, which as referenced before, should raise questions as to the validity of the processing as well as the placement of a proper seismic datum.**
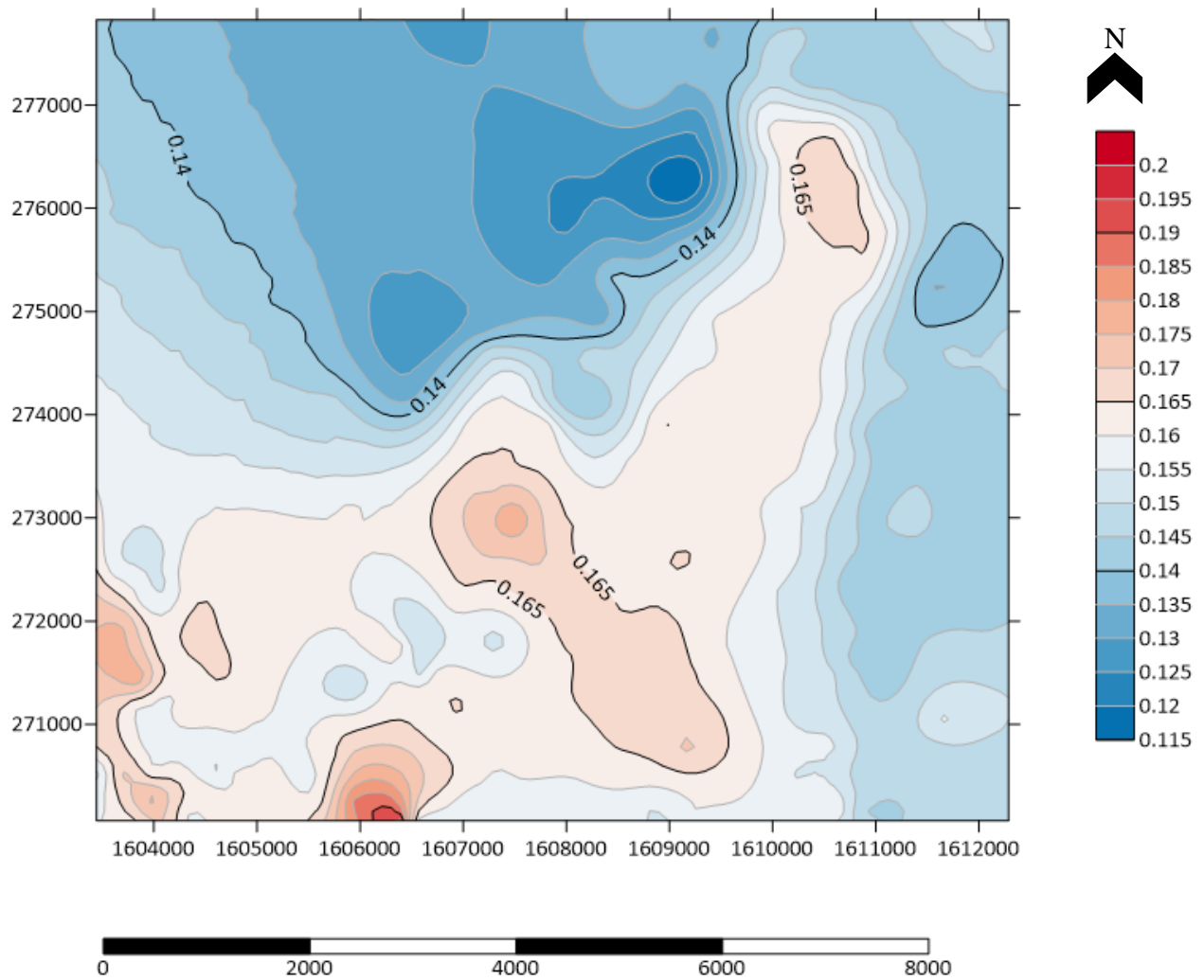
Figure 43 The figure above is a product of the correction equation listed above. The correction is in the time domain and as a static correction, can be applied to any surface within the seismic volume. The datum used for this is 1300 feet depth.
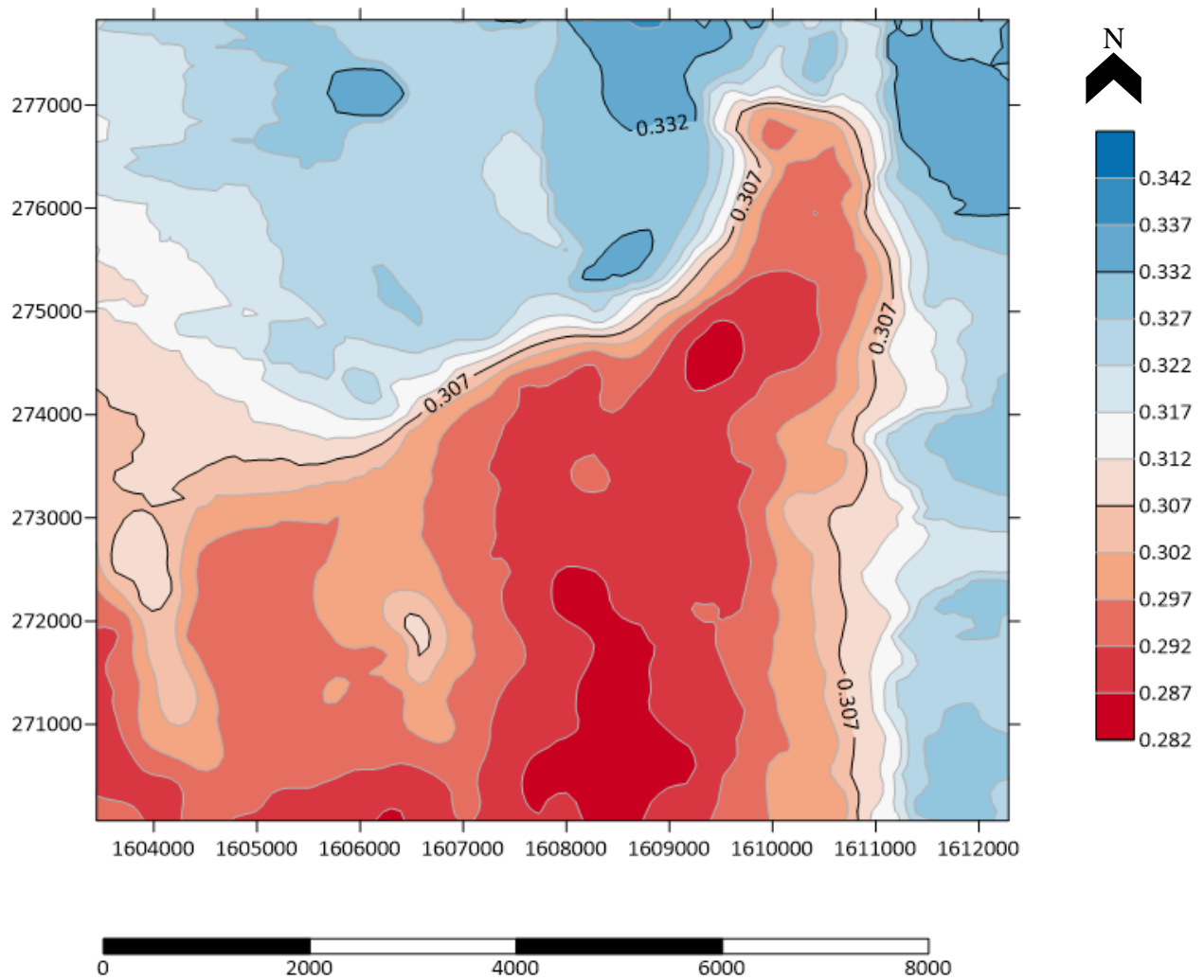
Figure 44 **The figure above is the Stone Corral formation picked in seismic two-way-time corrected using a datum of 2000 feet above sea level. This datum is most closely associated with the topographic elevation, notice the severity of the topographic impact on the subsurface.**
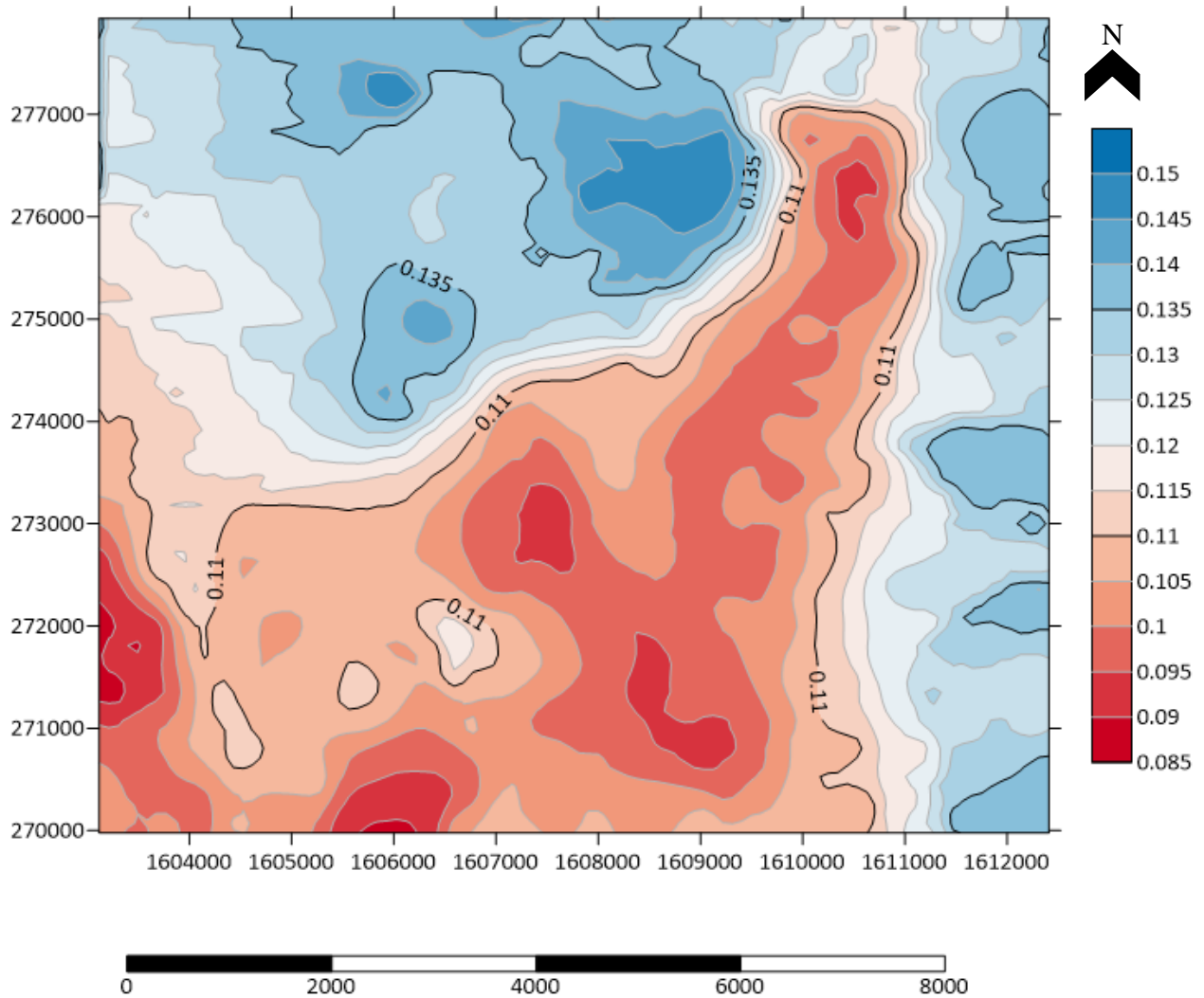
Figure 45 The figure above is an iteration of the Stone Corral formation as it was corrected using a seismic datum of 1100 feet elevation. If we compare the 1200 foot, 1300 foot and this, the 1100 foot datum elevation we can see that 1400 correction is too little correction, the 1100 foot elevation is too much which leaves the 1300 foot elevation as the optimal elevation for the datum correction.
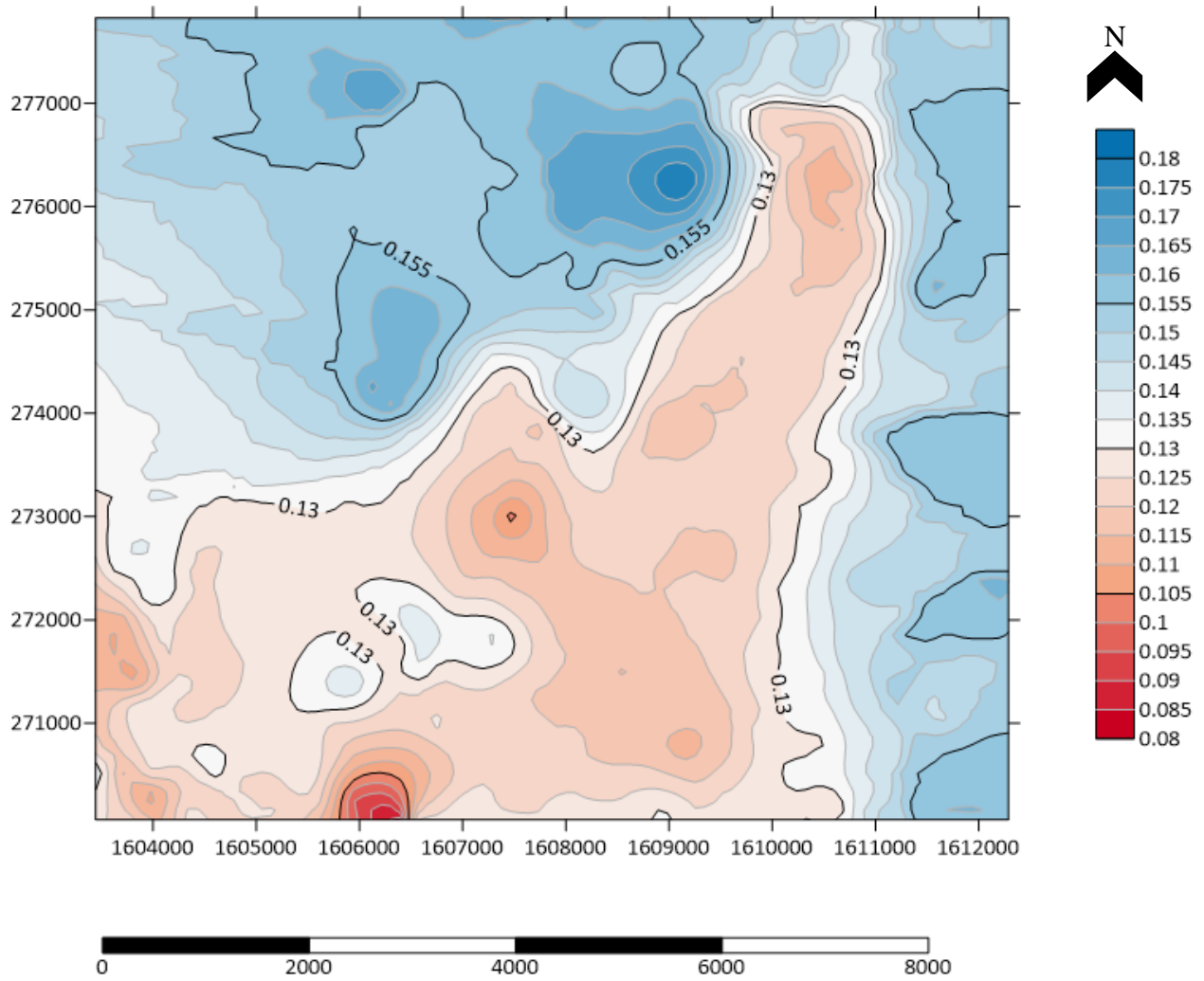
Figure 46 The figure above is an iteration of the Stone Corral formation as it was corrected using a seismic datum of 1200 feet elevation.
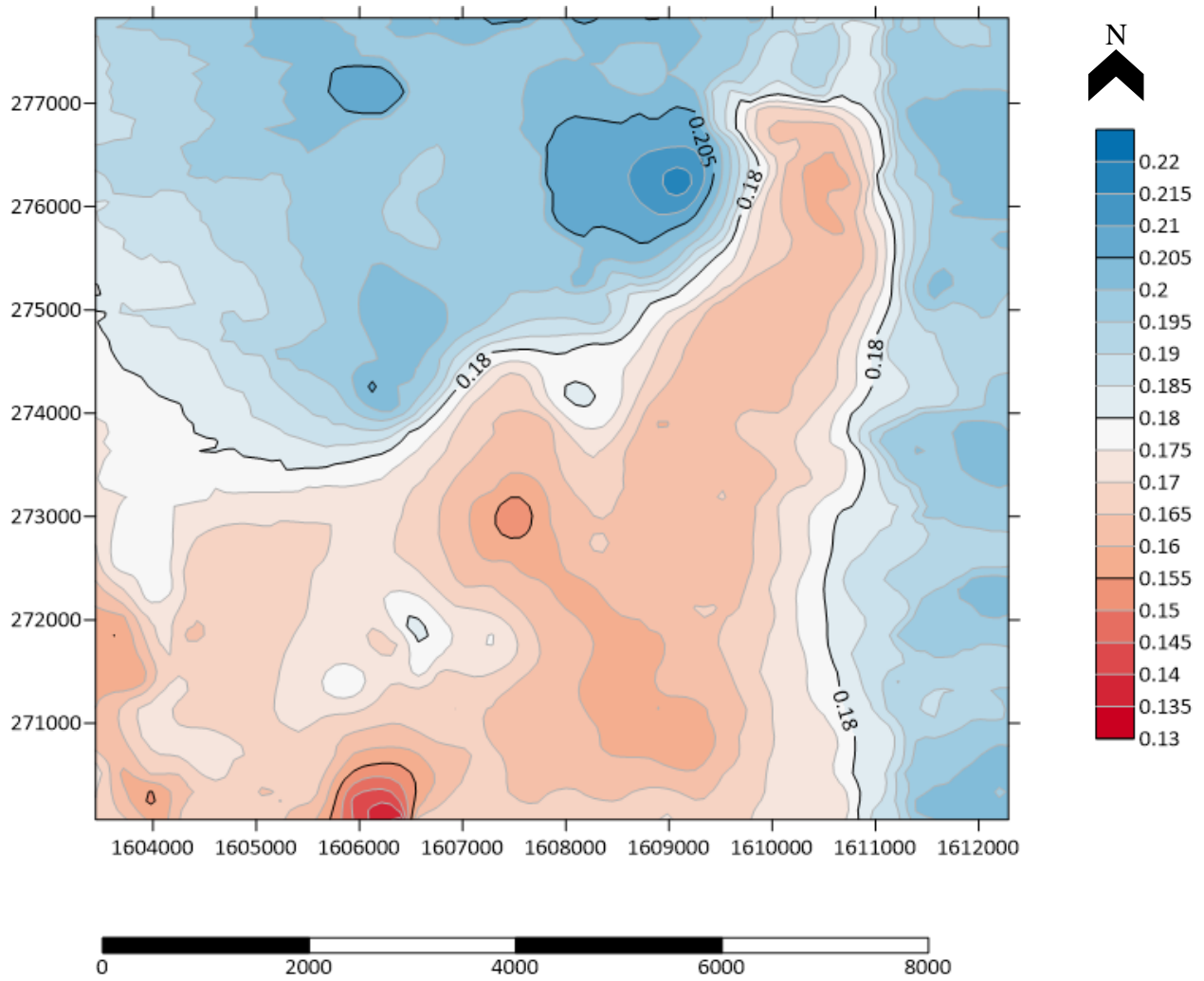
Figure 47 The figure above is an iteration of the Stone Corral formation as it was corrected using a seismic datum of 1400 feet elevation.
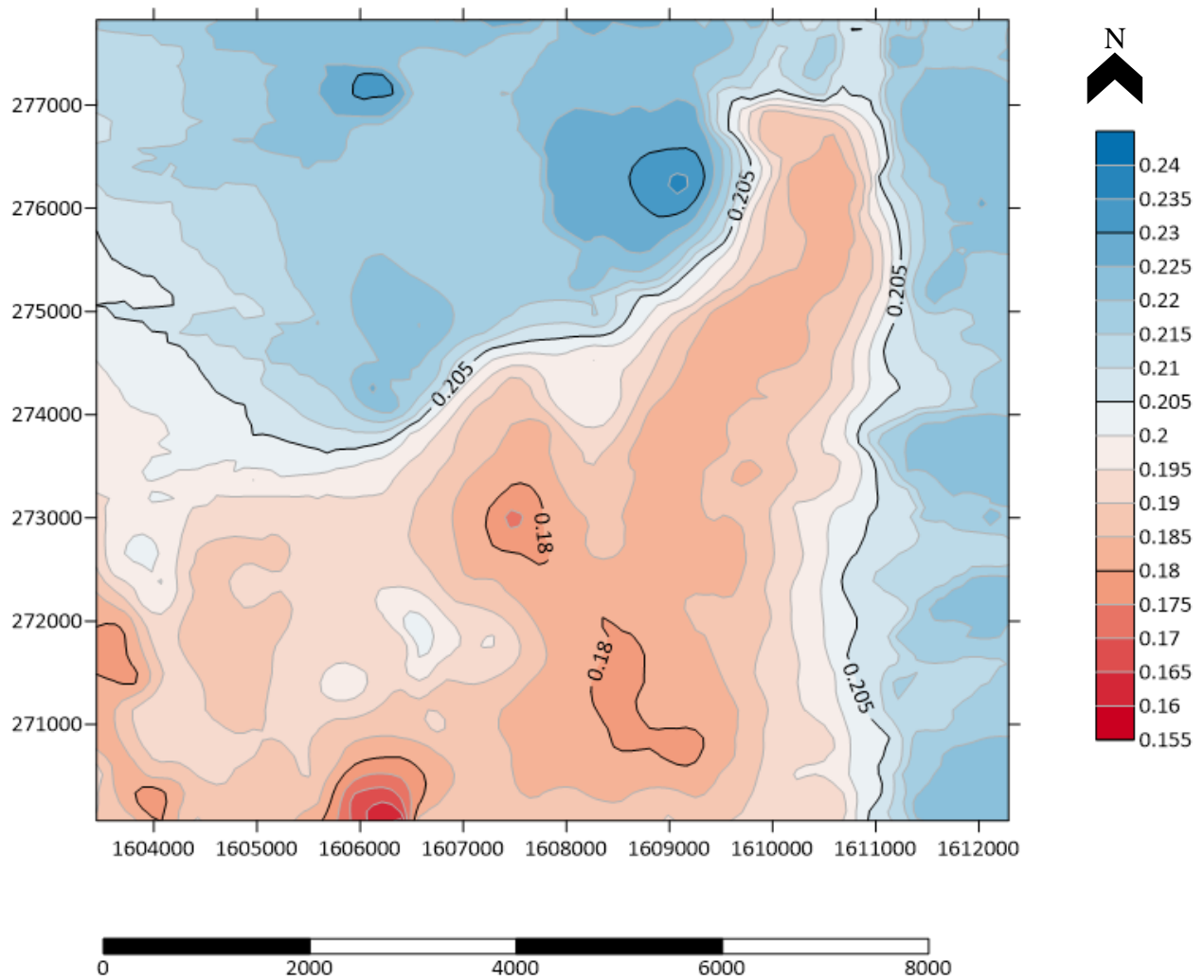
Figure 48 The figure above is an iteration of the Stone Corral formation as it was corrected using a seismic datum of 1500 feet elevation.
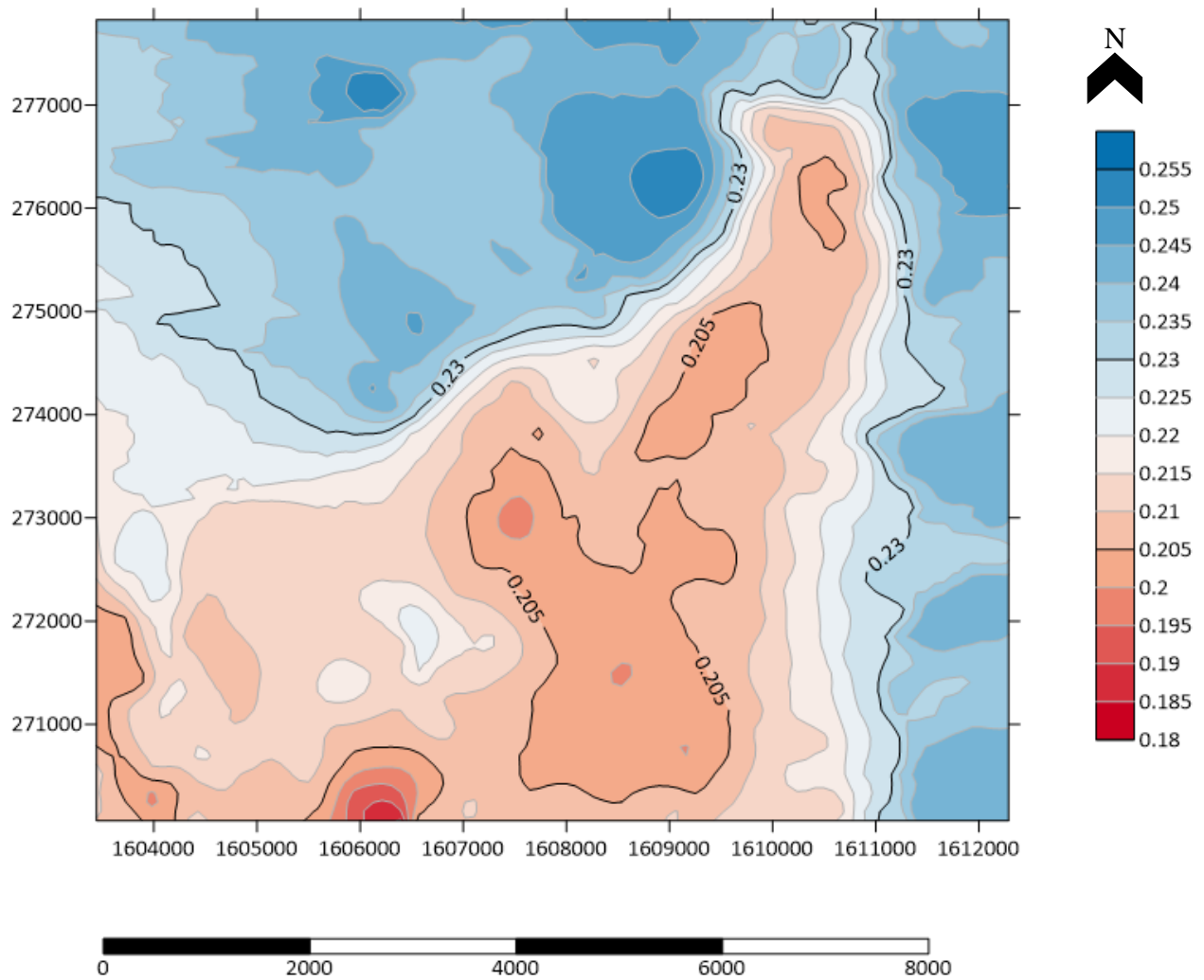
Figure 49 The figure above is an iteration of the Stone Corral formation as it was corrected using a seismic datum of 1600 feet elevation.
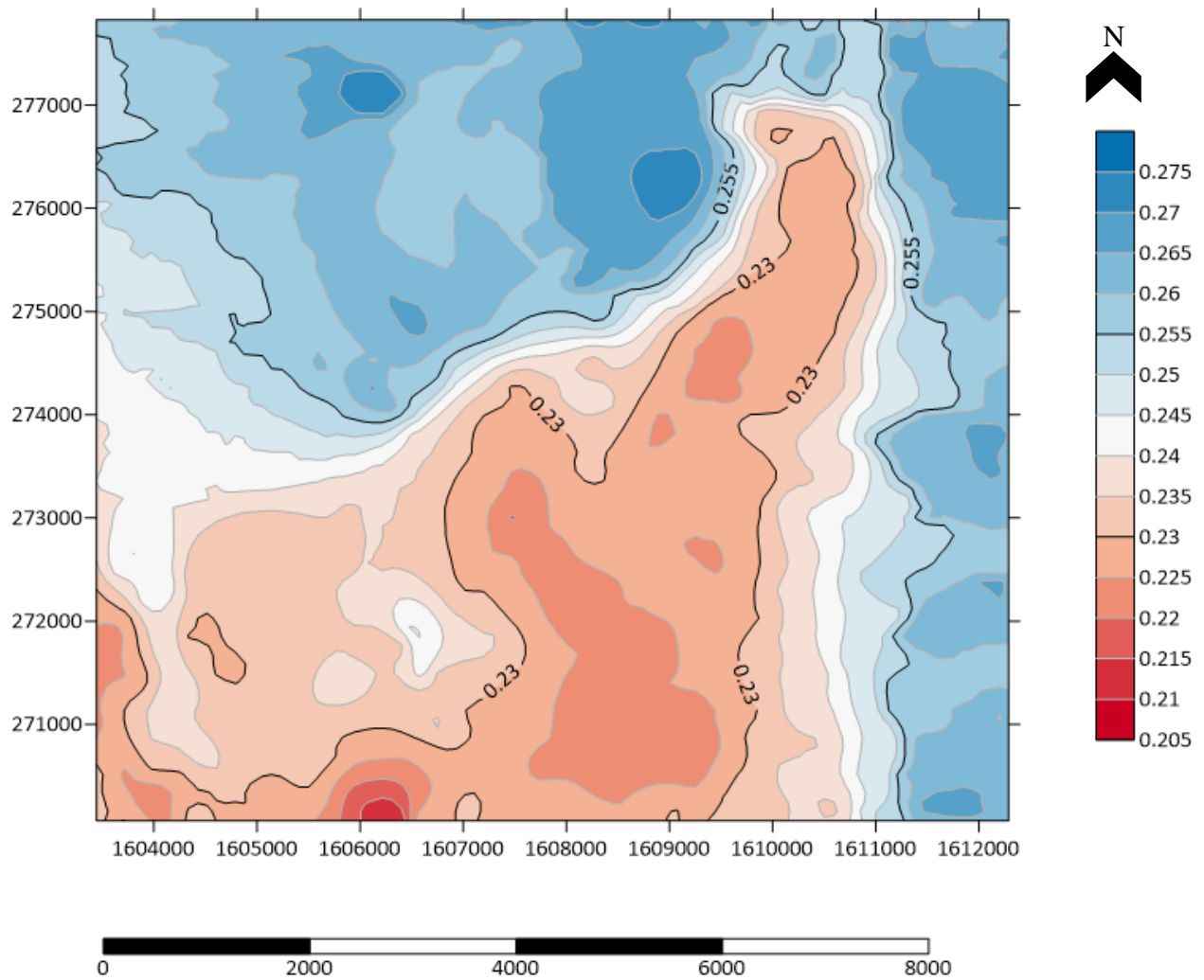
Figure 50 The figure above is an iteration of the Stone Corral formation as it was corrected using a seismic datum of 1700 feet elevation.
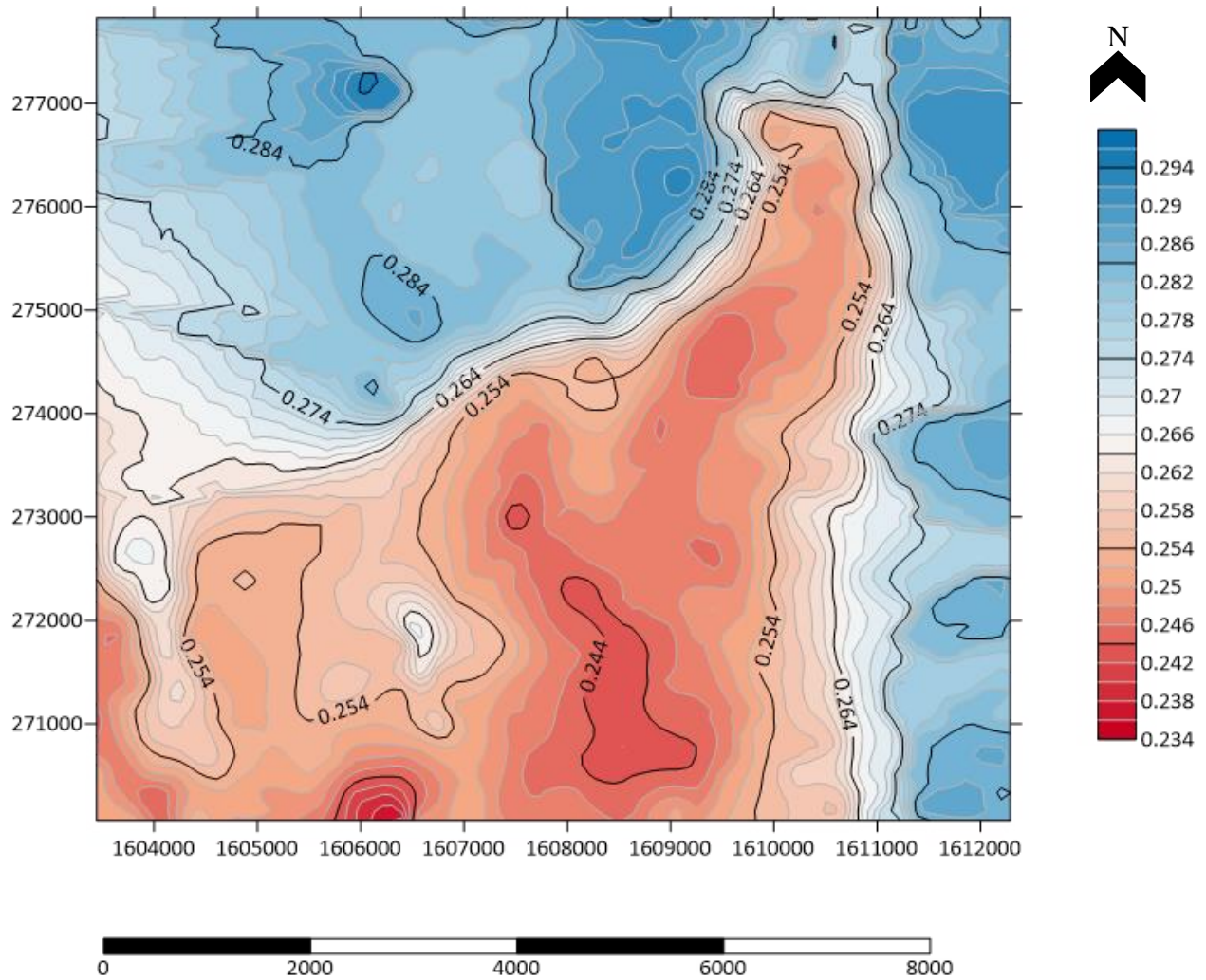
Figure 51 The figure above is an iteration of the Stone Corral formation as it was corrected using a seismic datum of 1800 feet elevation.
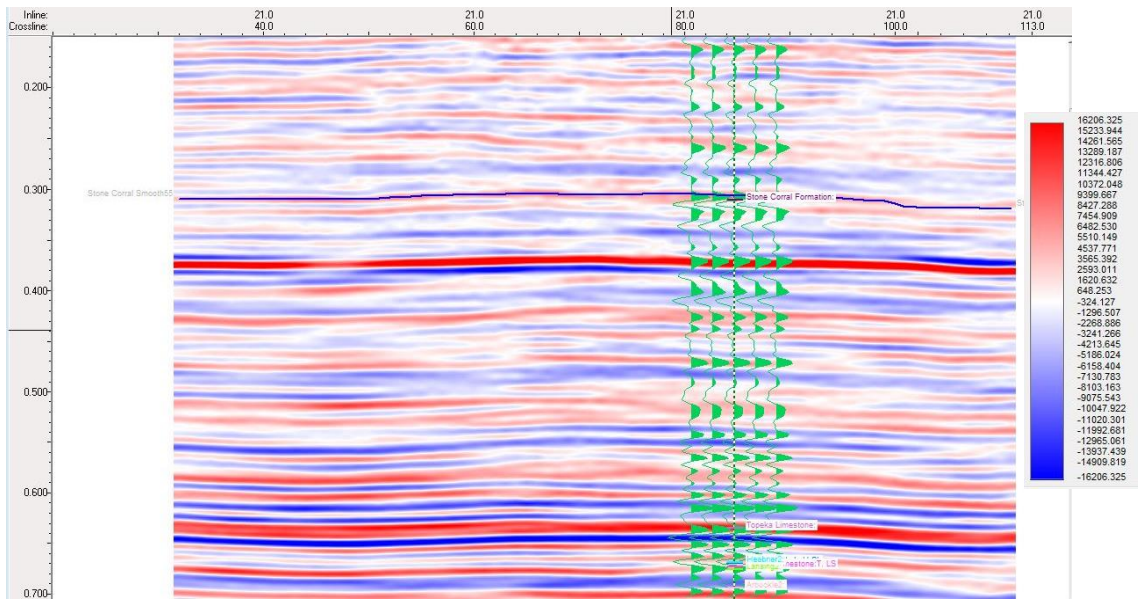
Figure 52 The figure above provides an interpretation of the Stone Corral based on the post-stack data provided to the author. A horizon velocity shift will correct this surface in three-dimensional space.

Chapter 6 - Seismic Interpretation

The Stone Corral is the formation on which the interpretation and comparison will be made. We will compare the previous interpretation supplied by the last interpreter to the interpretation made by the author based on the seismic workflow proposed. The interpretation will be made in two-way time (TWT) as well as the depth domain as the depth domain can be tied to well reports and reflects the accuracy of normal moveout and statics corrections. It can be seen in Figure 53and Figure 54 that the maps are TWT and depth domain and the Stone Corral lies at around 305 milliseconds and 1147 ft depth. In the pre-stack data interpreted by the author, the Stone Corral existed at an average depth of around 400 milliseconds in TWT depending on the local variation. Also, the Stone Corral is picked at 1147 feet in depth, but it is known from drilling reports in the area that the Stone Corral sits at around 1410-1420 feet in the subsurface. Even before looking at a reinterpreted section of the Stone Corral, based on the evidence provided by well control, the previously interpreted section is indeed incorrect. Whether or not this is due to misinterpretation of the actual Stone Corral reflector or the incorrect application of velocity and static modeling will be explained in the hitherto section.

Discussing the seismic interpretation as it pertains to the datum elevation, the author previously notes that the 1300-foot is the optimal datum for statics corrections as the 1400-foot and the 1100-foot datums either leave too little corrected or overcorrect respectively. This workflow suggests that by a trial and error methodology, one can derive the correct datum elevation and give the most accurate and highest fidelity seismic profile of a reflector in the subsurface. This workflow and general application of theory coincides with what Steeples et al.

propose in 1990 wherein reflection data can be used in the interpretation of static corrections,

validating the process used for this dataset.
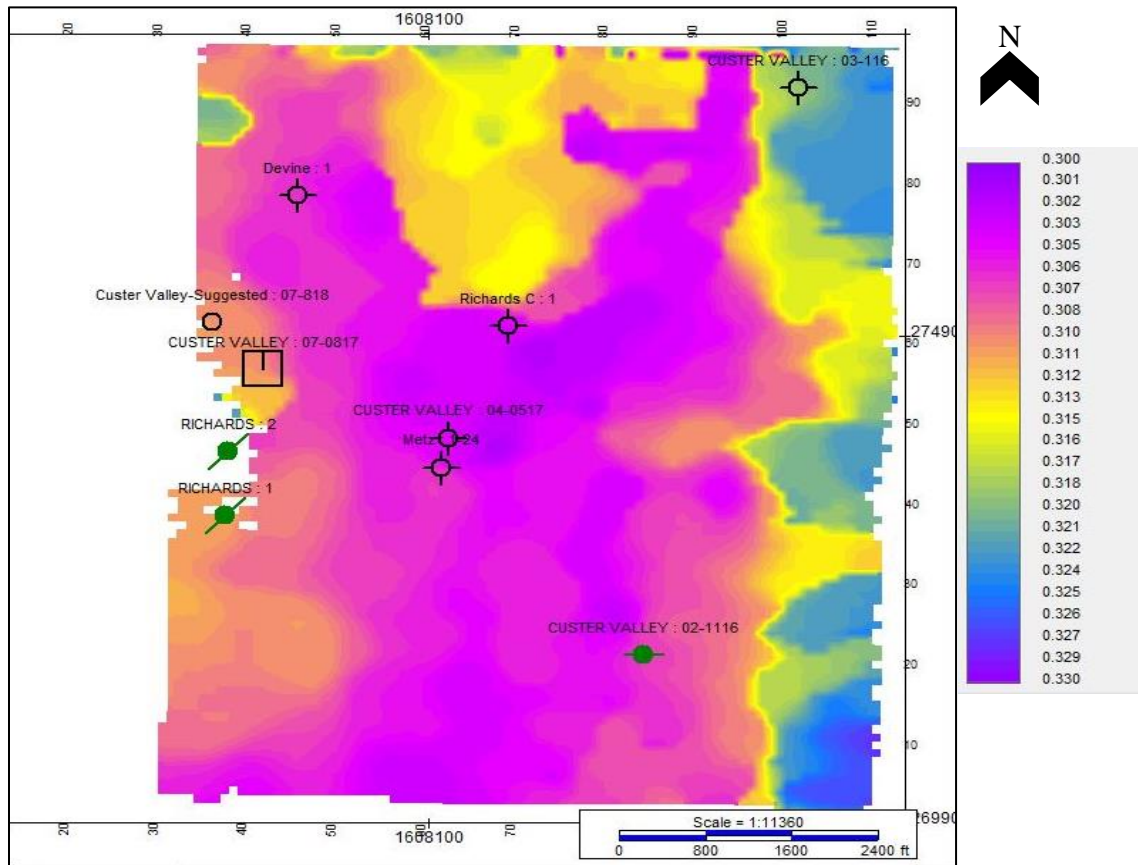
Figure 53 This is a figure of the Stone Corral formation interpreted from the post stack data given to the author with the pre-stack data. On overage the Stone Corral lies at about 305 ms in two-way time.
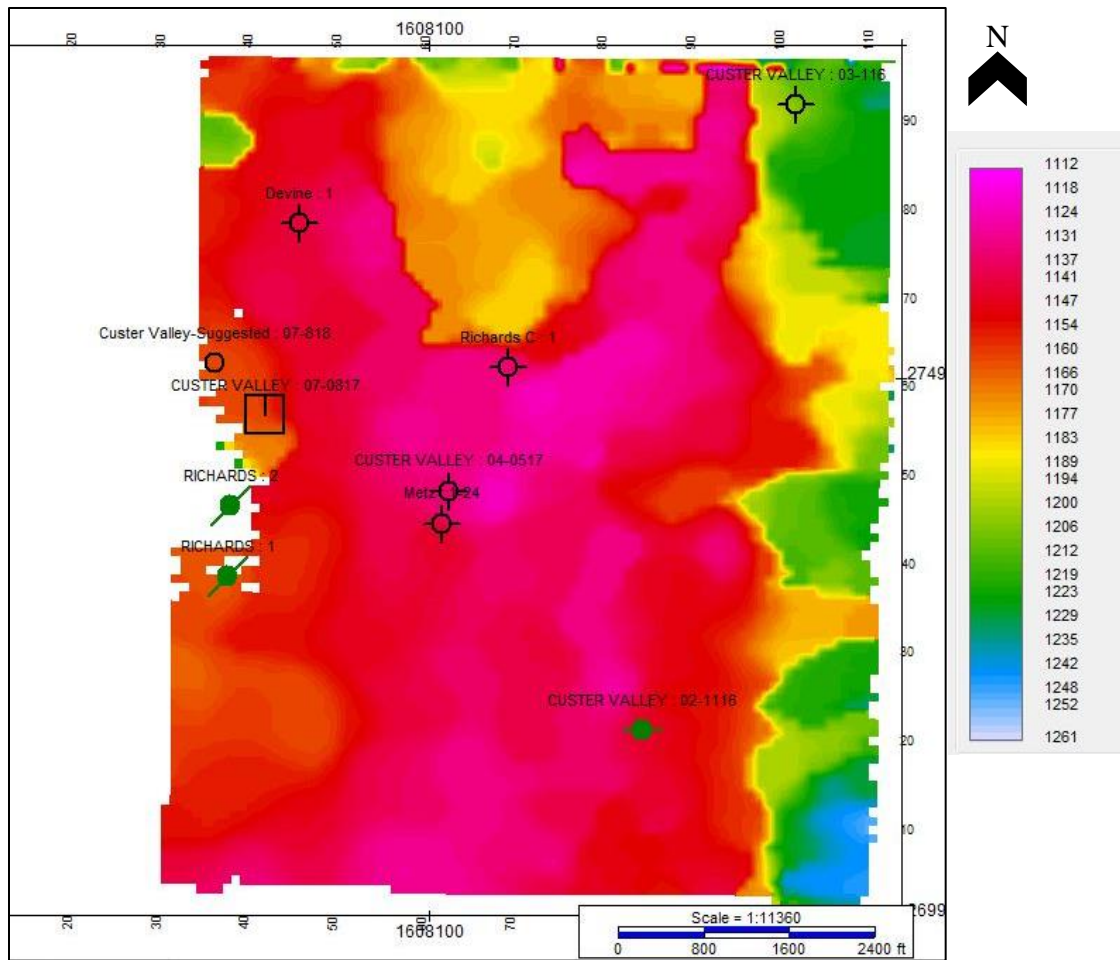
Figure 54 the figure above is a depth map of the Stone Corral formation based on the seismic reflector that was picked in the post stack data provided by the original interpreter.
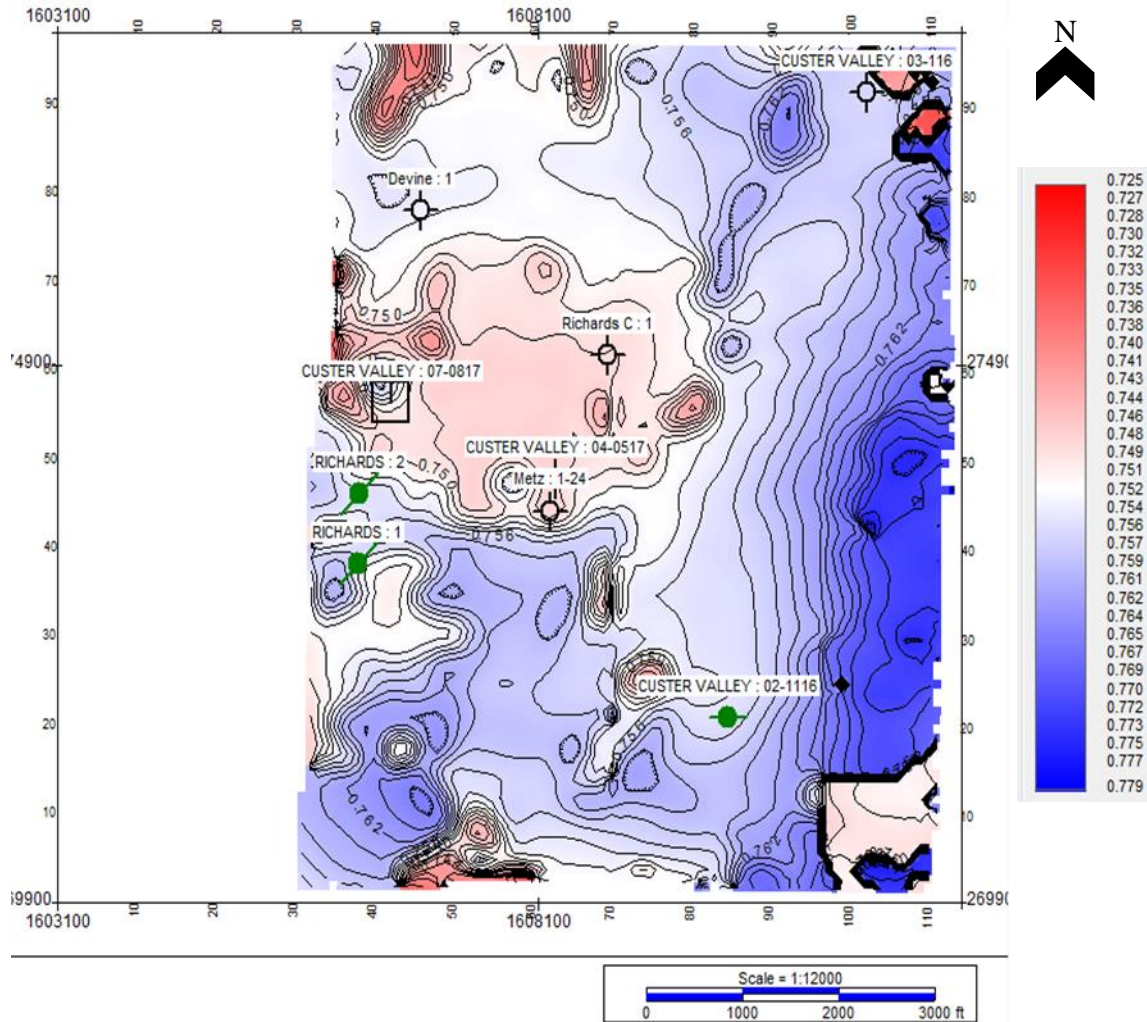
Figure 55 This figure shows the structure interpreted in the study area before the seismic processing workflow had been applied to the pre-stack data. Amplitude is the primary attribute used.
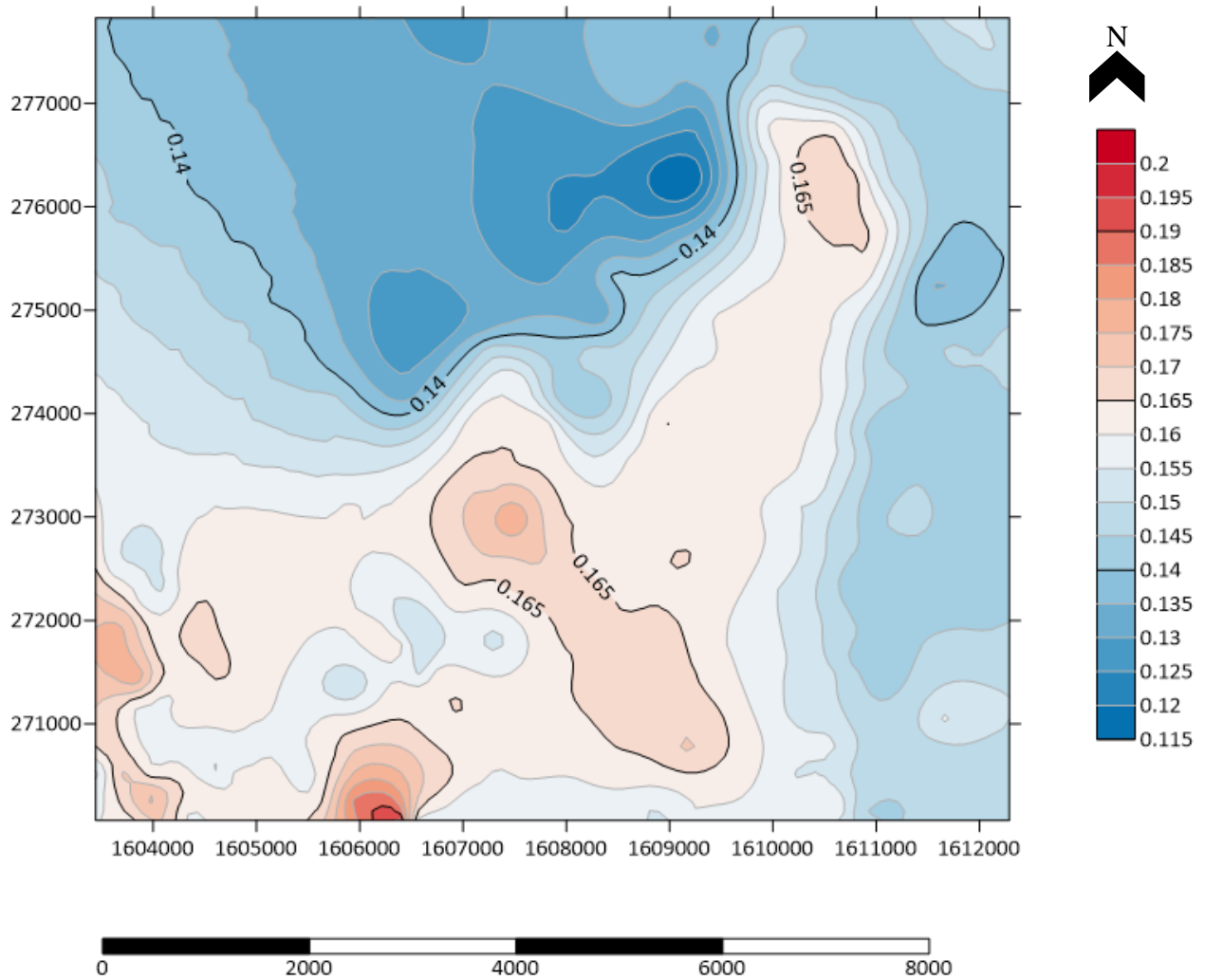
Figure 56 The figure above was listed previously as an iteration of Stone Corral corrections at a datum elevation of 1300 feet subsea. The improvement of the topographic imprint on the subsurface is proven in this iteration therefore proving the validity of the processing workflow.

Chapter 7 - Discussion of Data Quality Control

The steps that have been outlines in this thesis have aimed to take any dataset provided, regardless of data quality and content and provide a reliable workflow to properly process the given data based on the key fundamentals of seismic processing. These being (1) Data Initialization, (2) Assigning Correct Geometry, (3) Amplitude Processing, (4) Noise Attenuation, (5) Deconvolution, (6) Multiple Attenuation, (7) Velocity Analysis and Normal Move Out (NMO), (8) Migration, and (9) Stacking, as previously mentioned in Chapter 2. Each step in the seismic processing workflow is designed to improve the native data quality by enhancing the signal-to-noise ratio (SNR) so that more of the data will be usable for interpretation. Each step in the seismic processing workflow has individual modules and iterations that must be carefully considered when attempting to improve the SNR because as each step seeks to improve the quality of the data by changing parameters, there is also a chance to damage the native data so that aspects like seismic reflectors or refractors are lost. While occasionally this cannot be avoided, as there are tradeoffs, the basis of quality control seeks to safeguard against the possibility of catastrophic loss of data.

Seismic data geometry is often the most overlooked step in the processing of seismic data and often results in the most detrimental effects to the data id it is not properly accounted for. The chapter concerning seismic data geometry and the associated sections within this thesis surmise that if there is inconsistent data geometry correlation between the native data and what appears in the header geometry sheet, there will inevitably be data loss. The problems associated with the receiver and source line enumeration and hierarchy seen in this dataset are proof that if not corrected, the traces

will not be placed correctly within three-dimensional space. This leads to the character of

seismic reflectors being misrepresented, and in the worst-case scenario, data being

excised from the dataset to preserve the fidelity of the accurate and salvageable data. The

comparison of source line and receiver lines before and after correction verify the need

for quality control of the data.

Seismic velocity analysis can take place after the geometry is established

correctly and has been verified for accuracy. The velocity analysis is important in the fact

that it allows for normal moveout of the data and helps in establishing the time-depth

conversion of the data later with the use of a synthetic. Velocity data is considered one of

the most important aspects in seismic data processing outside of correcting geometry

because many of the aspects of the seismic process that come after are contingent upon

the accuracy of the velocity. Mentioned previously in the statics correction chapter of this

thesis, the processes for picking velocity is explained but while most processors pick

strictly based on the semblance spectrum of the data, checking for validity within the

stack response is a useful way to quality control the velocity picks so that aberrant picks

are not used. For instance, within this dataset there existed a pocket of high semblance in

the data at 400 milliseconds at over 11,500 feet/second. This semblance pick may seem to

be valid based solely on its highlight within the spectrum. However, knowing that at this

time-depth the Stone Corral reflector truly exists at closer to 9,200 to 10,000 ft/sec allows

for quality control of the velocity pick. The stack response of the pick in CVS and bulk

stack display allows for validation of the semblance pick that was based on what was

interpreted from the hyperbolic approximation of the Stone Corral originally. This

multifaceted approach provides the most robust way of picking the velocity for the

entirety of the survey, giving confidence that the velocities will be accurate for building the stack.

The next step in the seismic processing workflow, as listed in this thesis, is static corrections and how they affect the quality of the data. In this process, the effect on the data is different than that of the geometry but shares some similarities. The statics corrections seek to bring coherence to reflectors that are placed in space by correct geometry, considering the variations in the low velocity layer. If this step in the seismic workflow is not properly quality controlled, then there is loss of coherence as well as a loss of signal-to-noise ratio which will later make interpreting horizons in 3D seismic that much more difficult. Comparing the approach used in the proposed seismic workflow to that which was used previously on this dataset, there is notable changes in the quality of the data. This being that the previous workflow suggested that all seismic data above the Stone Corral seismic reflector has a constant replacement velocity of 9,000 feet per second and did not properly account for the changes in density and topography. These factors that were overlooked, influence the character and position of the reflectors in space. While other datasets may exhibit different needs in terms of time and effort in different quality control modules, this dataset was required extensive quality control and care in the aspect of geometry and velocity modeling. As previously discussed in the aforementioned chapters, the most discrepancy between seismic processing workflows appeared in these steps and accounts for the most variation. However, this is not to say this will be the case for all datasets, for the seismic workflow proposed here will consider the variations in datasets. For example, many datasets may rely heavily on dynamic corrections to improve the quality of the data, as there may be issues with the

deconvolution of reflectors or there may be issues posed by the incorrect account of wavefield attenuation with depth. As with any robust seismic processing workflow each of these steps and associated quality control was performed on this dataset to further provide more accurate data for interpretation.

The steps in the seismic processing workflow then give rise to what could be considered the final quality control iteration of pre-stack seismic data, the seismic interpretation of the stacked and migrated seismic volume. The summation of all the steps and iterations put forth in this thesis cumulate into a 3-dimensional seismic volume on which horizons and surfaces are interpreted. Therefore, all the steps taken to improve the quality of the data show their effect. This stage is where the problems with datasets compound but without close analysis of the pre-stack data, they would not reveal themselves in the volume. The final step to quality control a dataset from one seismic processing workflow to another would be to compare a known seismic reflector picked over a study area and compare the character of the reflector; the amplitude and frequency spectra as well as the location of the reflector in the subsurface. The depth location and dip character of the surface are directly impacted by the steps outlines by this workflow and are optimized by the quality control of each step and iteration. However, the work done on correcting the statics from the surface-time static shift can also be considered for the application of the seismic interpretation as most of these corrections are made post-stack. The surfaces for topography, velocity and time correction are useful in validating quality control as they provide tangible evidence for the steps of the processing workflow that go into correcting data and improving signal-to-noise. For example, if incorrect processing or insufficient attention has been paid to the steps in the processing workflow,

the issues that arise will become more apparent in these maps and surfaces than they would be in the native data that corresponds with these maps. This is because the maps provide more tangible evidence for interpreting the horizons and corrections. The surfaces provide visible evidence, rather than numerical, showing the effects of the processing workflow and how it impacts the native data and inherent quality.

Chapter 8 - Bibliography

Baars, D. L., and E. A. Brostuen, n.d., Petroleum: a primer for Kansas--Start: <http://www.kgs.ku.edu/Publications/Oil/index.html> (accessed January 5, 2019).

Beck, A., and Steinberg, J., 1986, Datum corrections using transfer velocity map: Presented at the 3rd Ann. Summer Res. Workshop: society of Exploration Geophysics

Brown, A. R., 2011, Interpretation of three-dimensional seismic data: Tulsa, OK, Published jointly by American Association of Petroleum Geologists and the Society of Exploration Geophysicists.

Chapin, C. E., 2008, Interplay of oceanographic and paleoclimate events with tectonism during middle to late Miocene sedimentation across the southwestern USA: Geosphere, v. 4, no. 6, p. 976–991, doi:10.1130/ges00171.1.

Cole, V. B., 1975, Subsurface Ordovician-Cambrian rocks in Kansas: Kansas Geological Survey: Subsurface Geology, p. 18.

Cox, M., E. F. Scherrer, and R. Chen, 1999, Static corrections for seismic reflection surveys: Tulsa, OK, Society of Exploration Geophysicists.

Franseen, Evan & Byrnes, Alan P. & Cansler, Jason & Steinhauff, D. & Carr, Timothy. (2004). The Geology of Kansas Arbuckle Group. Current Research in Earth Sciences. 250.

Frei, W., R. Bauer, P. Corboz, and D. Martin, 2015, Pitfalls in processing near-surface reflection-seismic data: Beware of static corrections and migration: The Leading Edge, v. 34, no. 11, p. 1382–1385, doi:10.1190/tle34111382.1.

Goupillaud, P. L., 1961, An Approach To Inverse Filtering Of Near-Surface Layer Effects From Seismic Records: Geophysics, v. 26, no. 6, p. 754–760, doi:10.1190/1.1438951.

Hatherly, P. J., 1982, A computer method for determining seismic first arrival times: Geophysics, v. 47, no. 10, p. 1431–1436, doi:10.1190/1.1441291.

Krey, T., 1954, A Remark Concerning The Problem Of How To Place The Reference Plane (Datum Level) In Reflection Seismic Prospecting*: Geophysical Prospecting, v. 2, no. 4, p. 281–284, doi:10.1111/j.1365-2478.1954.tb01293.x.

Li, Q., H. Feng, and Q. Li, 2011, Method of seismic interactive velocity analysis: Beijing 2009 International Geophysical Conference and Exposition, Beijing, China, 24–27 April 2009, doi:10.1190/1.3603593.

Miller, R. D., and J. Xia, 1998, Large near-surface velocity gradients on shallow seismic reflection data: Geophysics, v. 63, no. 4, p. 1348–1356, doi:10.1190/1.1444436.

Öncel, A. O., 20019, Introduction to Geophysics.

Opara, C., O. F. Adizua, and J. O. Ebeniro, 2018: Universal Journal of Geoscience, v. 6, no. 1, p. 1–7.

Rupnik, J.J., 1947, The constant level datum plane in areas of rough topography: The Mines Magazine, **37**, No. 11, 63-64.

Rogers, A. W., 1981, Determination of Static Corrections: Developments in Geophysical Exploration Methods, p. 1–36, doi:10.1007/978-94-009-8105-8_1.

Selem, A. M., 1955, Reflection Survey In Rough Topography*: Geophysical Prospecting, v. 3, no. 3, p. 246–257, doi:10.1111/j.1365-2478.1955.tb01375.x.

Sheriff, R. E., and L. P. Geldart, 1995, Exploration seismology: Cambridge, Cambridge University Press.

Sloss, L. L., 1963, Sequences in the Cratonic Interior of North America: Geological Society of America Bulletin, v. 74, no. 2, p. 93, doi:10.1130/0016-7606(1963)74[93:sitcio]2.0.co;2.

Steeples, D. W., R. D. Miller, and R. A. Black, 1990, Static corrections from shallow-reflection surveys: Geophysics, v. 55, no. 6, p. 769–775, doi:10.1190/1.1442889.

Steeples, D. W., and R. D. Miller, 1998, Avoiding pitfalls in shallow seismic reflection surveys: Geophysics, v. 63, no. 4, p. 1213–1224, doi:10.1190/1.1444422.

Thomas, R. P., and R. H. Morrison, 1963, Seismic Datum Construction in Areas of Rugged Topography: Geophysics, v. 28, no. 5, p. 855–868, doi:10.1190/1.1439284.

Thralls, H. M., and R. W. Mossman, 1952, Relation of Seismic Corrections to Surface Geology: Geophysics, v. 17, no. 2, p. 218–228, doi:10.1190/1.1437747.

Yilmaz Ozdoægan, S. M. Doherty, and Yilmaz Ozdoægan, 2001, Seismic data analysis: processing, inversion, and interpretation of seismic data: Tulsa, OK, Society of Exploration Geophysicists.

Zhang, L., J. Xia, and F. Kong, 2016, The shallow-reflection wave-based static-correction method and its effect: SEG Technical Program Expanded Abstracts 2016, doi:10.1190/segam2016-13686586.1.

Appendix A - R_Line Pattern

Reverse the R_Line Channel

32-38,55-58,74,75,77,78,79-81,94-98,111-114,128-132,146-149,162-166,176,180-184,199-205,212,218-223,227,228,232-236,241-243,245-250,253-256,261-265,267-271,275-280,282-285,296-300,302,303,307-310,312-316,318-322,324-327,330-333,336,340-342,357-360,363-368,371,372,376-379,383,387-390,397-399,403,407-410,417,424,427-434,440,442,443,446,447,450-452,455,456,459-462,465-467,470-475,482-486,489,491,494-496,499-501,503-505,507-510,514-517,525-527,530-532,534-540,543,549,550,552,556,559-562,565,568,569,571,575,576,581-583,589-593,597,598,601-605,609,611,613,614,617-620,623-625,630-634,637-644,240,521,524,179

Patterned R_Line Channel

49,105,139,188,311,347,400,520,528,574

Pattern where cables are good between R_lines 101-143

21,22,23-27,50-52,124,125,126,143,144,158,159,160,172,174,175,191,192,210,211,224-226,237-239,301,322,323,334,335,355,356,369,370,380-382,391-392,401-402,411,412,418-420,425,426,435,436,437,444,445,453,454,463,464,475,476,487,488,497,498,506,518,519,528,529,541,542,551,563,564,573,584,585,586,595,606,607,608,615,616,626-629,122,251,252,266,281

Acceptable R_Lines

1,2,3,4,5,6,19,20,28,29,30,31,48,54,72,73,76,89,90,91,93,107,108,110,127,145,161,177,178,193,195,196,197,198,214,215,216,217,230,231,244,257,258,259,272,273,274,288,290,291,292,293,294,304,305,306,317,328,329,337,338,339,348,349,350,362,373,374,375,384,385,386,394,395,396,404,405,406,413,414,415,416,421,422,423,438,439,448,457,458,468,469,480,481,490,492,502,511,512,513,523,533,544,545,546,547,548,553,554,555,558,566,567,570,577,578,579,580,587,588,599,600,610,612,621,635,636,449,522,557,622140,141,154,189,206,207,343,346,351